

A Lunar Far-Side Very Low Frequency Array

(NASA-CP-3039) A LUNAR FAR-SIDE VERY LOW
FREQUENCY ARRAY. (New Mexico Univ.) 75 p
CSCL 03A

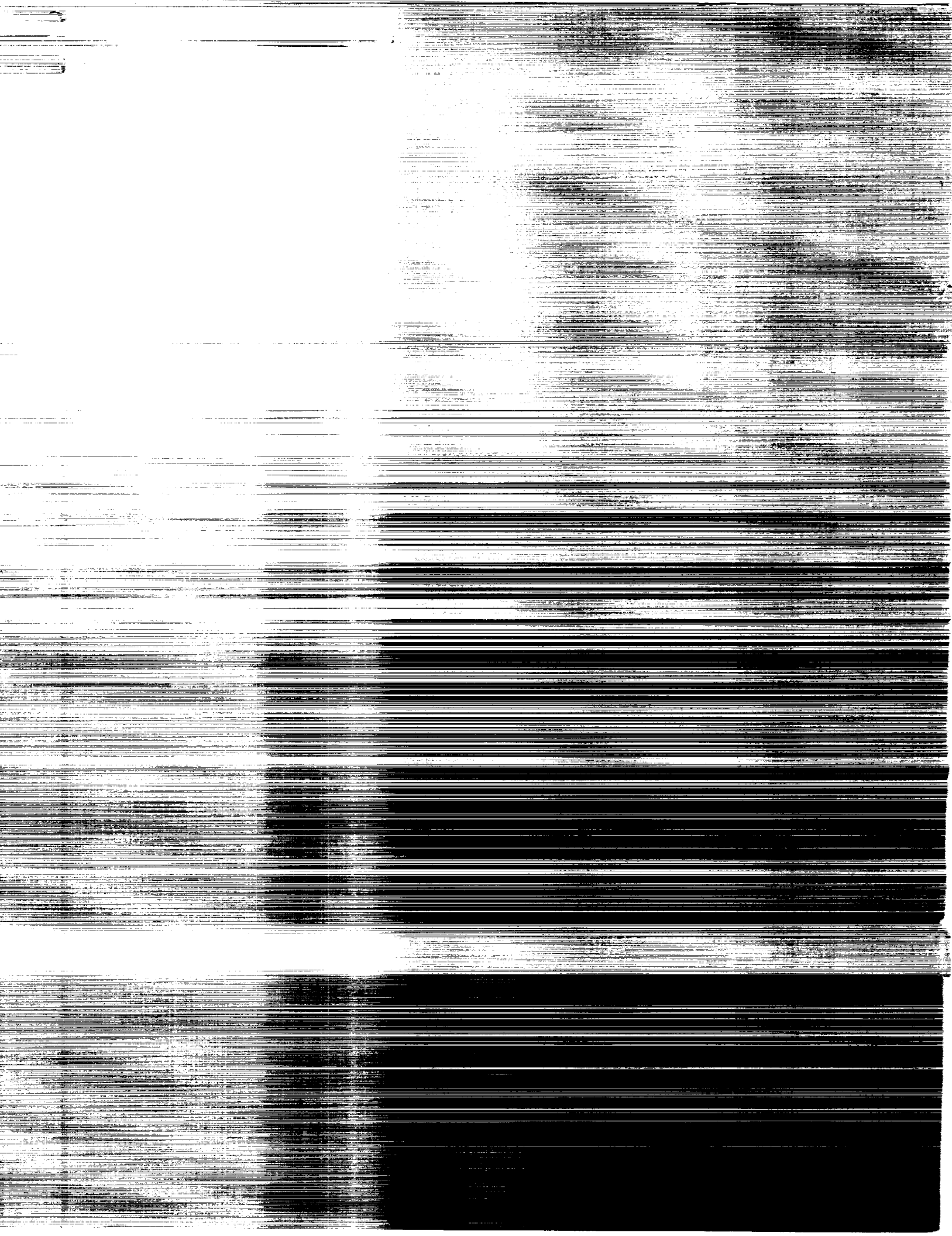
N90-10305

Unclass
0224710

H1/89

*Proceedings of a workshop held at
the IBM Corporation
Albuquerque, New Mexico
January 18-19, 1988*

NASA



NASA Conference Publication 3039

A Lunar Far-Side Very Low Frequency Array

Edited by
Jack O. Burns
and Nebojsa Duric
University of New Mexico
Albuquerque, New Mexico

Stewart Johnson
BDM Corporation
Albuquerque, New Mexico

G. Jeffrey Taylor
University of New Mexico
Albuquerque, New Mexico

Proceedings of a workshop sponsored by
the National Aeronautics and Space Administration,
Washington, D.C., the University of New Mexico,
Albuquerque, New Mexico, and the BDM Corporation,
Albuquerque, New Mexico, and held at
the BDM Corporation
Albuquerque, New Mexico
February 18-19, 1988

NASA

National Aeronautics and
Space Administration
Office of Management
Scientific and Technical
Information Division

1989

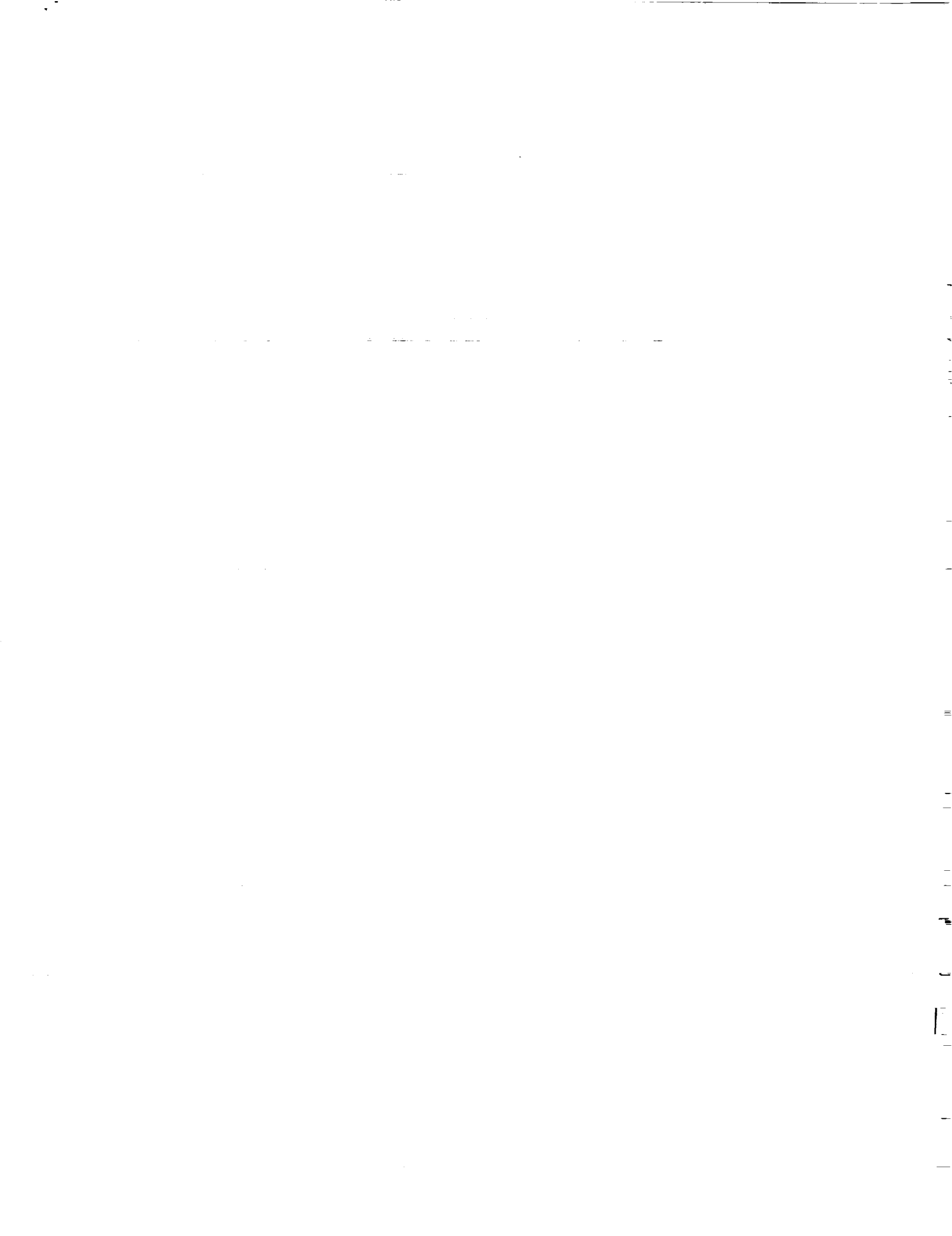
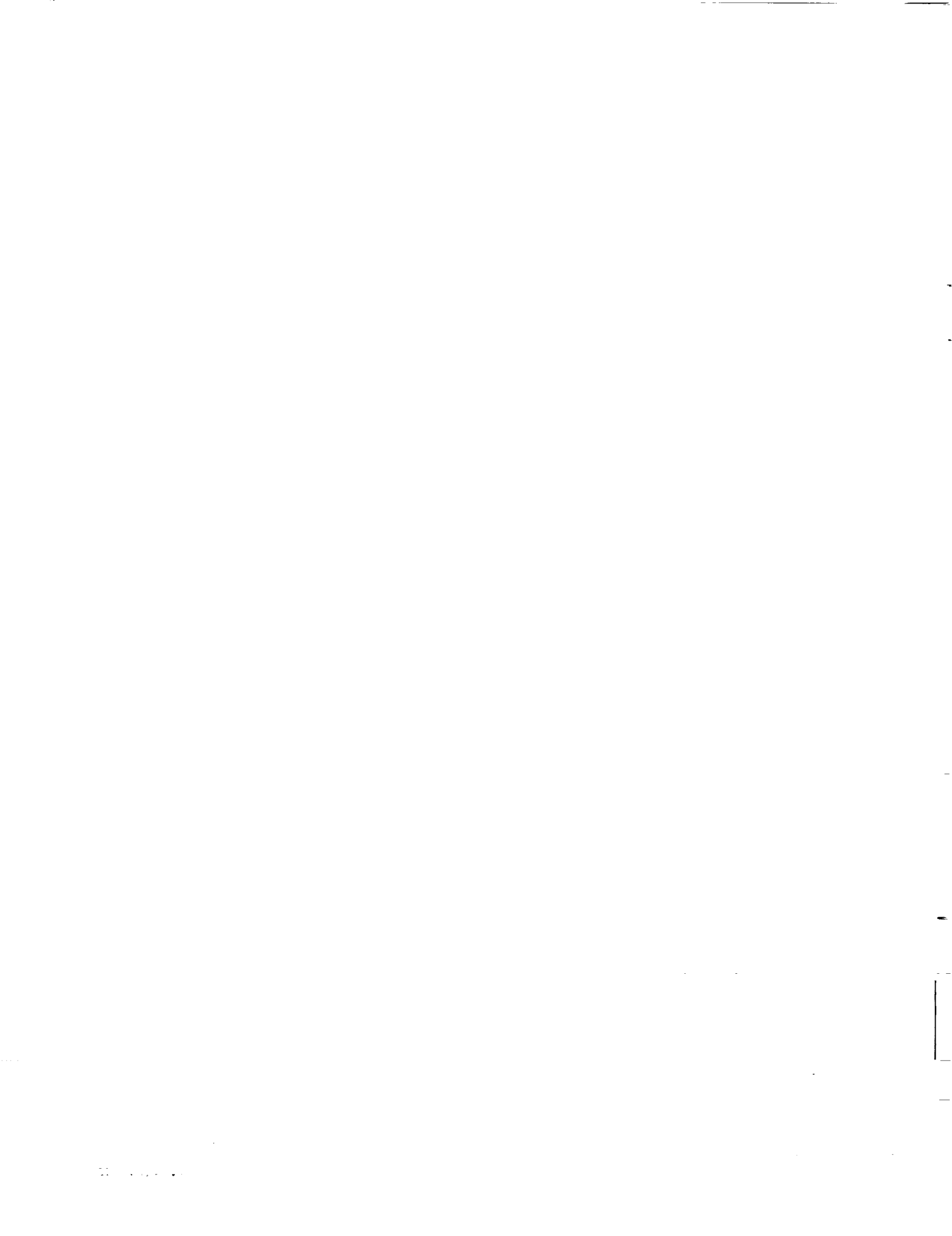


TABLE OF CONTENTS

	Page
PROLOGUE — J.O. Burns	v
LIST OF PARTICIPANTS	vi
WORKSHOP AGENDA	vii
INTRODUCTION — J.O. Burns	1
PART I — THE ENVIRONMENT AT THE LUNAR SURFACE	
G.J. Taylor	7
PART II — PREVIOUS AND PROPOSED LOW-FREQUENCY OBSERVATORIES	
THE CLARK LAKE TELESCOPE	
W.C. Erickson	13
THE BOULDER-AMES DECAMETER WAVELENGTH VLBI EXPERIMENT	
J.P. Basart	19
THE RADIO ASTRONOMY EXPLORER PROGRAM: VALUABLE LESSONS FOR FUTURE LOW FREQUENCY RADIO ASTRONOMY FROM SPACE	
M.L. Kaiser	23
THE 75 MHz LAV SYSTEM	
W.C. Erickson and R.A. Perley	27
PART III — SCIENCE WITH A LUNAR VLFA	
SCIENCE AT VERY LOW RADIO FREQUENCIES	
N. Duric	29
VOYAGER RADIO ASTRONOMY AND THE LOW FREQUENCY NEAR-EARTH RADIO ENVIRONMENT	
M.D. Desch	35
THE EFFECTS OF SCATTERING AND SCINTILLATION IN THE INTERSTELLAR AND INTERPLANETARY MEDIUMS	
B. Dennison	43
PART IV — DESIGN CONSIDERATIONS FOR A LUNAR VLFA	
ENGINEERING FOR A LUNAR FAR-SIDE VERY LOW FREQUENCY ARRAY	
S.W. Johnson	47
LUNAR FAR-SIDE VERY LOW FREQUENCY ARRAY	
J.P. Basart and J.O. Burns	53
PART V — POTENTIAL LUNAR VLFA SITE	
SITE SELECTION CRITERIA	
G.J. Taylor	61
PART VI — PROPOSAL FOR PRELIMINARY STUDIES	
PRECURSOR MISSIONS	
G.J. Taylor and J.O. Burns	65
PART VII — SUMMARIES, CONCLUSIONS, AND PROPOSALS FOR FUTURE WORK	
SUMMARY REMARKS	
J.N. Douglas	67
SUMMARY AND CONCLUSIONS	
J.O. Burns	75
SUGGESTIONS FOR FUTURE WORK	
J.O. Burns	77



PROLOGUE

On February 18th and 19th, 1988, a workshop was convened to discuss the scientific goals and preliminary designs of a potential Very Low Frequency Array (VLFA) to be constructed on the Lunar Far-Side. This two day meeting was conducted in the attractive, informal atmosphere of the BDM Corporation in Albuquerque. An attempt was made to gather together a small but representative group of astronomers who have participated in the construction of and observations with low frequency radio telescopes. The primary motivation behind the workshop was to seek guidance from our panel of experts on how we might plan for a VLFA on the Moon. We attempted to build upon previous foundations that were laid at other Lunar Base conferences and in other discussions of space-based very low frequency astronomy. We rolled our sleeves up, and asked some tough, detailed questions about the scientific justification for a lunar VLFA, the location and deployment of the array in the harsh environment of the lunar far-side, and the possible configuration of the antennas and their electronics. This report describes the results of our deliberations.

For the purposes of this workshop, we have defined very low radio frequencies to be < 30 MHz (> 10 meters wavelength). This is a practical definition for astronomical observations as discussed in this report. We do note, however, some inconsistency with radio frequency engineering that usually refers to very low frequencies as < 1 kHz.

The specific goals of the workshop were two-fold as follows:

(1) Define the scientific objectives of the Lunar Far-Side VLFA. We attempted to consider potential observations of the Sun, the magnetospheres of planets, the interstellar medium of the Galaxy, compact stellar objects, and active galaxies and quasars with the VLFA. Our efforts were restricted to defin-

ing in general what types of observations one might pursue for the purpose of guiding the design of the VLFA.

(2) Develop a preliminary design of the VLFA for further study. Among the areas of discussion were the frequencies for observation, the mode of operation (scan versus aperture synthesis), receiver and dipole design, computer requirements, data transmission, and antenna pattern and deployment. We reached a general consensus on these topics and have proposals that address these issues in this report.

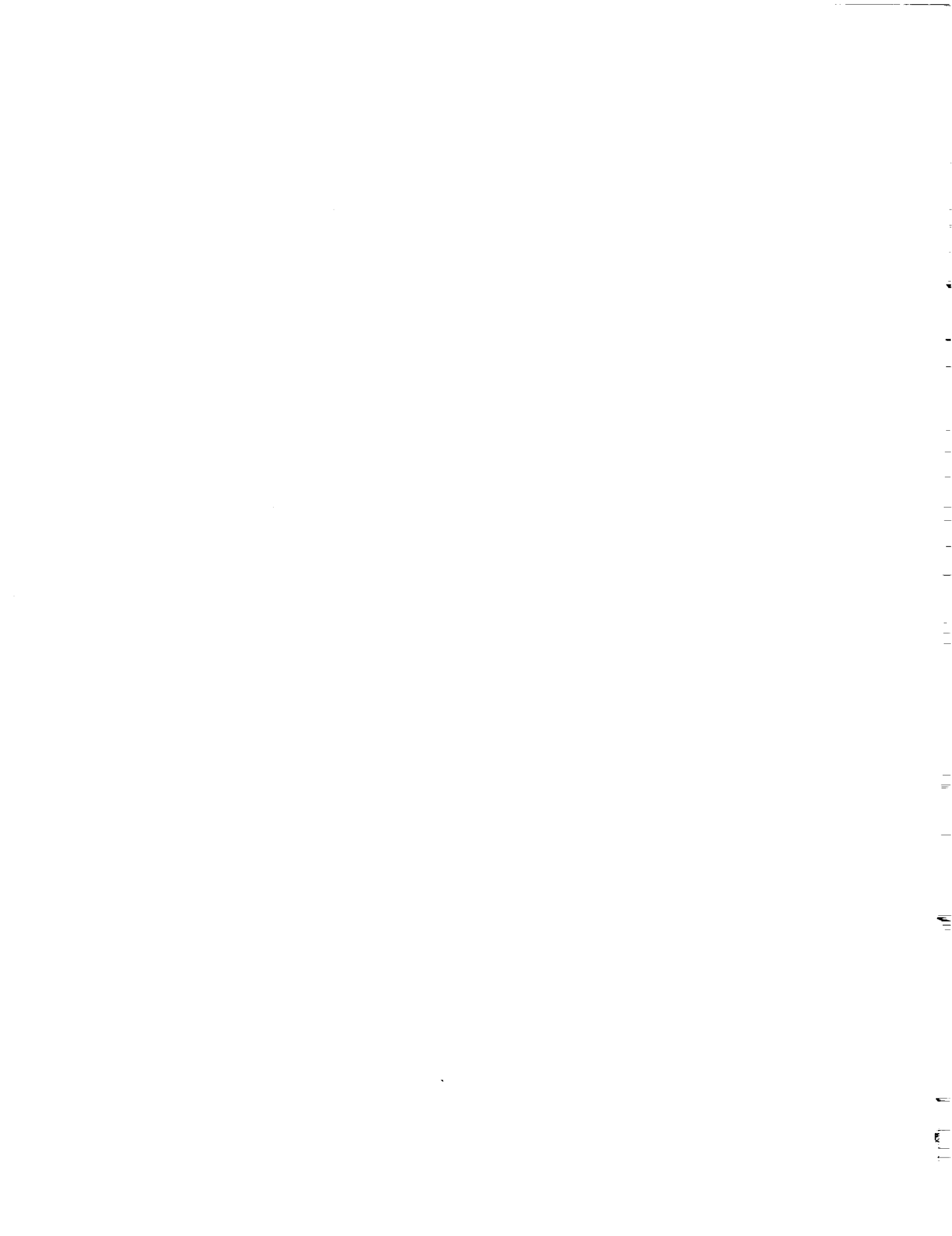
We adjourned feeling satisfied that we accomplished our primary mission which involved the first serious discussions of a lunar VLFA. However, this workshop was only the beginning of what we hope will become a permanent working group on the VLFA. Many technical questions were posed that will require further study. A series of recommendations for future work are offered in the last section of this report. As with many issues involving a manned lunar base, pursuit of answers to these questions will require funding of the research scientists and engineers so that adequate time can be devoted to this work.

I would like to thank Mike Duke and Barney Roberts from the NASA Johnson Space Center for their ongoing support of our studies of specific astronomical observations on the Moon. A special thanks goes to Wendell Mendell for his participation in the workshop and for providing important motivation for a lunar base over the last five years. Finally, I would like to acknowledge Dr. Stewart Johnson and the BDM Corporation for providing us with marvelous facilities that helped to make this workshop a success.

Jack O. Burns
The University of New Mexico
June, 1988

LIST OF PARTICIPANTS

1. Ferhart Akgul
Department of Civil Engin.
University of New Mexico
Albuquerque, NM 87131
2. Jodi Asbell-Clarke
Institute for Astrophysics
University of New Mexico
Albuquerque, NM 87131
3. Dr. John Basart
Electrical Engineering Dept.
Iowa State University
Ames, IA 50011
4. Dr. Jack O. Burns
Institute for Astrophysics
University of New Mexico
Albuquerque, NM 87131
5. Dr. Brian Dennison
Physics Department
Virginia Polytechnic Inst.
& State University
Blacksburg, VA 24601
6. Dr. Michael Desch
Code 690
Goddard Space Flight Center
Greenbelt, MD 20771
7. Dr. James Douglas
Department of Astronomy
University of Texas
Austin, TX 78712
8. Dr. Neb Duric
Institute for Astrophysics
University of New Mexico
Albuquerque, NM 87131
9. Dr. William Erickson
Astronomy Program
University of Maryland
College Park, MD 20742
10. Ilias Fernini
Institute for Astrophysics
University of New Mexico
Albuquerque, NM 87131
11. John Hull
Battelle, Columbus Division
505 King Avenue
Columbus, OH 43201
12. Dr. Stewart Johnson
BDM Corporation
1801 Randolph Rd. SE
Albuquerque, NM 87106
13. Dr. Michael Kaiser
Code 690
Goddard Space Flight Center
Greenbelt, MD 20771
14. Dr. Jerome Kristian
Mt. Wilson & Las Campanas Obs.
813 Santa Barbara St.
Pasadena, CA 91101
15. Dr. Wendell Mendell
Code SN3
NASA Johnson Space Center
Houston, TX 77058
16. Dr. G. Jeffrey Taylor
Institute of Meteoritics
University of New Mexico
Albuquerque, NM 87131



INTRODUCTION

Jack O. Burns
The University of New Mexico

In response to the recent report by Sally Ride (1987), NASA has begun to move aggressively into long-range planning beyond the Space Shuttle and the Space Station. A new Office of Exploration headed by John Aaron was recently added at NASA Headquarters to consider, among other things, how the U.S. might establish a permanent presence on the Moon and on Mars. With regard to a lunar base, a four-phase scenario is being considered. This will hopefully serve as a generic template for implementation definition and for a schedule required for analysis. The four phases are as follows:

- Phase I — Exploration and Base Site Selection
- Phase II — Scientific Outpost
- Phase III — Permanently Inhabited Base
- Phase IV — Self-Supported Base.

Some of the goals for each phase of exploration are shown schematically in Figure 1. More detailed facilities and a possible timeline for deployment are shown in Figure 2. These figures are courtesy of Mike Duke and Barney Roberts.

For the purposes of this report, we note that a far-side observatory is scheduled for Phase II, in the later half of the first decade of the 21st century. This would presumably include a VLFA that would likely be deployed with a minimum of human presence. At first glance, this timeline appears both optimistic and also a distant prospect for the future. Why should astronomers be concerned with such a futuristic observatory when we have yet to see the launch of the first of the Great Observatory Series, the Hubble Space Telescope, and have yet to secure funding for AXAF and SIRTF? The answer to this question lies in the long timescales required to develop support in the astronomical community and in Congress, and to develop good scientific and technical proposals for such space-based projects. The analogy to the Space Telescope may be particularly appropriate. Lyman Spitzer's first proposal for an Earth-orbiting large optical telescope appeared in print in the late 1940s, nearly 40 years ago. The first NASA-sponsored meetings began in 1962. Some 27 years later (1989), the Hubble Space Telescope is anticipated to be launched by the Shuttle. It is interesting to note that 27 years from the date of this workshop is 2015. Thus, it is not too early to begin to explore lunar observatories such as the VLFA on the far side.

The idea of observatories on the Moon can be traced

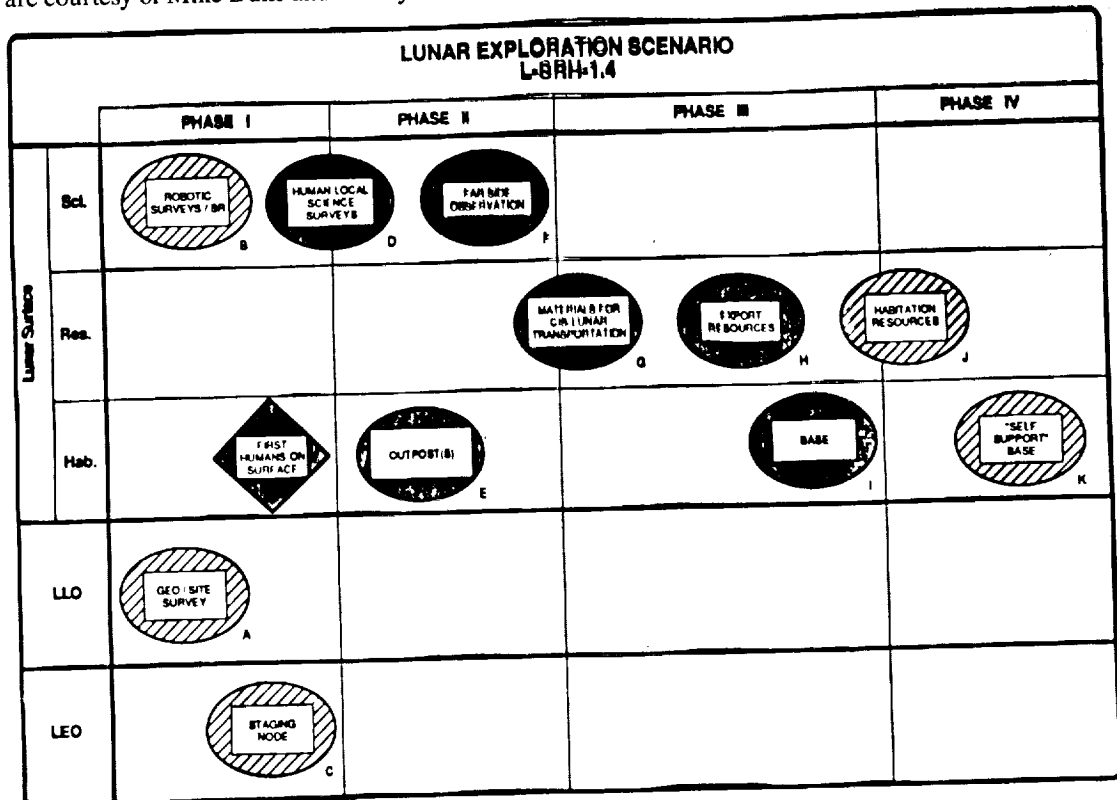


Figure 1.

this workshop that a VLFA on the lunar far side was one of the more interesting and important proposals for lunar observatories.

The National Commission on Space Report and the recently completed second Lunar Bases Symposium have further emphasized that the Moon is possibly the best location within the inner solar system from which to conduct astronomy, especially meter to kilometer wavelength radio astronomy. The Moon has several natural advantages over the Earth for low frequency radio astronomy. These include:

- (1) The Moon absorbs Earth radio noise for a far side observatory. The Earth's environment is very loud at low frequencies. First, man-made interference from radio, television, and communications dominates on the surface of Earth and leaks through the ionosphere at significant levels (Erickson, 1988). Thus, both on Earth's surface and in Earth orbit, one is faced with high levels of interference. Second, Earth's magnetosphere is a strong source of kilometric auroral radiation, especially below 1 MHz. This was first discovered in the early 1970s by the Radio Astronomy Explorer (RAE) satellite (see paper by Kaiser in Part II of this report). The Moon is a natural filter for these interfering signals.
- (2) The Moon has very little ionosphere. On Earth's surface, the ionosphere does not transmit radio frequency radiation below about 5 MHz. In addition, scintillation and scattering of radio waves by the ionosphere and troposphere limit both position accuracy and resolution of radio observations below about 30 MHz. The exact value of the global average electron density in the Moon's ionosphere is uncertain, but is believed to be low (~ 100 electrons/cm³). This corresponds to a plasma frequency of ~ 90 kHz which would be the lower bound on observations from the Moon. Other astronomical considerations discussed in this report would likely drive the lower bound on the frequency of the VLFA above 500 kHz. However, Vondrak (1988) has recently pointed out that a 100-m layer of negatively charged electrons and ions may hug the surface of the Moon on the day side. The electron levitation is believed to be due to the net positive charge of the surface produced by interaction with the solar wind. The density may be as high as 10^4 electrons/cm³ corresponding to a plasma frequency of 1 MHz. Clearly, this must be investigated further since it would impact on the design of the VLFA.
- (3) The Moon is a stable platform. This is an advantage over Earth-orbiting spacecraft. On the Moon, the dipole array can be deployed over large areas with accurate relative positions for phase coherence. In orbit, gravitational strains constantly move the relative positions of array components, thus varying one's ability to observe all sources in the same fashion (i.e., with the same u-v coverage for aperture synthesis) or monitor source variability.
- (4) The maintenance of a lunar VLFA will be very low. Once deployed there will be no erosion of the cables and com-

ponents by wind and rain. Although the temperature gradient from day to night is large (280 K), this is not expected to significantly alter the characteristics of the simple dipole antennas.

There are, however, some concerns that one has about placing the VLFA on the lunar far side. These include:

- (1) The possible damage integrated circuitry and computer chips in the receiver, correlator, and computers by cosmic rays. Since the Moon has no significant magnetic field, the surface is not shielded from the damaging cosmic radiation. However, radiation-hardened electronics are commonly produced for spacecraft that fly above Earth's van Allen radiation belts.
- (2) Human environmental hazards. The Moon is a very inhospitable place to live and work. Lack of oxygen and water, and radiation from the Sun and the Galaxy are major concerns. The deployment of the VLFA over tens of kilometers on the far side could potentially be very time-intensive. Such concerns would appear to demand that the array be deployed by intelligent robots. This increases the technical complexity of an otherwise simple instrument.
- (3) Remote basing on the far side. The likely location of lunar colonies for the first decade or two will be on the near side. Operations on the far side must be remotely controlled and semi-autonomous. In addition to the deployment problem noted above, one must also deal with the operation of the VLFA in a completely remote mode. Repair and upgrades of components, and initial processing and transmission of data must all be handled without human presence.
- (4) Cost. Establishment of a lunar base is expensive. Sellers and Keaton (1985) estimate the cost will be about \$80 billion in 1984 dollars. However, spread over 20 plus years, the yearly cost could be less than the Apollo program. Clearly, astronomy cannot bear this burden. This must be a national or international effort that is driven by political as well as scientific motivations. Once a permanent manned presence is established on the Moon, the cost of a VLFA is relatively low because of the simplicity and low mass of the components.

Astronomy and Astrophysics for the 1980s. Report of the Astronomy Survey Committee, Vol. 1, National Academy Press, 1982, pp. 165 - 166.

Burns, J.O. and Mendell, W.W. 1988, editors, *Future Astronomical Observatories on the Moon*, NASA Conference Publication #2489.

Douglas, J.N. and Smith, H.J. 1985 in *Lunar Bases and Space Activities of the 21st Century*, Vol. 1, ed. W.W. Mendell (LPI: Houston), p. 301.

Erickson, W.C. 1988, U. of Maryland Report.

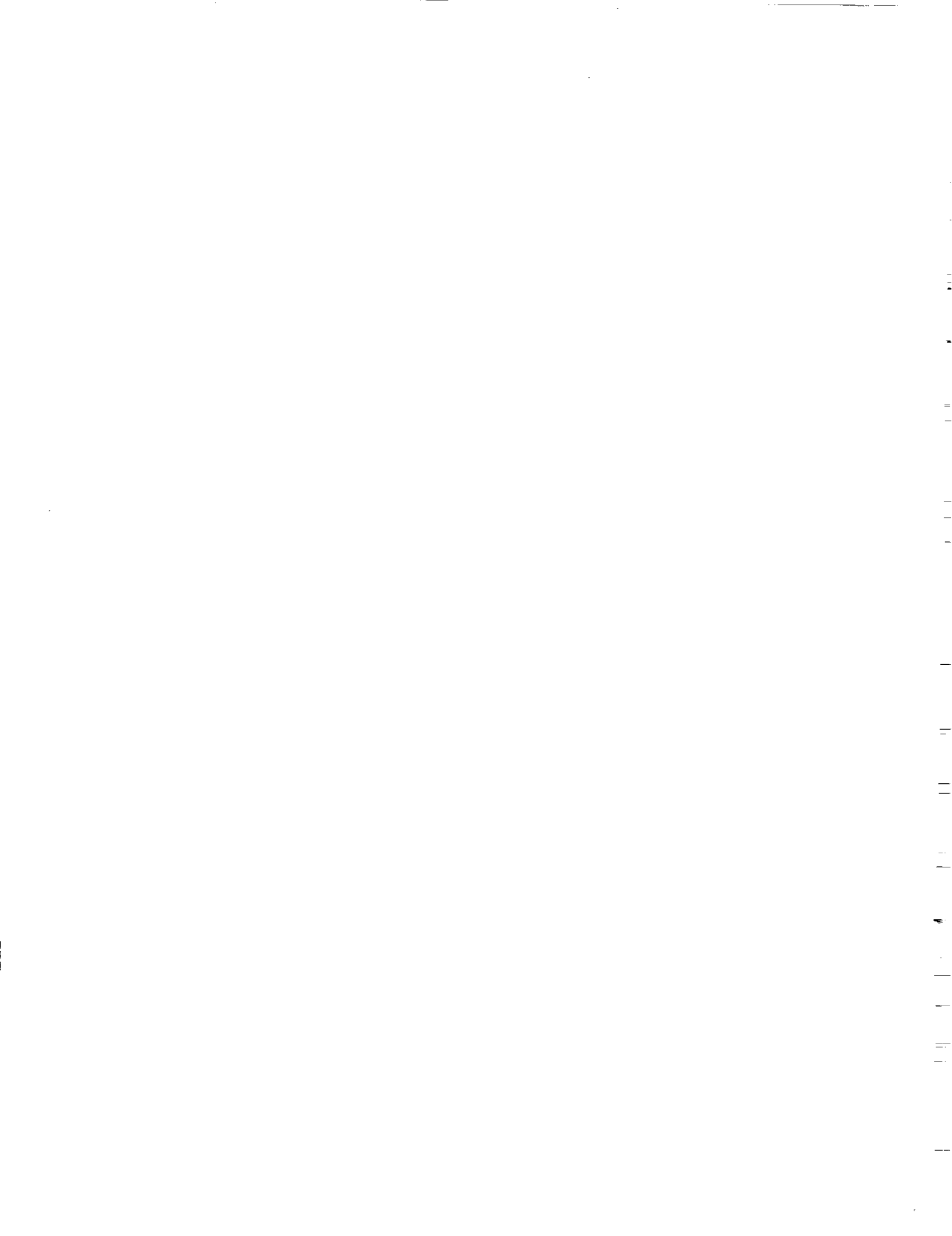
NASA Summer Conference on Lunar Exploration and Science, 1965, NASA Report, pp. 369-391.

NASA Summer Study of Lunar Science and Exploration, 1967, NASA Report, pp. 371-390.

Ride, S. 1987, NASA Report.

Sellers, W.O. and Keaton, P.W. 1985, in *Lunar Bases and Space Activities of the 21st Century*, Vol. 1, ed. W.W. Mendell (LPI: Houston), p. 711.

Vondrak, R.R. 1988, in *Lunar Bases and Space Activities of the 21st Century*, Vol. 2, in press.



PART I — THE ENVIRONMENT AT THE LUNAR SURFACE

THE ENVIRONMENT AT THE LUNAR SURFACE

G. Jeffrey Taylor

Department of Geology and Institute of Meteoritics
University of New Mexico, Albuquerque, NM 87131, USA

ABSTRACT

The Moon's geologic environment features 1) a gravity field one-sixth that of Earth; 2) a sidereal rotation period of 27.3 days; 3) a surface with greater curvature than Earth's surface; a chord along a 60-km baseline would have a bulge of 260 meters; 4) a seismically and tidally stable platform on which to build structures and transportation systems; total seismic energy released is 10^8 times less than on Earth, and most moonquakes have magnitudes of 1 to 2, within Earth's seismic noise; 5) a tenuous atmosphere (the total mass at night is only 10^4 kg) that does not cause wind-induced stresses and vibrations on structures; 6) a large diurnal temperature variation (100 to 385 K in equatorial regions), which facilities must be designed to withstand; 7) a weak magnetic field, ranging from 3 to 330×10^{-5} oersted compared to 0.3 oersted on Earth at the Equator; 8) a surface exposed to radiation, the most dangerous of which are high-energy (1–100 Mev) particles resulting from solar flares; 9) a high flux of micrometeorites which are not slowed down from their cosmic velocities because of the lack of air; data indicate that microcraters 10 m across will form at the rate of $3000/\text{m}^2/\text{yr}$; 10) a regolith 2 to 30 meters thick which blankets the entire lunar surface; this layer is fine-grained (average grain sizes range from 40 to 268 μm), has a low density (0.8 to 1.0 g/cm^3 in the upper few millimeters, rising to 1.5 to 1.8 g/cm^3 at depths of 10–20 cm), is porous (35–45%), cohesive (0.1 to 1.0 kN/m^2), and has low thermal diffusivity (0.7 to $1.0 \times 10^{-4} \text{ cm}^2/\text{sec}$) and electrical conductivity ($10^{-14} \text{ ohm}^{-1}\text{m}^{-1}$); 11) a rubbly upper several hundred meters in which intact bedrock is uncommon, especially in the lunar highlands; and 12) craters with diameter-to-depth ratios of 5 if fresh and 15 km across; larger and eroded craters have much larger diameter-to-depth ratios.

The Moon's geologic environment is dramatically different from Earth's and presents fascinating challenges to engineers designing facilities on the lunar surface. This paper summarizes the geologic nature of the stark lunar surface and its tenuous atmosphere.

GENERAL CHARACTERISTICS

The strength of the Moon's gravitational field is about one-sixth that at Earth's surface; the surface gravity is 162 cm/sec^2 and the escape velocity is 2.37 km/sec . The

lower gravity allows use of materials of lower strength than on Earth for structures of equivalent size. Alternatively, much larger structures can be built on the Moon. The Moon has a slow sidereal (the time it takes to complete one revolution) rotation period of 27.3 Earth days, so days and nights last almost two weeks. Consequently, solar energy systems require some way to store energy and plants will need artificial light during the long lunar night. Finally, because of the Moon's smaller radius, its surface has a larger curvature than does Earth's surface. For example, a chord along a 10-km baseline would have a bulge along it of 7.2 meters; a 60-km baseline would have a bulge of 260 meters.

STABLE PLATFORM

The Moon provides a stable platform on which to build. Seismic properties are summarized in Table 1, which is adapted from Goins et al. (1981). There are two main categories of lunar seismic signals, based on the depth at which they originate. Almost all occur deep within the Moon at depths of 700 to 1100 km; on average, about 500 deep events were recorded during the eight years that the Apollo seismic network operated. These deep moonquakes are related to tidal forces inside the Moon.

Moonquakes also occur at much shallower depths (200 km), but apparently below the crust (Nakamura et al., 1979). They occur much less frequently than do deep moonquakes, only about 5/year. Shallow moonquakes do not appear to be related to tidal flexing of the Moon or to surface features. For comparison, most earthquakes occur at depths of 50 to 200 km.

Lunar seismic activity is drastically less than terrestrial seismicity (Table 1). Lunar seismographs detected only 500 quakes per year. In contrast, 10,000 detectable earthquakes occur each year on Earth. Note that the magnitudes of detectable quakes are different on Earth and the Moon, due mostly to greater seismic noise on Earth. In fact, most moonquakes are in the magnitude 1 to 2 range, which is in Earth's seismic background.

The total seismic energy released in the Moon is about 10^8 times less than in Earth. The magnitudes of the largest events on the Moon are also much less than the largest events on Earth (Table 1). The most energetic lunar events are the shallow ones, the largest recorded one being only 4.8 magnitude, corresponding to an energy of 2×10^{17} ergs.

Table 1. Comparison of moonquake and earthquake intensities (from Goins et al., 1981)

	Moon	Earth
Number of events/year	5 shallow (m 2.2)* 500 deep (m 1.6)*	10 ⁴ (m 4)*
Energy release of largest event	2 × 10 ¹⁰ joule (shallow) 1 × 10 ⁶ joule (deep)	10 ¹⁹ joule
Magnitude of largest event	4.8 (shallow) 3.0 (deep)	9
Seismic energy release/year	2 × 10 ¹⁰ joule yr ⁻¹ (shallow) 8 × 10 ⁶ joule yr ⁻¹ (deep)	10 ¹⁸ joule yr ⁻¹

*m = magnitude

The largest recorded earthquake measured 9.5 magnitude on the Richter scale, corresponding to an energy of 10²⁶ ergs.

Seismic waves are intensely scattered near the lunar surface. This causes the energy of the waves arriving at a given point to be spread out, so the damaging effects of a moonquake would be less than those of an earthquake of the same magnitude. (In fact, values of seismic energy and magnitudes reported for the Moon by Goins et al. (1981) are greater than those reported by Lammlein et al. (1974) because the latter authors had not accounted for scattering of seismic waves near the lunar surface or for some instrument effects.) Consequently, it appears that the lunar surface is far more stable than any place on Earth.

The scattering of seismic waves in the Moon is significant down to a depth of 25 km, but is most intense in the upper few hundred meters. This implies a lack of coherent layering in this region.

Tidal forces raise and lower the lunar surfaces about as much as on Earth, where body tides deflect the ground about 10–20 cm twice each day. Because the Moon is locked into a synchronous orbit, the main tidal bulge on the Moon is a permanent feature. Nevertheless, small tidal deflections stemming from librations do occur, but have much longer periods than on Earth. The tidal flexing of the lunar surface in both horizontal and vertical directions is about 2 mm along the length of a 10-km baseline (Dr. James Williams, personal communication, 1986). The precise amount of motion depends on position on the Moon. Tidal motions must be taken into account when designing, for example, long transportation systems or telescope arrays that require accurate alignment.

ATMOSPHERE

The lunar atmosphere is a collisionless gas. The total nighttime concentration is only 2 × 10⁵ molecules/cm³ (Hoffman et al., 1973). Its total mass is only 10⁴ kg, about the mass of air in a movie theater on Earth at 1 bar. This flimsy

atmosphere will eliminate engineering problems associated with wind (Johnson, 1986), but might add others, such as difficulty in lubricating moving parts.

The composition of the lunar atmosphere appears in Table 2. The gases derive from the solar wind, except for ⁴⁰Ar, which is produced by the decay of ⁴⁰K inside the Moon and then diffuses out. No daytime measurements of gas concentrations were made due to instrument limitations, but Hodges (1976) calculates that gases of carbon compounds, specifically CO₂, CO, and CH₄, probably dominate. They are absent at night because they condense out of the atmosphere onto soil particles.

Table 2. Composition of the lunar atmosphere at night (from Hoffman et al., 1973)

Gas	Concentration (mol m ⁻³)
H ₂	1.1 × 10 ⁻¹³
⁴ He	6.6 × 10 ⁻¹⁴
²⁰ Ne	1.3 × 10 ⁻¹³
³⁶ Ar	5.0 × 10 ⁻¹⁵
⁴⁰ Ar	1.2 × 10 ⁻¹⁴
O ₂	3 × 10 ⁻¹⁶
CO ₂ *	5 × 10 ⁻¹⁵

*Carbon gases (CO₂, CO, CH₄) probable dominate the daytime lunar atmosphere (Hodges, 1976).

The tenuous lunar atmosphere can be altered significantly by large-scale operations on the Moon. Vondrak (1974) has calculated that if the density of the lunar atmosphere is increased, a point is reached where the rate at which gas is lost is slowed dramatically. This could compromise a number of scientific experiments requiring a hard vacuum, such as

observations of the solar wind. Considering that each Apollo mission contributed 10^4 kg of gas (Johnson, 1971), temporarily doubling the atmosphere's nighttime mass, it would appear easy to contaminate the Moon's fragile atmosphere when regular flights to and from the lunar surface begin. The atmosphere must be monitored carefully when a lunar base is established. Studying the evolution of the Moon's atmosphere will, in fact, be an interesting research project in itself.

SURFACE TEMPERATURES

Surface temperatures change drastically from high noon to dawn on the Moon, presenting a challenge to those designing lunar structures subject to thermal expansion and contraction. At Apollo 17, for example, the temperature ranged from 384°K to 102°K during the month-long lunar day (Keihm and Langseth, 1973). Furthermore, the temperature decreases rapidly as sunset approaches, falling about 5°K/hr . These data apply to equatorial regions only. In polar regions, the predawn temperature is about 80°K (Mendell and Low, 1970). The temperature in permanently-shadowed areas at the poles could be lower. The cold nighttime temperature will permit cooling of many systems without use of cryogenics.

The temperature variation is damped out rapidly at depth in the lunar soil (Keihm and Langseth, 1973). At a depth of 30 cm the temperature is about 250°K and varies only 2° to 4°K from noon to dawn. This steady temperature might be useful for some purposes, but not as a heat sink because the lunar soil has a very sluggish thermal conductivity (see below).

MAGNETIC FIELD

No magnetic field is now being generated inside the Moon, although there was a source of magnetism several billion years ago. It is not known whether this was generated by a dynamo in a metallic core, as on Earth, or by local, transient events such as meteorite impacts. Whatever its source, the lunar magnetic field is much weaker than is Earth's (Dyal et al., 1974). On the surface, the lunar magnetic field strength ranges from 3 to 330 gamma (1 gamma = 10^{-5} oersted = 10^{-5} gauss). For comparison, Earth's field at the equator is 30,000 gamma. Also, the lunar field varies locally on the Moon. For example, at the Apollo 16 landing site, the field varied from 113 ± 4 to 327 ± 7 gamma.

There is also a field external to the Moon, derived from the solar wind. This ranges from 5 gamma in the free streaming solar wind to about 10 gamma in Earth's geomagnetic tail, in which the Moon resides 4 days during each lunation.

RADIATION ENVIRONMENT

Because of the Moon's small magnetic field and nearly absent atmosphere, solar and galactic nuclear particles hit its surface unimpeded. There are three sources of radiation with

different energies and fluxes; see Taylor (1975) for a summary. The energy sources are 1) high energy (1-10 GeV/nucleon) galactic cosmic rays, with fluxes of about $1/\text{cm}^2/\text{sec}$ and penetration depths of up to a few meters; 2) solar flare particles with energies of 1-100 MeV/nucleon, fluxes up to $100/\text{cm}^2/\text{sec}$, and penetration depths up to 1 cm; and 3) solar wind particles, which have much lower energies of about 1000 eV, tiny penetration depths (10^{-8} cm), but high fluxes ($10^8/\text{cm}^2/\text{sec}$). These penetration depths refer to the primary particles only. Reactions between them and lunar material cause a cascade of radiation that penetrates much deeper (Silberberg et al., 1985), up to several meters. The combination of high flux and energy make solar flare particles the most dangerous to people working on the lunar surface and to electronic devices deployed directly on the surface.

MICROMETEORITE FLUX

The lack of a significant atmosphere on the Moon allows even the tiniest particles to impact with their full cosmic velocities, ten to several tens of km/sec. This rain of minute impactors could damage some structures and instruments on the lunar surface. Almost all lunar rock samples contain numerous microcraters, commonly called zap pits, on surfaces that were exposed to space while on the lunar surface. Studies of lunar rocks (Fechtig et al., 1974) have revealed the average flux of projectiles over the past several hundred million years. However, data from the Surveyor 3 TV camera shroud returned by the Apollo 12 mission and study of Apollo windows (Cour-Palais, 1974) indicate that the present flux of particles smaller than 10^{-7}g , which are capable of making craters up to 10 microns across, is about ten times greater than that measured on lunar rocks. Study of louver material from the Solar Max satellite (Barrett et al., 1988) confirm that fluxes are greater now than the average of the past several hundred million years. Combining the fluxes of particles $< 10^{-7}\text{g}$ measured on spacecraft with those $> 10^{-7}$ measured in Apollo rocks, one arrives at the flux estimate in Table 3.

Table 3. Micrometeorite fluxes on the moon, calculated from data given by Fechtig et al., (1974)

Crater diameter (μm)	Craters $\text{m}^{-2}\text{yr}^{-1}$
0.1	30,000
1.0	1,200
10	300
100	0.6
1000	0.001

REGOLITH

The lunar regolith, also called the lunar soil, is a global veneer of debris generated from underlying bedrock by meteorite impacts. It contains rock and mineral fragments and glasses formed by melting of soil, rock and minerals. It also contains highly porous particles called agglutinates, which are glass-bonded aggregates of rock and mineral fragments. Agglutinates are produced by micrometeorite impacts into the lunar regolith.

Regolith depth ranges from 2 to 30 meters, with most areas in the range 5 to 10 meters. Impacts by micrometeorites have reduced much of the regolith material to a powder. Its grain size ranges from 40 to 268 μ m and varies in a highly complex fashion with depth (Heiken, 1975). The chemical composition of the regolith reflects the composition of the underlying bedrock, modified by admixture of material excavated from beneath or thrown in by distant impacts.

The mechanical properties of lunar regolith samples were measured by Mitchell et al. (1972). The bulk density of the regolith is very low, 0.8 to 1.0 g/cm^3 , in the upper few millimeters, but increases to 1.5 to 1.8 g/cm^3 at depths of 10 to 20 cm. Its porosity is 35 to 45% in the upper 15 cm, accounting in part for the low density. Except for the uppermost few millimeters, the lunar regolith is more cohesive, 0.1 to 1.0 kN/m^2 , than most terrestrial soils and has an angle of internal friction of 30 to 50°. Agglutinates and shock-damaged rock fragments are weak and break under loads, leading to an increase in soil density (Carrier et al., 1973).

The lunar regolith is an excellent insulator. Its thermal diffusivity at depths of 30 cm is 0.7 to 1.0 $\times 10^{-4}$ cm^2/sec and its thermal conductivity is 0.9 to 1.3 $\times 10^{-4}$ W/cm K (Langseth et al., 1976). This is not surprising considering the high porosity and lack of air. At depths of 30 cm, the thermal diffusivity is somewhat lower.

The lunar regolith is also an excellent electrical insulator. The dielectric properties of the regolith have been summarized by Olhoeft and Strangeway (1975) and by Olhoeft (1988). For soils, conductivities are about 10^{-14} $(\text{ohm}\cdot\text{m})^{-1}$. Lunar soils have dielectric constants ranging from 1.5 to 4, with a systematic variation with density: $k = (1.93 \pm 0.17)p$ where k is the dielectric constant and p is the density (g/cm^3). This relation holds for rocks as well. There is no systematic variation with soil composition (Olhoeft and Strangeway, 1975), almost no dependence on temperature, and no dependence on frequency above 1 MHz. Loss tangents have also been measured on lunar materials. This quantity is strongly dependent on density and on composition, and somewhat dependent on temperature and frequency. The loss tangent is given by:

$$\log \text{ loss tangent} = (0.38(\% \text{ TiO}_2 + \% \text{ FeO}) + 0.312p - 3.260)$$

where p is the density.

A small amount of lunar dust might be transported by charge differences built up by photoconductivity effects.

Criswell (1972) described a bright glow photographed by Surveyor 7 and explained the phenomenon as levitation of dust grains about 6 μ m in radius. The grains were lifted only 3 to 30 cm above the local horizon, and had a column density of 5 grains/ cm^2 . This does not appear to be a significant transport mechanism on the lunar surface.

UPPER FEW HUNDRED METERS

The upper few hundred meters of the Moon have been intensely fragmented by meteorite impacts. In the heavily cratered highlands and regions underlying mare basalt flows, the fragmental region extends for at least a few kilometers. Consequently, it might be difficult to find extensive areas of intact bedrock.

Active seismic experiments (Cooper et al., 1974) indicate that the velocity of compressional waves is about 100 m/sec at depths of less than 10 meters, which is in the regolith, and about 300 m/sec at depths between 10 and 300 meters. These velocities are too slow to correspond to coherent rock, implying that the upper few hundred meters of the lunar surface is rubble (Cooper et al., 1974). Rocks returned from the highlands confirm the fragmental nature of the upper lunar crust. Most are complicated mixtures of other rocks, and many are weakly consolidated. Furthermore, the rims of all craters are by their nature weakly consolidated or unconsolidated materials and, therefore, not able to withstand tensional stresses.

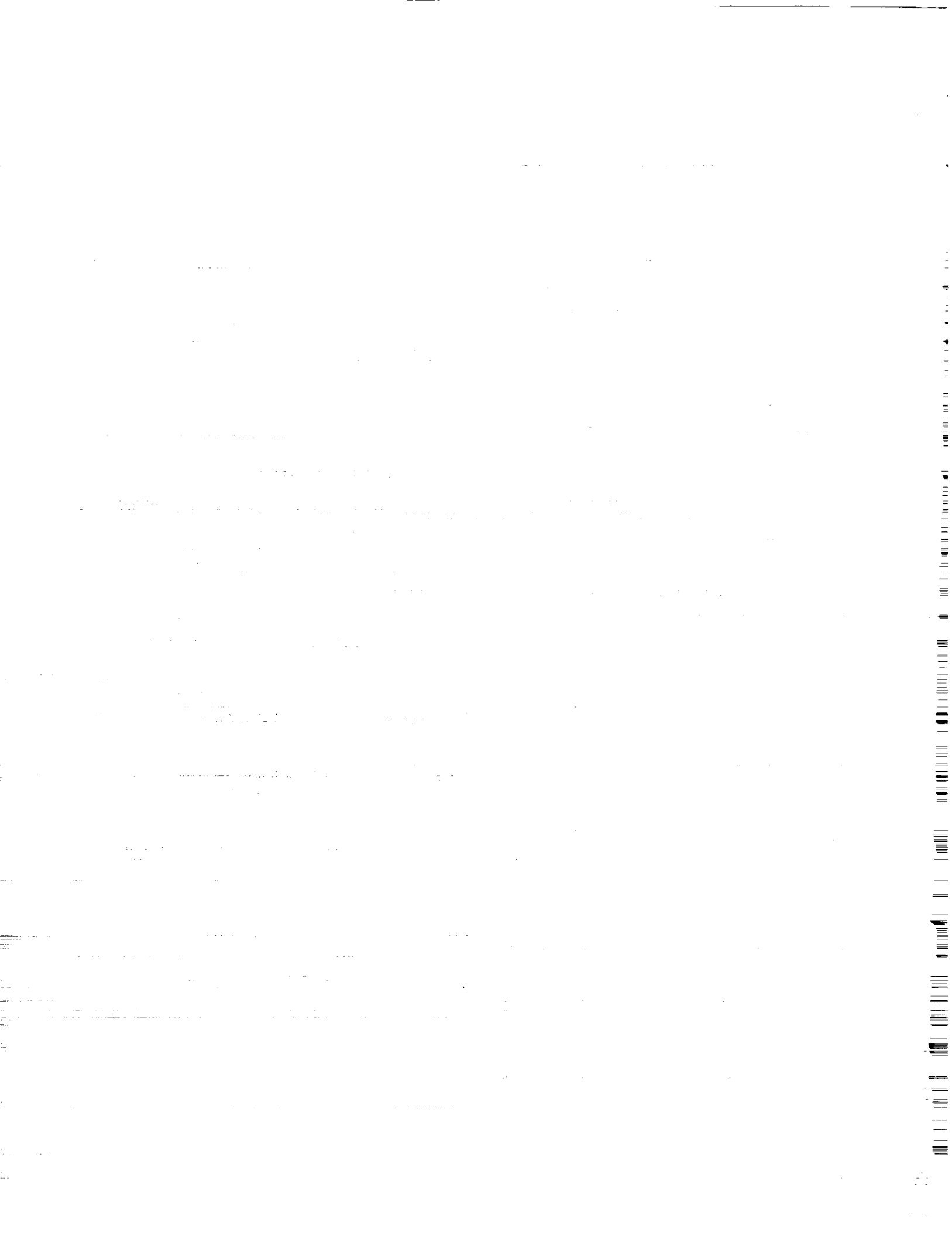
A few localities might have intact bedrock, however. Many mare basalt flows, for example, form visible layers in crater walls or, as at the Apollo 15 landing site, in the walls of sinuous rilles. Also, extensive sheets of impact-generated melt rocks occur on the floors of many large craters, such as Copernicus, which is 95 km in diameter.

CRATER MORPHOLOGIES

Fresh lunar craters up to 15 km in diameter have a consistent diameter/depth ratio of 5 (Pike, 1974). More specifically, craters 15 km across follow the relation $R_i = 0.196 D_r^{1.010}$, craters 15 km follow the relation $R_i = 1.044 D_r^{0.301}$ where R_i is the crater depth and D_r is the diameter as measured from rim crest to rim crest (Pike, 1974). Large craters are much shallower for their diameters than are smaller ones. Crater morphology changes as a crater is eroded by meteorite bombardment, during which a crater becomes wider and shallower, thereby increasing the diameter-to-depth ratio. Thus, even the smoothest areas on the lunar surface are undulating plains, so building horizontal transportations systems might require cut and fill operations. Finally, as noted above, rim materials consist of weak, unconsolidated rock. This could present problems for construction if certain facilities had to be built on crater rims.

REFERENCES

- Barrett, R.A.; Bernhard, R.P.; and McKay, D.S. (1988) Impact holes and impact flux on returned solar max. louver material. *Lunar and Planet. Sci. XIX*, 39-40. Lunar and Planetary Institute, Houston.
- Carrier, W.D. III; Bromwell, L.G.; and Martin, R.T. (1973) Behavior of returned lunar soil in vacuum. *J. Soil Mech. Found. Div., ASCE* 99, 979-996.
- Cooper, M.R.; Kovach, R.L.; and Watkins, J.S. (1974) Lunar near-surface structure, *Rev. Geophys. Space Phys.* 12, 291-308.
- Cour-Palais, B.G. (1974) The current micrometeoroid flux at the moon for masses 10^{-7} g from Apollo window and Surveyor 3 TV camera results. *Proc. Lunar Sci. Conf. 5th*, 2451-2462.
- Criswell, D. (1972) Lunar dust motion. *Proc. Lunar Sci. Conf. 3rd*, 2671-2680.
- Dyal, P.; Parkin, C.W.; and Daly, W.D. (1974) Magnetism and the interior of the Moon. *Rev. Geophys. Space Phys.* 12, 568-591.
- Fechtig, H.; Hartung, J.B.; Nagel, K.; and Neukum, G. (1974) Lunar microcrater studies, derived meteoroid fluxes and comparison with satellite-borne experiments. *Proc. Lunar Sci. 5th*, 2463-2474.
- Goins, N.R.; Dainty, A.M.; and Toksoz, M.N. (1981) Seismic energy release of the Moon. *J. Geophys. Res.* 86, 378-388.
- Heikien, G. (1975) Petrology of lunar soils. *Rev. Geophys. Space Phys.* 13, 567-587.
- Hodges, R.R., Jr. (1976) The escape of solar-wind carbon from the moon. *Proc. Lunar Sci. Conf. 7th*, 493-500.
- Hoffman, J.H.; Hodges, R.R.; and Johnson, F.S. (1973) Lunar atmospheric composition results from Apollo 17. *Proc. Lunar Sci. Conf. 4th*, 2865-2875.
- Johnson, F.S. (1971) Lunar atmosphere. *Rev. Geophys. Space Phys.* 9, 813-823.
- Johnson, S.W. (1986) Engineering for a 21st century lunar observatory. Submitted to *J. Aerospace Eng.*
- Keihm, S.J. and Langseth, M.G. (1973) Surface brightness temperatures at the Apollo 17 heat flow site: Thermal conductivity of the upper 15 cm of regolith. *Proc. Lunar Sci. Conf. 4th*, 2503-2513.
- Lammlein, D.R.; Latham, G.V.; Dorman, J.; Nakamura, Y.; and Ewing, M. (1974) Lunar seismicity, structure, and tectonics. *Rev. Geophys. Space Phys.* 12, 1-21.
- Langseth, M.G.; Keihm, S.J.; and Peters, K. (1976) Revised lunar heat-flow values. *Proc. Lunar Sci. Conf. 7th*, 3143-3171.
- Mendel, W.W. and Low, F.J. (1970) Low-resolution differential drift scan of the moon at 22 microns, *J. Geophys. Res.* 75, 3319-3324.
- Mitchell, J.D.; Houston, W.N.; Scott, R.F.; Costes, N.C.; Carrier, W.D. III; and Bromwell, L.G. (1972) Mechanical properties of lunar soil: density, porosity, cohesion, and angle of internal friction. *Proc. Lunar Sci. Conf. 3rd*, 3235-3253.
- Nakamura, Y.; Latham, G.V.; Dorman, H.J.; Ibrahim, A.-B.K.; Koyama, J.; and Horvath, P. (1979) Shallow moonquakes: depth, distribution and implications as to the present state of the lunar interior. *Proc. Lunar Planet. Sci. Conf. 10th*, 2299-2309.
- Olhoeft, G.R. (1988) Electrical and magnetic properties. In *Lunar Sourcebook* (G. Heiken and D. Vaniman, eds.), Cambridge University Press, in preparation.
- Olhoeft, G.R. and Strangeway, D.W. (1975) Dielectric properties of the first 100 meters of the Moon. *Earth Planet. Sci. Lett.* 24, 394-404.
- Pike, R.J. (1974) Depth/diameter relations of fresh lunar craters: revision from space-craft data. *Geophys. Res. Lett.* 1, 291-294.
- Silberberg, R.; Tsao, C.H.; and Adams, J.A., Jr. (1985) Radiation transport of cosmic ray nuclei in lunar material and radiation doses. In *Lunar Bases and Space Activities of the 21st Century* (W.W. Mendell, ed.), 663-669, The Lunar and Planetary Institute, Houston.
- Taylor, S.R. (1975) *Lunar Science: A Post-Apollo View*. Pergamon Press, New York, 372 pp.
- Vondrak, R.R. (1974) Creation of an artificial lunar atmosphere. *Nature* 248, 657-659.



PART II — PREVIOUS AND PROPOSED LOW-FREQUENCY OBSERVATORIES

THE CLARK LAKE TELESCOPE

W.C. Erickson¹
Department of Physics and Astronomy
University of Maryland
College Park, MD 20742

INTRODUCTION

Most radio astronomical observations below 100 MHz have been the result of considerable effort on the part of a relatively small number of astronomers and engineers. The size required for the instruments has precluded the construction of more than a few in the world and, until recently, technology has not allowed the design of a large decametric array which would operate over more than a limited frequency range and be steerable in two coordinates with reasonable speed. Consequently, this part of the radio spectrum has attracted very few astronomers even though much information about the physics of celestial objects may be found from the study of radiation from the cosmos at these low frequencies.

Advances in the technology of decade bandwidth antennas [Rumsey, 1966], and low cost, reliable, wideband, solid state devices have made large fully-steerable decametric systems practical. Around these developments, the design of the Clark Lake telescope evolved during the 1970s. It was operable anywhere between 10 and 125 MHz with nearly instantaneous frequency and beam positioning capability. Unfortunately, recent cuts in Federal funding have forced us to discontinue operation of the system and it has now been dismantled.

OUTLINE OF THE ARRAY AND ELECTRONICS

The array was a 3.0×1.8 km "T" with the direction of its legs being approximately east, west, and south. The array was laid out in the plane of the Clark's dry lake which is not exactly tangential to the geoid. The south arm, which was perpendicular to the E-W arms, was laid out 18 arcsec from the plane containing the Earth's axis and the center of the array. The EW arm contained 32 banks, each with 15 individual elements; the N-S arm contained 16 similar banks. The signals from each of the EW banks were cross-correlated with those from the N-S banks to determine the two-dimensional visibility function of the area of sky under observation. This visibility function was then Fourier transformed to produce a map of the field-of-view. The beam shape of the three-armed "T" is equivalent to that obtained with a full cross but the collecting area of the fourth arm is lost. Phase

tolerances between the orthogonal arms are more critical in the "T" array than in a full cross [Christiansen and Hogbom, 1969], but these phases were easily adjusted in software after calibration by the observation of strong, small angular diameter sources.

Each log spiral element (teepee, hence the nickname "TPT") had a collecting area of about $(\text{wavelength})^2/3$, and was designed to operate between 20 and 125 MHz. The low frequency limit was extended to ≈ 10 MHz at reduced efficiency by terminating the base of each spiral with resistors. The teepees were at 6.25 meter intervals in the E-W arm and 7.5 meter intervals in the south arm. This spacing gives rise to grating responses above 50 MHz. The response due to these grating lobes was reduced by adjusting real-time delays to make the radiation coherent only for the desired lobe. Since the elements were all fixed in the vertical direction, beam positioning was accomplished purely through adjustment of the phase gradient across each arm. The gain of the system was modulated by the response pattern of the individual elements. For good zenith distance coverage, the response pattern must be wide ($\approx 90^\circ$ in this case), and the gain of each element was correspondingly low.

As shown in Figures 1 and 2, phasing of the array was accomplished in two stages. The elements were divided into 48 banks of 15, and the signals from the 15 antennas in each bank were combined, then preamplified and sent to the central building on separate coaxial feed lines. Phasing within a bank was accomplished by electronically "rotating" each conical spiral antenna with a diode switch controlled from the central building. Phasing between the banks was adjusted in software before the map of the field of view was formed by Fourier transformation.

SINGLE ELEMENT CONSTRUCTION AND OPERATION

The basic building block of the array was the conical log spiral antenna. Ideally this antenna would consist of two conducting sheets wound on the surface of a cone but, in this case, these sheets were approximated by sets of wires. The antenna was self-conjugate with a characteristic impedance of

¹Present address: Department of Physics, University of Tasmania, GPO Box 252C, Hobart, Tasmania 7001, Australia.

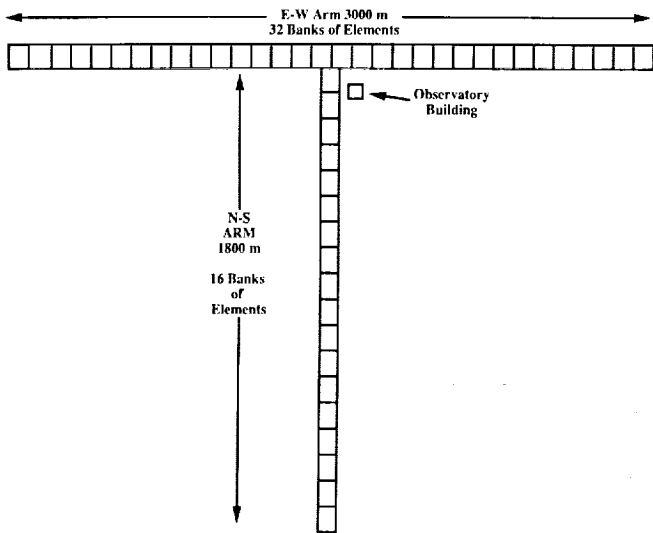


Figure 1. The layout of the array. Signals from each bank of elements were amplified and transmitted to the observatory by separate coaxial cables.

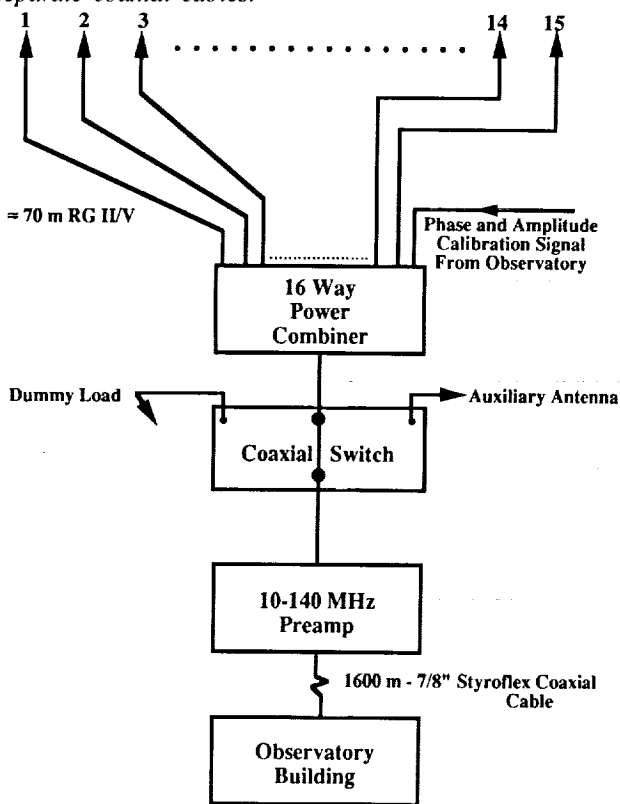


Figure 2. One bank of 15 conical spiral antennas.

189Ω and it was a backward-wave antenna fed by a balanced transmission line at its apex.

The electrical and radiative properties of this antenna were as follows: The antenna radiates primarily from the region where the circumference of the spiral is approximately equal to the wavelength, thus low frequencies are radiated from near the base of the element and high frequencies are

radiated from its top. The low-frequency limit of the antenna is determined by the size of the base of the spiral (circumference \approx wave-length) and the high frequency limit is set by the point at which the top of the spiral is truncated. This low frequency limit was extended by terminating the base of the spiral with a resistive load. Power that would ordinarily be reflected from the base of the antenna was dissipated in the load, and a constant antenna impedance was maintained to very low frequencies. At low frequencies, however, power is absorbed in the terminating resistors rather than being launched into space and the antenna efficiency decreases. Therefore the low frequency limit on the operating frequency was set by the loss of efficiency that one could tolerate rather than by impedance mismatches. Since the galactic background is intense at low frequencies, the background noise dominated receiver noise to below 10 MHz and the system could be operated down to about that frequency. The radiation pattern and the circularity of the polarization remained the same at these frequencies below the nominal cut-off of the antenna.

The radiation is unidirectional toward the apex and the polarization is in the opposite sense from the opening direction of the spiral, i.e., a right-hand (clockwise opening) spiral as viewed from the top radiates predominately a left circular wave. The far field radiation pattern is determined by the apex angle of the cone and the pitch angle of the conductors. More details may be obtained from other sources [Rumsey, 1966; Dyson, 1965; Yeh and Mei, 1967, 1968].

In actual practice the use of conducting sheets is very difficult because of cost and wind resistance for large antennas. A good approximation to a conducting sheet can be made by using three wires, one at the location of each edge of the conductor and one in the center. Thus the elements in this array used six coaxially wound spiral wires, three connected to each side of the transmission line.

Each element in the array was phased by electrically rotating it in 45° increments. Antenna rotation was a practical phasing scheme in this array because the polarization remained nearly circular in all directions observed. The conical spiral antennas have this property between the half-power points of their radiation patterns ($\pm 45^\circ$). Antenna rotation was accomplished by winding the spirals with eight instead of six wires and a diode switch was devised to select six of the wires at any given time. With the simplicity of this phasing scheme comes the disadvantage of not having continuous rotation. The phase error of any element can be as much as 22.5° due to incremental phasing. However, these phase errors caused only rather minor sidelobes (Erickson and Fisher, 1974).

Although the antenna was designed to operate only to zenith distances of 45°, it was found in practice to operate quite well to considerably larger angles. In fact, several objects were well-observed only 15° above the southern horizon.

ELEMENT GROUPING AND PHASING SCHEME

The phasing within each bank is accomplished by rotating each element, so there is no real time delay added to the signals from individual elements. All time delays are added to the 48 signal paths in the central building.

The use of simple phasing as opposed to delays in the 15-element banks limits the size of banks due to coherence loss with wide receiver bandwidths. Each bank was approximately 100 meters in length. This resulted in a coherence loss of 9% with a bandwidth of 3 MHz at a zenith distance of 45°. The loss was normally much less with smaller bandwidths and zenith distances.

TP IMPEDANCE CHARACTERISTICS

Because the conical spiral elements in this array incorporated several features which have not been tried before, it was imperative that impedance and radiation characteristics be investigated before building 720 units. For practical reasons the antenna impedance could not be measured directly. There was a length of cable, a transformer, and the phase switch between the impedance bridge and the antenna terminals. Since we were interested in the operation of the total system, the standing wave ratio (VSWR) and impedance measured through these components are perfectly valid provided the power loss in the individual components is not more than about 20%.

Significant stray reactances in the feed system arise due

to the physical layout of the diode switch inside the central support pipe. These reactances were measured and compensated with small inductors incorporated in the switch. The combination of stray and lumped reactances forms a nearly symmetrical low pass filter with a cutoff frequency of about 250 MHz in series with each antenna wire. Impedance measurements were made at the base of the TP and corrected for delay feeder cable. The maximum VSWR was 1.4:1, which corresponds to a reflected power loss of 4%. Ohmic losses in the transformer and switch were less than 1 db (20%) and the loss in the feeder cable was 0.4 db (8%) at 110 MHz. The characteristic impedance of the antenna was close to 189Ω, the theoretical value for a self-conjugate antenna.

The eight wires were wound around a support system that consists of eight parallel filament, dacron ropes. The ropes were protected by polyethylene jackets. The N-S arm of the array is shown in Figure 3.

ELECTRONICS SYSTEM

A separate receiver channel was attached to the output of each of the 48 banks. Each channel employed an up conversion from the frequency being observed to 170 MHz. This conversion places all image frequencies well above the frequency range of observation. After some amplification, the signals were converted to 10 MHz where the principle amplification occurred. Four IF bandwidths, ranging from 3 to 0.15 MHz, were selectable. A diagram of these channels is shown in Figure 4.

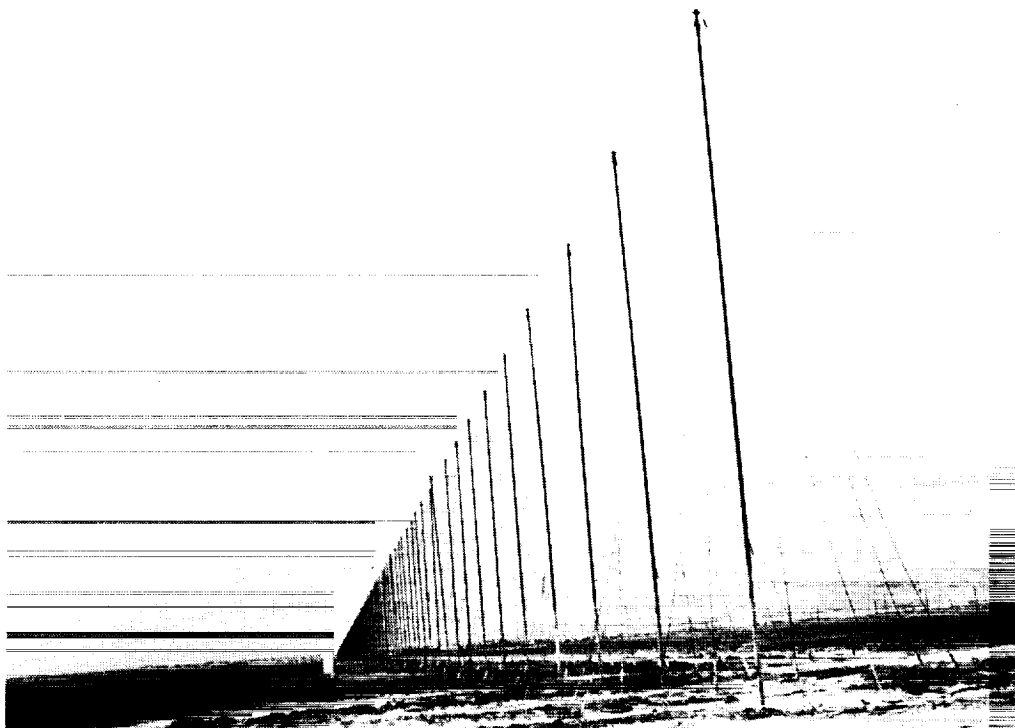


Figure 3. A photograph of the N-S arm of the array.

DATA PROCESSING

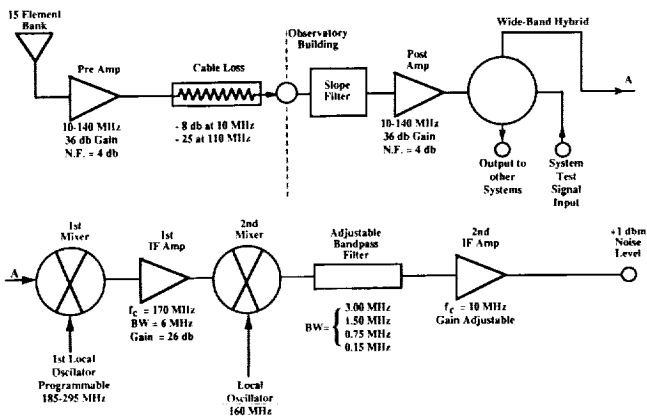


Figure 4. Block diagram of one of the 48 channels in which signals from the 15-element banks were processed.

The 10 MHz output of each receiver channel was sampled at a frequency of 12 MHz, digitally delayed, and then cross-correlated. The correlator outputs from the 512 simultaneous interferometers were preintegrated for periods from 10 millisecond to 10 sec — periods short enough that the phase rotation for a source moving at a sidereal rate is negligible on any of the interferometer baselines — and after each preintegration period, the digital data were written on magnetic tape. Later, an off-line processor was used to remove the phase rotation and to integrate the signals for periods of up to 5 minutes. A Fourier transform then produced a map of the area of sky under observation. These maps may be averaged to effectively integrate the signals for periods of hours. A detailed description of the electronics system is to be found in von Arx, Cafilisch, and Erickson (1978). The specifications of the system are summarized in Table 1.

Table 1. TPT Specifications

PARAMETER	VALUE
Frequency range	10-125 MHz
Instantaneous bandwidths	0.15-3 MHz
Total collecting area	250
Resolution	
20 MHz	17'
110 MHz	3'
Steering and frequency changing time	1 millisecond
Sky coverage	≈ 45° zenith distance
Sensitivity (and confusion limit)	1 Jy at all frequencies
Polarization	left circular

The TPT was different from most other synthesis-type radio telescopes in that all the Fourier components from a minimum spacing of about one wavelength to the maximum aperture of the systems were available simultaneously. Also, the telescope operated in a frequency range where terrestrial interference is very common. It appeared to be necessary to develop procedures to reject low level interference after formation of the maps, as well as to reject obvious interference in the visibility-plane data. Therefore, rather than averaging the visibility-plane data for hours, then gridding them and transforming them, we transformed the data frequently and averaged the selected maps [Erickson, Mahoney, and Erb, 1982]. Since maps were formed frequently, this processing scheme is also more appropriate for observation of rapidly varying solar emission regions.

The length of time over which we could integrate the visibility-plane data before Fourier transformation was limited to ≈ 5 minutes; longer integration would begin to smear the visibility data because of the rotation and foreshortening of the arrays caused by Earth rotation. The T-shaped antenna provides data automatically in a 32×32 grid; we do not project them onto the (u-v)-plan or regrid them before transformation. In practice, a transformation was performed and a new integration was begun whenever the phase gradients across the banks of elements were updated to follow the source under observation. Maps were generally produced at intervals of 1 second to 5 minutes. Use of longer intervals facilitates the processing speed but requires that more data be discarded when interference occurs.

OPERATION

The system operated very well. All of the design specifications listed in Table 1 were met or exceeded in practice. Only one area of problems turned out to be somewhat more troublesome than anticipated. We encountered nearly constant, low-level interference which appeared to come from a variety of sources. Much of this interference was apparently man-made radio noise reflected at a glancing incidence by the ionosphere or diffracted over the mountains surrounding the telescope site. Interference from the extremely strong natural sources, Cas-A and Cyg-A, also prevented sensitive observations in their vicinity, i.e. within about 10° of their positions. Solar radio bursts could interfere with daytime observations. Strong interference was easily recognized and rejected from the raw data. However, much effort was expended in developing sophisticated algorithms to recognize and excise low-level interference that could not be found until the signals from the banks were cross-correlated and time integrated. In practice this meant that we were unable to reach the confusion limit of the system as quickly as we anticipated in its design. It should have been possible to reach the confusion limit (≈ 1 Jy) with only a few minutes of integration; because it was

necessary to excise much of the data and to average over interfering sources, about 30 minutes integration was required to reach the confusion limit.

The confusion limit depended upon the direction of observation. In simple regions near the Galactic poles we were able to reliably observe sources down to a flux density of 0.5 to 0.7 Jy, in complex regions along the Galactic plane we could only work down to about 2 Jy. In any event, the system was 10 to 50 times more sensitive than any other existing or planned telescope in this frequency range. For a variety of reasons (Erickson and Fisher, 1974), the confusion and sensitivity limits of the system were fairly independent of frequency.

The system was used as a multifrequency radioheliograph for solar studies and as a synthesis telescope for sidereal studies. As a radioheliograph it was used to determine the radio signatures of coronal mass ejection events, to show that Type III emitting electron streams propagated in dense coronal streamers, to discover meter-decameter microbursts, to determine the three-dimensional structure of coronal streamers, to measure coronal electron densities on a routine basis, and to determine the spectrum and brightness distribution of the quiet Sun. In the field of sidereal astronomy Clark Lake observations lead to the discovery of the first millisecond pulsar and to the discovery of the millisecond pulsar in M28, many supernova remnants were mapped, HII absorption was studied to determine the synchrotron emissivity of the Galaxy, a steep-spectrum radio lobe near the Galactic center was discovered and the Galactic plane was mapped. About one-third of the sky was surveyed with unprecedented sensitivity and resolution before we were forced to discontinue operation. These survey data are now being analyzed.

REFERENCES

- Christiansen, W.N. and J.A. Hogbom, 1969, *Radiotelescopes*, pp.155-156, Cambridge University Press, London.
- Dyson, J.D., 1965, "The characteristics and design of the conical log-spiral antenna," *IEEE Trans. Antennas Propagat.*, AP-13(4), 488-499.
- Erickson, W.C. and J.R. Fisher, 1974, "A new wideband, fully steerable, decametric array at Clark Lake," *Radio Science*, 9, 387-401.
- Erickson, W.C., M.J. Mahoney and K. Erb, 1982, "The Clark Lake Teepee-Tee Telescope," *Astrophys J. Suppl.*, 50, 403.
- Rumsey, V.H., 1966, *Frequency Independent Antennas*, pp.39-54, Academic Press, New York.
- von Arx, B., M. Caflisch and W.C. Erickson, 1978, "The TPT Electronics System," U. of MD Technical Note AP 78-027.
- Yeh, Y.S. and K.K. Mei, 1967, "Theory of conical equiangular-spiral antennas, 1, Numerical technique," *IEEE Trans. Antennas Propagat.*, AP-14(5), 634-639.
- Yeh, Y.S. and K.K. Mei, 1967, "Theory of conical equiangular-spiral antennas, 2, Current distributions and input impedances," *IEEE Trans. Antennas Propagat.*, AP-16(1), 14-21.



THE BOULDER-AMES DECAMETER WAVELENGTH VLBI EXPERIMENT

John P. Basart
Department of Electrical and Computer Engineering
Iowa State University
Ames, Iowa 50011

ABSTRACT

This paper reviews the VLBI experiments at 26.3 MHz conducted in the early 1970s between Boulder and Haswell, Colorado, and between Boulder, and Ames, Iowa. The longest baseline was 83,000 wavelength. While it was possible to get fringes on this baseline, the reliability of the data was very poor because of the extreme amount of ionospheric-induced phase and amplitude fluctuations. Clearly, in order to obtain reliable data, very-long-baseline interferometers operating at frequencies of 26 MHz and lower must be placed above the ionosphere.

INTRODUCTION

The objective of the VLBI experiments at a decameter wavelength was to determine source structure in order to identify radio sources of small angular extent to be used in future interplanetary scintillation experiments at low frequencies. The observing source list consisted of point-like sources, or sources with point-like components, with measured or extrapolated flux densities greater than 20 Janskys at 26 MHz. Additionally, their declinations were between -2° and 68° . Sources with right ascensions in the range 8^h to 14^h were omitted because of competing solar noise and interplanetary scintillation effects. The observing list consisted mostly of extragalactic sources in the 3c catalog plus a few supernova remnants, pulsars, the sun, Jupiter, and Saturn (Shawhan et al., 1973). Sources with similar right ascensions, but quite different declinations, were divided into two observing schedules to accommodate constraints on manually phasing the antennas. Each schedule consisted of an 18-hour program starting at about 6:00 p.m. local time and stopping at noon with the last runs on the Sun. Each day 3C48 and 3C144 were observed as calibrators.

INTERFEROMETER DESCRIPTION

Two different interferometer baselines were used in three series of experiments. In November 1970 and July 1971, telescopes in Boulder and Haswell, Colorado, were used. The baseline length was $22,000\lambda$ at a position angle of 135° . The fringe width was 9 arc seconds and the 3σ detection limit was about 20 Jy. In August 1971 the Boulder and Ames, Iowa, telescopes were used. This interferometer had a baseline of $83,000\lambda$ at a position of 76° . The fringe width was 2.5 arc

seconds with about the same detection limit as the Boulder-Haswell baseline.

The antennas in all three telescopes consisted of 160 pairs of crossed full-wave dipoles in rectangular arrays. However, the Ames configuration was different than that of the other two antennas. The Ames rectangular array geometry was 10 dipole pairs east-west by 16 dipole pairs north-south. The Boulder and Haswell arrays were 20 dipole pairs east-west by 8 dipole pairs north-south. The reason for the difference in geometry was that the Boulder array was phased along its local meridian while the Ames array was phased to the west. Moving the array beam off center broadened it, hence, the shorter east-west array dimension made the Ames beam more similar to the Boulder beam.

Crossed dipoles were used in the array to avoid Faraday fading problems in the ionosphere. The orthogonal antennas were connected together to be receptive to left-elliptical polarization. (The choice of LEP was arbitrary.) Most of the observations were made in a southerly direction so we oriented the dipoles in a way to keep the signal level high. The crossed dipole pairs were aligned in the northeast-southwest and southeast-northwest directions rather than north-south and east-west. This eliminated a possible low-amplitude response by observing "off the end" of a north-south dipole.

The interconnections of antenna elements in a large array are always a problem. The method used here was to connect all antennas in one E-W row to one transmission line. This was repeated for each E-W row. There were two complete and identical configurations for each polarization of the crossed dipoles so only one polarization will be explained. In the Ames array, there were 16 rows of E-W transmission lines for each dipole polarization. Ten dipoles of the same polarization were connected to each E-W transmission line. The Colorado arrays had 8 rows for each polarization with 20 dipoles per row. There was no impedance matching of each antenna to its transmission line. The input impedance of full-wave-length dipoles is relatively high compared to the transmission line. Hence, the antenna-to-line coupling is low. This reduces the amount of signal transferred to the line, which is a negative factor, but it also loads the line very little, which is a strong positive factor. We can get by with small coupling between the antenna and the transmission line at these low frequencies because the signal level is high.

The interconnection of the E-W rows was done with a branch (corporate) feed. The first step in the interconnection

PAGE 18 INTENTIONALLY BLANK

was to connect each two adjacent E-W rows together with an impedance-matched network. This resulted in eight connected pairs. Then, each of these two adjacent pairs were connected by an impedance-matched network. This pairs-of-pairs connecting scheme was repeated until there was just one transmission line containing the output of the entire array. The final transmission lines from each polarization were connected together with an extra quarter-wavelength section of cable to form a left-elliptically polarized signal which then went to the receiver.

During the observing runs, all antennas were operated in transit mode by manually phasing the branch feed networks in the north-south direction before each observation and then letting the source drift through the beams. The phased position of the beams was determined by the equations.

$$\sin \xi = \cos \delta \sin H$$

$$\sin \eta = \sin \phi \cos \delta \cos H - \cos \phi \sin \delta$$

where ξ is the angle from the zenith to the west, η is the angle from the zenith to the south, and ϕ , δ , and H are the latitude, declination, and hour angle, respectively.

The receivers were conventional radio-telescope type superheterodyne receivers with extra radio-frequency filtering to reduce out-of-band interference. The bandwidths were 500 kHz and noise figures were approximately 2 dB. The recording terminals used at each site were standard Mark I terminals (Moran, 1976) borrowed from the National Radio Astronomy Observatory.

DATA ANALYSIS

As much as possible, the data analysis proceeded along the standard path for VLBI analysis in that era. Additional difficulties were encountered because of the very high phase noise, and the uncertainty about the detection of fringes. The signal-to-noise ratio of the fringes was always low. The often desirable 5σ threshold criterion was reduced to 3σ . To increase the reliability of the detection, three more criteria were used. One criterion was to put $+5$, and then -5 , microseconds delay offsets about the presumably correct delay and let the correlation program search for fringes once more for each offset. If a detection had been originally hypothesized and the residual delay after these two additional offset searches was consistent with the original residual delay, the criterion was satisfied. The second criterion was to compare two or more detections from different days. The result of this test was not always positive because the ionosphere varied so much from day to day. However, if the day-to-day results were consistent, the test was considered to be satisfied. The third criterion was to have a residual fringe rate near zero. Since the source positions were well known by high-frequency measurements, the fringe frequency was

predictable. If the residual fringe frequency was near zero, this criterion was satisfied.

The resulting correlated fluxes for any particular source were scattered from day to day because of variations in the ionosphere over the two antenna locations. All multiply observed sources for all observing runs were placed on one calibration grid of normalized flux density versus time. Each flux density was normalized by the mean observed flux density for that particular source. This plot showed systematic changes in flux with time which were contributed to ionospheric variations. Correction factors were obtained from the systematic changes in the grid of sources and applied to the individual measurements. Rates of change of trends in the observed fringe amplitude due to the ionosphere ranged from zero up to 16% per day. If amplitude changes were large and abrupt, the data were likely not to be used at all because of extreme uncertainties in how to correct them (or because they may not have been real). After applying corrections to the grid of sources, the rms scatter about the normalized means was 8%.

Flux calibration was difficult because no source initially appeared to be unequivocally unresolved. The initial procedure was to estimate the apparent observed size of the Crab Nebula pulsar using the VLBI measurement of Mutel et al. (1974). To estimate the scattered size in the interplanetary region, we used the formula of Erickson (1964)

$$\theta_s = 0.649 P^{-2} \pm \lambda^{-2} \text{ arc second}$$

where P is the closest distance the radio wave passes by the Sun in astronomical units and λ is the wavelength in meters (11.4 in our case). For an average solar elongation angle of 65° , $\theta_s = 1.77$ arc sec. This was combined in quadrature with the interstellar scattering size of 1.30 arc sec. (Mutel et al., 1974) to give an estimated apparent size of the Crab pulsar of 2.20 arc secs. Assuming a total flux density of 800 Jy for the Crab pulsar at 26.3 MHz gave a visibility of 0.064 for a Gaussian model. After adjusting the Boulder-Ames data to comply with this visibility, a check was made with 3C48. The estimated observed size of 3C48 using the Boulder-Ames data was 0.60 arc sec. (Gaussian model). With this size, the predicted Boulder-Haswell visibility was 0.98 which was in reasonable agreement with the measured visibility as calibrated by the Crab pulsar. With consideration of the data on the Crab pulsar and 3C48, plus some consistency checks with 3C43, we set the flux calibration using the apparent size of 3C48 as 0.60 arc sec. with a circular Gaussian brightness distribution. The total flux density was set equal to 37 Jy as given by Viner and Erickson (1975).

RESULTS

As an illustration of the results, Tables 1, 2, and 3 are presented. These data should not be taken as definitive. The

Table 1. Sources Detected on Three Experiments

Source	Assumed 26 MHz Total Flux, Janskys	BH November 1970			BH August 1971			BA August 1971		
		Vis	Solar Elongation Angle,°	No. of Obs.	Vis	Solar Elongation Angle,°	No. of Obs.	Vis	Solar Elongation Angle,°	No. of Obs.
3C48	37	0.98	152	2	0.98	107	4	0.81	112	3
3C66	149	0.30	152	2	0.16	88	2	0.12	99	2
3C123	828	0.048	160	2	0.027	64	2	0.030	78	2
3C144 (compact component)	800	0.86	149	7	U.D.	52	2	0.064	65	8
3C456	92	0.76	119	1	0.79	141	1	0.40	152	2
3C459	90	0.52	118	2	0.69	144	1	0.47	158	3

U.D. means Unreliable Data.

Table 2. Sources Detected on B-A and One B-H Experiment

Source	Assumed 26 MHz Total Flux, Janskys	BH				BA August 1971		
		Vis	Solar Elongation Angle,°	No. of Obs.	Date	Vis	Solar Elongation Angle,°	No. of Obs.
4C13.01	28*	0.88	123	1	August 71	1.05	137	1
3C9	91	0.77	125	2	August 71	0.33	137	3
3C71	73	0.72	159	1	November 70	0.65	122	3
3C196	218	0.52	115	1	November 70	0.080	43	3
3C295	72	No Det	67	1	August 71	0.25	63	1
3C345	34	No Det	95	3	August 71	0.73	89	3
1645+17		U.D.**	106	2	August 71	54.3 Jy	95	3

*Determined by extrapolation.

**U.D. means Unreliable Data.

extreme noisiness caused by ionosphere permeated the analysis so thoroughly that it was impossible to calculate reliable error bars. Most of the total flux densities were from Viner and Erickson (1975). The uncertainties in these fluxes range from 5% to 18%. Errors in the visibilities contain the errors in the total flux densities plus, say, 25% more error due to ionospheric variations in visibility measurements.

Table 1 contains sources detected on all three experimental runs between Boulder and Haswell, and Boulder and Ames. Table 2 contains sources detected on the Boulder-Ames baseline and one Boulder-Haswell run. Finally, Table 3 contains sources detected on the Boulder-Haswell baseline only. Dashes in this table indicate that these sources were not scheduled for observation. The consistency of the results is remarkably good considering the noisiness of the data. For the Boulder-Haswell 1971 results, the average rms variation of multiple observations of the same source was 3% and for BA it was 8%. A comparison of the eight sources in common on the two Boulder-Haswell runs shows deviations varying from 0% to 47% between the two epochs.

Interpretation of the data was very limited in the early 1970s. At the most we had two points in the uv plane (other than the origin) from our data. High-resolution mapping at centimetric wavelengths was only beginning so we had little knowledge of the source structure at any wavelength. We used available information from scintillations, occultations, and interferometry at all radio wavelengths. We essentially were constrained to testing the agreement between our data and the published parameters of single and double-component sources. The agreement was tested by using our uv values in models reported in the literature and then comparing the predicted visibility with our measured visibility.

DISCUSSION

We detected 36 out of a possible 49 radio sources on one or both of the baselines. From a simple comparison of our measured visibilities with the predicted visibilities using models determined from higher-frequency data, we found that in a large majority of cases, for which comparisons could be

Table 3. Boulder-Haswell Sources

Source	Assumed 26 MHz Total Flux, Janskys	November 1970			August 1971		
		Vis	Solar Elongation Angle, °	No. of Obs.	Vis	Solar Elongation Angle, °	No. of Obs.
3C2	56	0.80	160	2		U.D.**	
3C16	65	0.26	140	1	0.19	124	1
3C23	56	0.86	144	1	0.85	117	2
3C33	222				0.19	118	3
3C43	46	0.70	153	2	0.70	107	2
3C55	88	0.26	158	1			
W3					31 Jy	81	2
3C147	39	0.64	138	2	—	—	—
3C153	42	0.63	135	2	—	—	—
3C154	119	0.28	140	2	—	—	—
3C157	132	0.20	124	1	—	—	—
3C181	57	0.42	121	1	—	—	—
3C186	54	0.70	120	1	—	—	—
3C190	64	1.22	113	2	—	—	—
3C191	46	0.97	112	1	—	—	—
3C196.1	167	0.62	105	2	—	—	—
3C208	83	0.34	101	2	—	—	—
3C336	64	—	—	—	0.42	101	1
3C380	271	—	—	—	0.076	105	1
PSR1919		—	—	—	35 Jy	133	1
3C409	381	—	—	—	0.12	138	2
3C432	59	—	—	—	0.61	147	1
3C446	55	—	—	—	1.0	141	1

A dash means no scheduled observation.

**U.D. means Unreliable Data.

made, our data were consistent with those models. Wilkinson et al. (1974) had discussed the consistency of some sizes over a frequency range from 408 to 2695 or 5000 MHz. Our results suggested that this consistency extended down to 26 MHz, an overall factor of 100 or more in frequency. Within the accuracy of our consistency checks, we found no straight-spectrum source with a component that was optically thick at 26 MHz.

Our experiments showed that it is possible to find correlations in 26 MHz data collected over an 83,000λ baseline. But considering the overall effort of erecting and maintaining the telescopes, collecting the data, and calibrating and interpreting the data, very little hard information came from a large amount of work. The cause of the minimal amount of information deduced from the data was the ionospheric variation. At times, the ionosphere caused the signals to completely disappear. At all other times, the signals were severely disturbed in amplitude and phase. Another contributing factor to significant loss of data was lightning. Lightning located many miles away disrupted the correlations. During the summer season, lightning often occurs, with or without an accompanying storm. It is very clear, that to make regular quantitative high-resolution observations at frequencies of 26 MHz and lower, the antennas must be above the ionosphere.

ACKNOWLEDGMENTS

Other principal investigators in this project were Stanley Shawhan, Thomas Clark, and William Erickson.

REFERENCES

- Erickson W.C., 1964, *Ap.J.*, 139, 1290.
- Moran, J.M., 1976, in *Methods of Experimental Physics*, Meeks, M.L., ed., 12, Part C, 174.
- Mutel, R.L., Broderick, J.J., Carr, T.D., Lynch, M., Desch, M., Warnock, W.W., and Klemperer, W.K., 1974, *Ap. J.*, 193, 279.
- Shawhan, S.D., Clark, T.A., Cronyn, W.M., and Basart, J.P., 1973, *Nature, Physical Science*, 243, 65.
- Viner, M.R. and Erickson, W.C., 1975, *Astron. J.*, 80, 931.
- Wilkinson, P.M., 1972, *M.N.R.A.S.*, 160, 305.

THE RADIO ASTRONOMY EXPLORER PROGRAM VALUABLE LESSONS FOR FUTURE LOW FREQUENCY RADIO ASTRONOMY FROM SPACE

Michael L. Kaiser
Laboratory for Extraterrestrial Physics
Goddard Space Flight Center
Greenbelt, MD 20771

The Radio Astronomy Explorer (RAE) program of the late 1960s and early 1970s represents mankind's first attempt to perform low frequency radio astronomy measurements from above the Earth's ionosphere with a dedicated set of instruments. A review of the results of this program have been given recently by Kaiser [in *Radio Astronomy From Space*, NRAO, 1986], so only those lessons learned that have direct application to a possible lunar low frequency radio observatory will be presented here.

Figure 1 is a drawing of RAE-2, which was placed in circular orbit around the Moon in 1972. RAE-1, launched into a 6000 km altitude orbit around the Earth, was very similar. The spacecraft was gravity gradient stabilized and an active libration damper was used to try to remove excess yaw due to deviations from a perfectly spherical orbit. Both spacecraft were equipped with two sets of 229-meter long Vee configuration antennas oppositely oriented, one set pointing radially upward and one set pointed toward the center of gravity, namely, the Earth or the Moon. A third antenna system, a short dipole, bisected the two Vees.

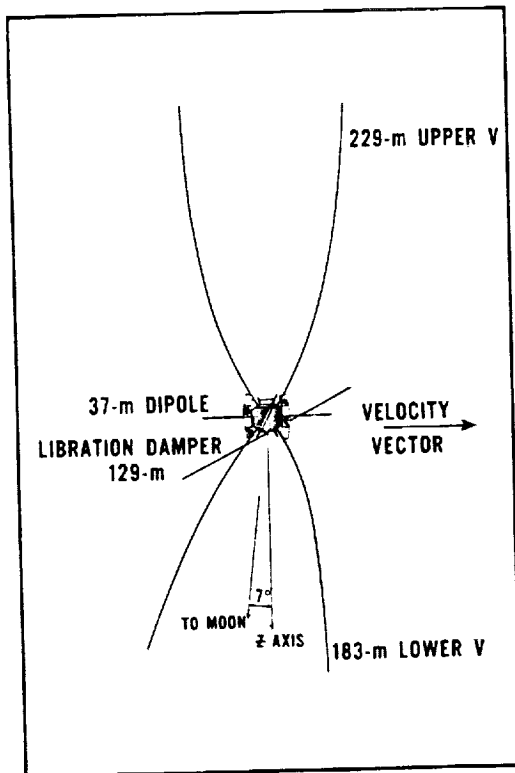


Figure 1.

Connected to these antenna systems were two basic types of radio receivers, Ryle-Vonberg and total power (burst), both operating in the 25 kHz to 13 MHz range. The basic difference between these two types of receivers from a practical point of view was the way in which their preamplifier sections operated. The total power receivers were driven by a wide bandwidth preamplifier section covering essentially the entire operating frequency range, and with significant gain even outside of the nominal range. The Ryle-Vonberg receivers, on the other hand, were made up of relatively narrow band pre-amp sections, one for each operating frequency. A lesson learned very early in the life of the RAE program was that the receivers using wide bandwidth preamplifiers, although easier and cheaper to build, suffered severely from distortion due to strong signals anywhere in their passband, even at frequencies not directly sampled by the receiver. More on this will be mentioned later in connection with the terrestrial emissions observed by the RAE spacecraft. The resulting power pattern of the receiving system was not good by terrestrial standards. At frequencies of a few MHz, typical beam widths were of the order of a steradian with significant side and back lobes.

The major scientific achievements of the two RAE spacecraft fell into several categories including solar physics, planetary non-thermal emissions concentrating primarily on the Earth's auroral kilometric emission (AKR), in situ plasma physics, and cosmic background mapping and spectra. In fact, the study of solar type II and III radio bursts and the study of AKR were extremely successful, accounting for more than half of all the ~60 scientific papers published from the RAE program. However, the galactic background studies were, at best, only marginally successful due to a combination of the poor angular resolution and strong interference from AKR and other signals of terrestrial origin (e.g., thunderstorm sferics and manmade).

The effects of the terrestrial noise spectrum were alleviated for RAE-2 because of its distance ($60 R_E$) from the source. However, even this large attenuation was not enough as can be seen in Figure 2 where four months of data from RAE-2 in lunar orbit are shown. At the two lower channels shown, 40 kHz and 290 kHz, AKR dominates the emission spectrum, at times reaching saturation levels and frequently causing receiver intermodulation products throughout the entire operating frequency range stemming from the wide band pre-amp mentioned above. The AKR maximizes at full Moon, which corresponds to RAE being

above the midnight sector of the Earth, directly in the main beam of AKR. Even at frequencies of 1.27 and 3.93 MHz, well above the natural band of AKR (50 kHz to 750 kHz), terrestrial effects are important, especially over the night hemisphere. This higher frequency noise is a combination of thunderstorm sferics from the whole "visible" hemisphere, manmade broadcast stations and intermodulation from the AKR.

Perhaps an even better appreciation of the dominance of AKR can be obtained from Figure 3, again observed by RAE-2 in lunar orbit. In the top panel is a dynamic spectra showing received power as a function of frequency and time. The black band in the middle (near 400 kHz) is AKR and the dark strips near the top are other terrestrial signals. Just before 15:00, the AKR and terrestrial signals are abruptly cut off and do not reappear until about 15:30. This interval

corresponded to the time when RAE-2 was above the back side of the Moon so that the Earth was occulted by the lunar disk. In the bottom panels are individual frequency channels where one can see that this occultation effect is extremely dramatic. This single figure represents probably the strongest reason for placing a lunar low frequency observatory on the far, well away from the terminator.

In summary, the RAE program gave us two very valuable lessons for use in any future low frequency observatories. First, do not use wide bandwidth preamplifiers or receivers. Specifically, avoid the AKR frequency range. Second, avoid direct view of the Earth itself, because AKR and other terrestrial noise, all of which is many orders of magnitude above cosmic background, will greatly hinder observations of intrinsically weak radio sources.

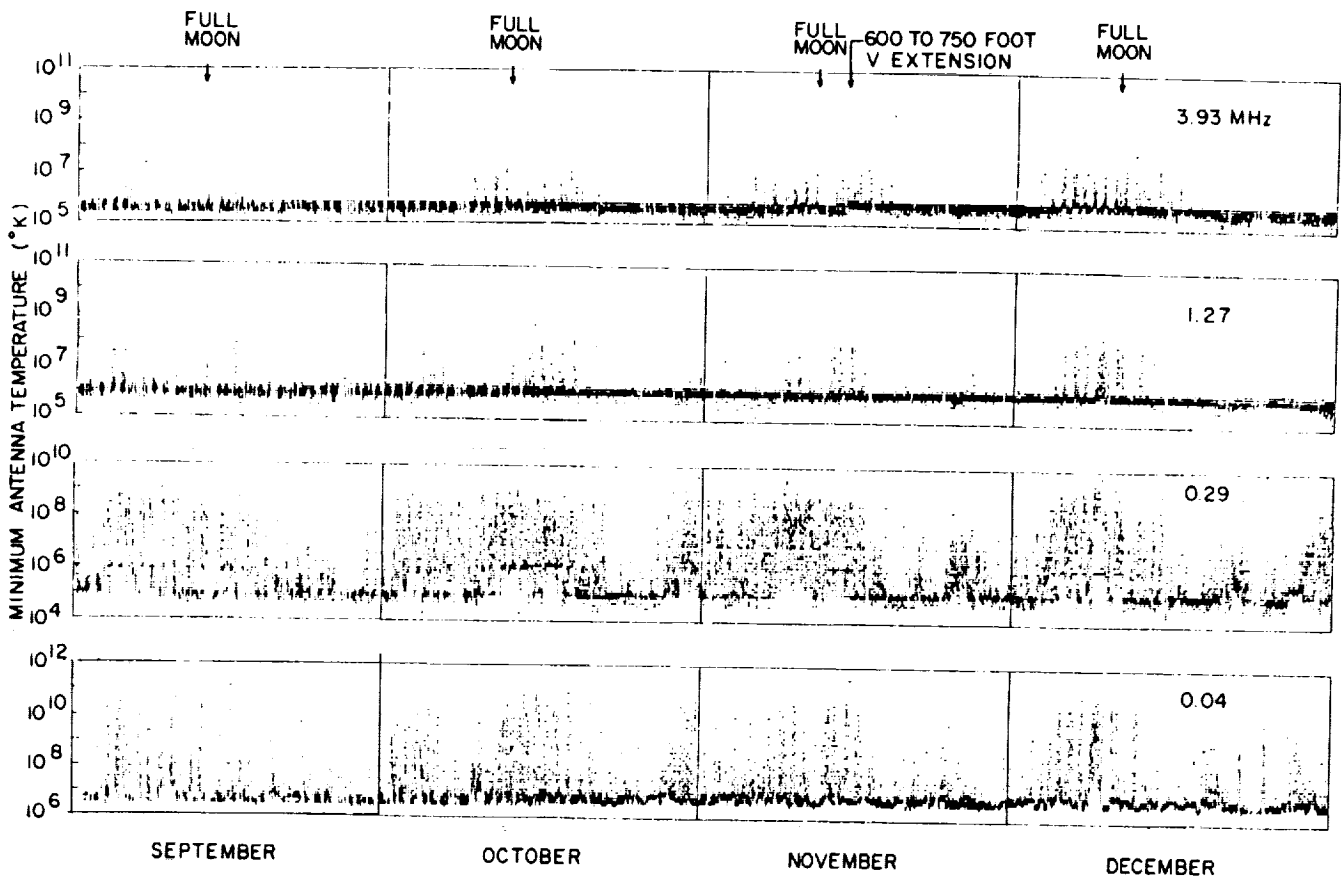


Figure 2.

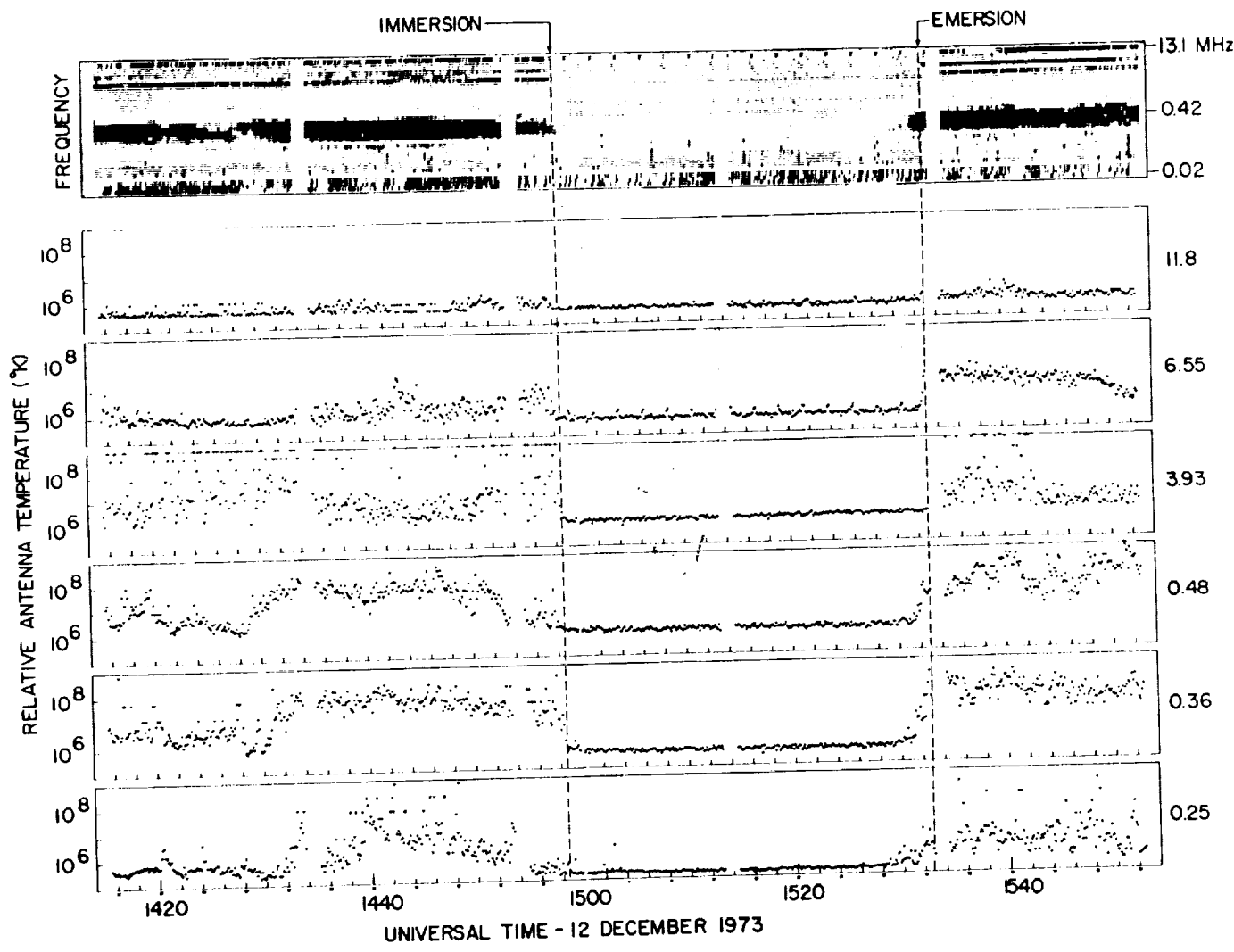
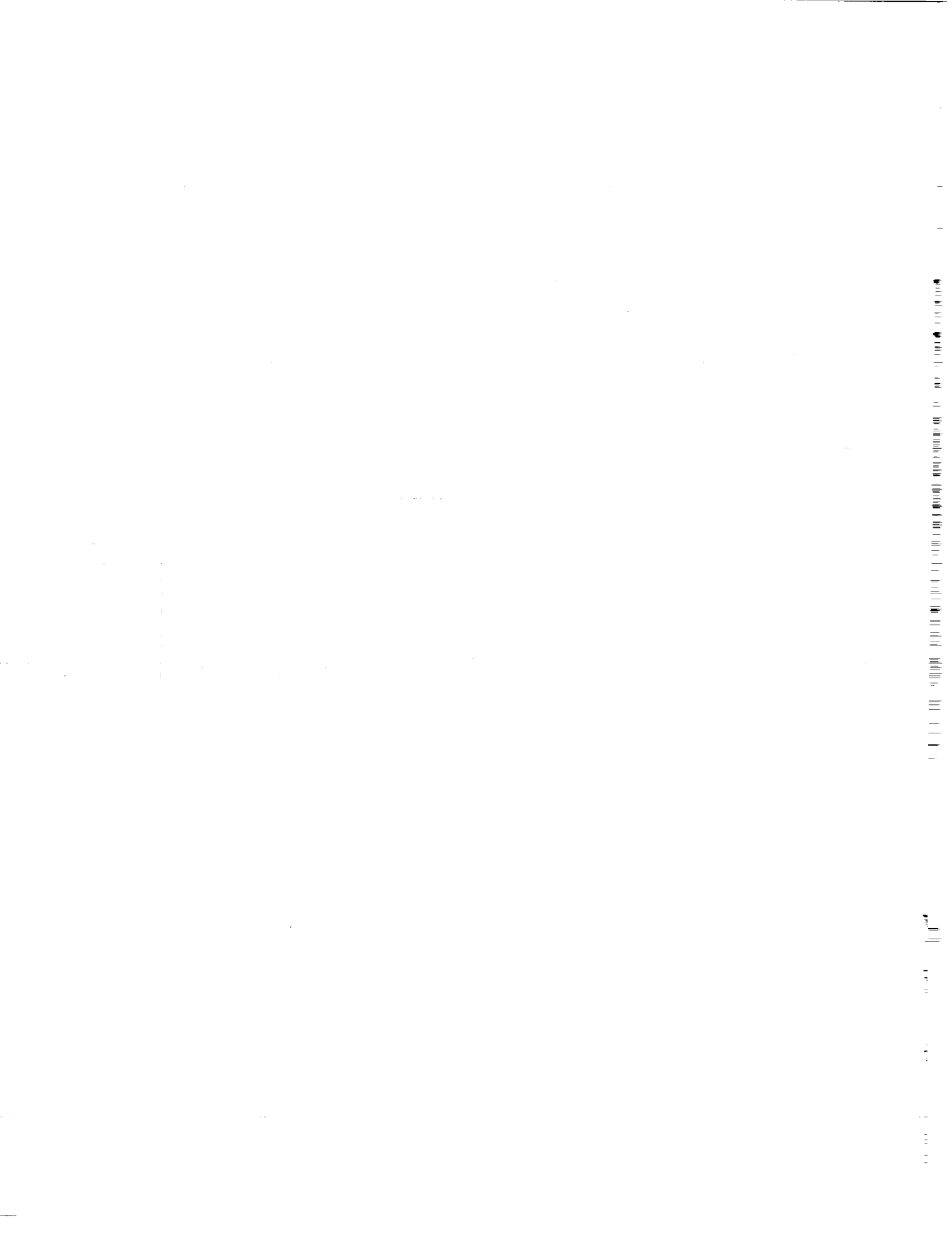


Figure 3.



THE 75 MHz VLA SYSTEM

W.C. Erickson¹
Department of Physics and Astronomy
University of Maryland
College Park, MD 20742

and

R.A. Perley
National Radio Astronomy Observatory
Very Large Array
Socorro, NM 87801

INTRODUCTION

The diffraction-limited resolution of radio astronomical instruments has encouraged the development of interferometric techniques. The technique known as 'Earth-rotation synthesis' has been utilized by numerous instruments (notably the VLA), and has proved immensely successful in providing full-field mapping of celestial radio emission with resolutions orders of magnitude better than that provided by the largest single antenna.

However, the use of Earth-rotation synthesis has been almost wholly limited to centimeter wavelengths. At longer wavelengths, ($\gg 1$ meter), the only instruments which utilize the technique (the University of Maryland's TPT, and Cambridge's 151 MHz array) operate over limited (5 km) baselines. There are two reasons why high resolution, low frequency interferometry has remained undeveloped. First, the very long baselines required to obtain useful resolution imply a prohibitive cost in transmission of the data to a correlator. Second, and more importantly, the disruptive effects of the ionosphere make calibration of the data very difficult on baselines longer than 5 km. Recent hardware and software developments now enable serious consideration of a high resolution, low frequency instrument. The completed VLA waveguide system contains ample unused bandwidth for transportation of low-frequency astronomical signals over useful baselines, and new software techniques developed to improve the dynamic range of VLA data should enable calibration of low-frequency data taken from long baselines. These considerations lead to the development of a meter-wavelength synthesis instrument at the VLA.

THE PROPOSED SYSTEM

In 1984 we proposed a low-frequency synthesis array that would utilize facilities already existing at the VLA site and

would be operated in conjunction with the VLA [Perley and Erickson, 1984]. A useful array could be constructed for about one million dollars, and would represent an excellent investment with regard to the science that would be returned. The array design and construction present no technological problems. We believe that data calibration can be accomplished using recently developed algorithms combined with a priori information on the sources in the field of view obtained at higher frequencies.

In examining various design options, we adopted the following constraints:

(1) Operation of the low-frequency array should not displace or inconvenience the current VLA.

(2) Maximum use should be made of the currently existing hardware and software at the VLA site, without violating the first constraint.

(3) The total cost should be kept within reasonable expectations of what the NRAO RE (Research Equipment) budget can provide.

The proposed instrument would be a powerful tool for work on a broad range of astrophysical problems. The design beamwidth of $10''-20''$ at 75 MHz will resolve thousands of objects whose structures have never been studied at frequencies below 100 MHz.

Since the ionosphere is a turbulent and highly refractive medium, it strongly affects the propagation of low-frequency radio waves. We have considered the expected effects on the data and have outlined a method of calibration. In addition, the problem of non-coplanar baselines was considered. These topics were discussed in some detail by Perley and Erickson [1984]. We showed that a general solution to the calibration problem should exist, based upon the fact that the system noise is entirely determined by galactic emission in the field of view and not by the receivers. We showed that for maps larger than 1° in extent, there should exist sufficient flux density from background sources to allow calibration of the data,

¹Present address: Department of Physics, University of Tasmania, GPO Box 252C, Hobart, Tasmania 7001, Australia.

assuming that an appropriate initial model of the stronger sources is provided.

We emphasized that these conclusions were based on certain ideas concerning the typical behavior of the ionosphere. Tests are needed to confirm that the proposed method of calibration is actually practical. These tests can be made with elements of the 327 MHz system in the 'A' configuration or with the existing 25-meter VLA dishes instrumented for 75 MHz. The tests would be completed before any major expenditures are scheduled to occur. If the calibration is as simple as we anticipate (for a reasonable fraction of the total observing time), only modest computing facilities will be required. We expect that the calibration will be simple when the ionosphere is quiet, and difficult or impossible when the ionosphere is disturbed. What we have not been able to estimate accurately is what fraction of the time each of these conditions are to be expected.

The proposed design can be summarized as follows:

1. Continuum capability at or near 75 MHz. Moderately wide-band antennas are recommended for frequency flexibility, both in order to avoid terrestrial interference and to allow bandwidth synthesis. Dual polarization is strongly preferred.
2. A maximum bandwidth of 4 MHz (probably limited by interference), with two narrower bandwidths available. Attention should be paid to bandpass shaping to minimize confusion from sources outside the field-of-view.
3. An array consisting of at least 27 banks of antennas which will be permanently located near 'A' array stations. In addition, we propose to place banks with those VLBA stations within 400 km of the VLA. The proposed array will operate only when the 'A' array stations are occupied by existing 25-meter antennas. The effective collecting area of each bank should be between 100 and 200 square meters. The banks should be equatorially mounted, and fully steerable. It is highly desirable to build more than 27 banks, since this will considerably reduce the severe aliasing problems that are expected.
4. Preamplifiers will be located at each bank so the signals can be conducted to the nearest VLA antenna with no significant loss in signal-to-noise. Further amplification plus frequency and bandwidth selection will be done at the VLA antenna. The signals will then be injected into the existing electronics for transmission to the control building.
5. At the control building, the signals will be extracted and recorded with a VLBA (or similar) recording system. These signals will then be played back into a special, dedicated correlator. A modest, dual-channel, narrow-bandwidth correlator is proposed. Multiple fields of view can be mapped by repeated passes of the data through the correlator.
6. Calibration and mapping will be done using currently existing self-calibration algorithms.
7. Presuming 27 banks with 2 MHz bandwidth and 8 hour integration with dual polarization, the expected rms noise at 75 MHz will be about 3 mJy, two orders of magnitude lower than any other system at this frequency.

This would provide an array which would operate when the current VLA is in the 'A' configuration—approximately 3 to 4 months per year. We estimate the cost of this system to be about one million dollars. A full-time array would cost approximately three times more.

AN ALTERNATIVE SYSTEM

After we made this proposal in 1984 it became obvious that, in spite of strong support from potential users, funding at the million dollar magnitude would not be available in the reasonably near future. We therefore considered a lower cost alternative that would take us at least part way towards our goal of the system outlined above. This alternative was to instrument the existing 25-meter VLA dishes at 75 MHz. A system was developed in which 75 MHz crossed dipoles (consisting of thin wires) are stretched between the feed support legs of the dishes. These dipoles, with the subreflector acting as a crude backplane, feed the dishes from their prime foci. With this crude feed system an aperture efficiency of about 20% and a collecting area of $\approx 100 \text{ m}^2$ per dish is achieved. This collecting area is marginal for calibration except when the ionosphere is quiet. However, the system should permit many of the investigations that were originally proposed. It does not satisfy constraint (1) as given above, i.e., use of this alternative 75 MHz system will require that the dishes be pointed at the object being observed and will thus strongly affect the simultaneous use of the VLA at other frequencies. Since many 75 MHz observations will be destroyed by ionospheric scintillations and will need to be repeated several times, this is not an efficient use of the VLA system.

The 75 MHz dipoles are in the shadow of the feed support legs and their presence does not affect the other VLA frequencies. Instrumentation at 75 MHz consists of only the dipoles and simple transistor preamplifiers; the preamplifier outputs are connected directly to an alternate input port on the 327 MHz modules. The principal problem with the system is caused by interference radiated by the digital equipment in the telescope. We have developed effective shielding for this interference.

Four VLA dishes are now instrumented at 75 MHz and operate satisfactorily. These have allowed us to demonstrate that strong, stable interference fringes can be obtained when the ionosphere is quiet. However, four elements do not yield enough baseline combinations for us to test mapping algorithms or to do useful science at this frequency. More dishes will be instrumented when resources permit. Once we have demonstrated that valid maps can be obtained and that useful scientific results can be produced with this alternative system, we hope to construct the full, stand-alone system that we originally proposed.

"A Proposal for a Large, Low Frequency Array Located at the VLA Site," R.A. Perley and W.C. Erickson, 1984, VLA Scientific Memorandum #146.

PART III — SCIENCE WITH A LUNAR VLFA

SCIENCE AT VERY LOW RADIO FREQUENCIES

N. Duric
University of New Mexico

ABSTRACT

The broad scientific goals of a lunar based Very Low Frequency Array are presented. The frequency range of 1 – 30 MHz is defined to be the operative VLF window. The low frequency end of this window is useful for studies of the interstellar medium since the large scale distributions of thermal and relativistic gas are traceable at these frequencies. Studies of discrete objects, both galactic and extragalactic, are possible at the higher frequency end of the window. The VLF window is ideally suited for studies of phenomena not manifested in any other spectral band. These include studies of low energy cosmic ray particles, thermal environments of discrete radio sources and coherent radiation arising from collective plasma processes.

INTRODUCTION

Very low frequency radio astronomy is bounded by two major constraints. The first is the Earth's ionosphere. It has a characteristic and variable plasma frequency of ≈ 10 MHz. Combined with radio interference, both man-made and geomagnetic, routine observations are limited to > 30 MHz. Reliable, straightforward observations at lower frequencies can only be made outside the ionosphere and a handful of satellite-borne antennas have been used to do this (Kaiser, this workshop). A more fundamental limit to VLF observations is set by the interstellar medium (ISM). Although its plasma frequency is relatively low (≈ 30 kHz), the ISM absorbs and suppresses radio emission, in a number of ways, at frequencies substantially greater than the plasma frequency. The Razin-Tsytoich effect, free-free absorption and synchrotron self-absorption are examples of mechanisms that inhibit radio emission near, and sometimes above 1 MHz. These mechanisms limit observations of discrete galactic and extragalactic objects but afford a better opportunity to probe the properties of the ISM. In fact, the VLF window defined by the 1 – 30 MHz range spans a wide enough frequency range to allow both studies of the ISM and studies of discrete objects, relatively immune from foreground plasma effects.

Density fluctuations in the interstellar plasma lead to another effect, namely interstellar scintillation. Refraction by the inhomogeneities distorts the incoming wavefront, thereby blurring the observed image. This interstellar "seeing" sets a fundamental limit to the achievable resolution in direct VLF observations. At 1 MHz, this limit is ≈ 0.5 degrees, whereas at 30 MHz it falls to $\approx 2''$. As discussed by Dennison (this

workshop) some resolution can be recovered, under certain conditions.

The inhomogeneous nature of the ISM all but eliminates the possibility of polarization studies at these frequencies. Within the effective beam of the VLF array, the ISM presents many such inhomogeneities with differing densities and magnetic field strengths. This leads to differential Faraday rotation which acts to depolarize the observed source. Polarization measurements will therefore only be possible for the closest sources. This does not present a great setback because polarization measurements can be obtained at higher frequencies with Earth-based telescopes.

The presence of a strong nonthermal background, which has a mean flux density of ≈ 1 Jy/(arcminute)² at 1 MHz (Cane, 1979), also limits VLF observations. The observed noise level depends on the system temperature

$$\Delta T_{rms} \propto T_{sys}^5 T_A + T_R,$$

where T_A and T_R are the antenna and receiver temperatures, respectively. For normal cm-wave observations $T_A \ll T_R$ and the system temperature is dominated by the receiver noise. However, for strong sources at low frequencies the condition $T_A \gg T_R$ can be met. In those cases the signal-to-noise ratio becomes independent of the receiver noise and therefore independent of integration time since,

$$\Delta T_{rms} \propto T_A \approx 30S(\text{Jy})/\Omega(Sr)$$

at 1 MHz. The measured flux density is S and the angular size of the beam is Ω . In the case of the galactic background $T_A \approx 2 \times 10^7 K$, much greater than the receiver noise temperature (Erickson, 1988; Douglas, this workshop). Furthermore, local enhancements in the background augment this effect. The extra sources of noise will limit the dynamic range of the observations and therefore limit the possible science.

Finally, the ISM is a source of coherent plasma processes which are manifested at very low frequencies. Such processes have been observed in solar radio bursts and in the magnetospheres of Jupiter, Saturn, Uranus, and the Earth. Coherent effects are expected to be important near 1 MHz. The reduction and analysis of such observations is not straightforward as described later in the paper.

VLF radio astronomy is, today, in an analogous position to where X-ray astronomy was in the late 1960s. The Sun and a few strong galactic sources dominate the known sources in

the VLF sky, as observed from the Earth. Unlike X-ray astronomy though, balloon-borne VLF astronomy is not possible since it is necessary to climb above the ionosphere. Only direct satellite observations can be made and these have been few with rudimentary antennas. An array could be constructed in space but this would not obviate the problems associated with the emissions from the Earth's magnetosphere (Kaiser, this chapter). VLF astronomy is therefore in the untenable position of being bounded by the presence of the Earth itself. It is these disadvantages which have slowed the development of VLF radio astronomy relative to X-ray and even γ -ray astronomy. An important lesson to be learned from X-ray precursor missions is that not all the science can be predicted and quantified. The precursor missions themselves provided much of the guidance in defining the scientific goals of more advanced missions such as the Einstein X-ray telescope. It is therefore desirable that the VLF lunar base mission be preceded by precursor projects aimed at mapping out the sky with an IRAS-style all sky survey. The scientific goals currently envisioned are summarized below, keeping in mind that better focus and even some redirection will be dictated by the proposed precursor missions.

SOURCE SPECTRA

The synchrotron spectrum of a radio source is determined by the shape of the energy spectrum of the radiating electrons. The slope and the energy cut-offs of the energy spectrum have a one-to-one correspondence with the radio spectrum. The emissivity of the source depends on the strength of the ambient magnetic field and the density of relativistic electrons so that:

$$S_\nu \propto N B^{(1-\gamma)/2} \nu^{-(\gamma-1)/2} \quad (1)$$

between the 2 energy cutoffs, where S_ν is the synchrotron emissivity (incoherent radiation) at the observing frequency ν and γ is the index of the power law energy spectrum ($N(E) \propto E^{-\gamma}$).

Observations of synchrotron sources reveal surprisingly similar energy spectra having implied slopes close to the universal value of 2.5. High frequency cutoffs can generally be observed (although they don't always fall into the radio window). The low energy cutoffs, on the other hand, have rarely been observed because they fall below 30 MHz. The same holds true for direct detections of Earth-bound galactic cosmic rays for which the high energy end has been studied through air-shower experiments but the lower energy end (below $\approx 0.1 - 1$ GeV) is inaccessible because of solar modulation. Interestingly enough, the particle detector experiments and radio observations, both fail as probes of energetic particles in the same energy range. It is true to say that almost nothing is known about the spectra of relativistic particles at energies corresponding to the VLF window.

The calculation of radio source luminosities is directly dependent on the spectral cutoffs according to:

$$L \propto n_{max}^{1-\alpha} - \nu_{min}^{1-\alpha} \quad (2)$$

where L is the luminosity and the frequency cutoffs are labeled as *max* and *min*. The lower cutoff is important for steep spectrum source having α close to greater than 1. This is of direct consequence to equipartition calculations of the energetics of radio sources since these are dependent on the source luminosities. The knowledge of the lower frequency cutoffs will improve calculations of the magnetic fields strengths and the energy contents of relativistic particles in steep spectrum sources such as pulsars and the lobes of radio galaxies. Better equipartition calculations, combined with observations of absorption effects and polarization studies at higher frequencies, will shed more light on the energetics and environments of radio sources.

A relativistic electron radiates at a characteristic frequency given by

$$\nu_{syn} = 10^{18} B_1 E^2 \text{Hz}. \quad (3)$$

An electron with an initial energy E_0 , will lose half its energy in

$$t_{1/2} = 8 \times 10^9 \left(\frac{B}{\mu G} \right)^{-2} \left(\frac{E}{\text{GeV}} \right)^{-1} \text{yrs}. \quad (4)$$

Energy losses of relativistic electrons quickly steepen an injected spectrum at the high frequency end. The longer the source ages without further particle injection, the lower the frequency, ν_k , at which the spectrum begins to steepen. Combining equations 3 and 4, it is possible to relate the turn-over frequency ν_k to t , the age of the source. This frequency is given by:

$$\nu_k = 3.4 \times 10^8 B^{-3} t^{-2} \text{ Hz} \quad (5)$$

where t is in years. For $\nu_k = 1$ MHz and $B = 3 \times 10^{-6} G$, $t = 3 \times 10^{10}$ years. Thus, once accelerated, the lower energy electrons remain for a long time and may represent the original injection spectrum. VLF radio observations can therefore trace low energy electrons and, in a sense, probe the fossil records of radio sources.

The shape of the low frequency end of the radio spectra (free of absorption effects) will also provide a useful constraint on theories of particle acceleration which are relevant to the more general problem of the origin of cosmic rays. Perhaps the most widely proposed acceleration mechanism is the diffusive shock acceleration process which is a first-order Fermi process by which particles are accelerated across shock fronts. Direct observational evidence for such a mechanism has come from *in situ* observations in the interplanetary medium, with particles up to a few MeV in

range, observed. In astrophysical settings, such as SNRs, radio observations indicate the presence of particles having energies of a few GeV to hundreds of GeV. The overlap between the lower energy particles produced in the Solar System and the higher energy particles at astrophysical sites has not been observed because of the dearth of observations at the appropriate energies. Such an overlap is needed in order to test the applicability of the observationally verified acceleration processes in the Solar System to the more extreme astrophysical environments. Most theories of particle acceleration predict approximate energy cutoffs for the energized particles (e.g., Volk, 1988; Blandford, 1988). Observations of the low energy end of the particle distribution function will strongly constrain these theories.

VLF RADIO SPECTRA

The spectra of radio sources below 30 MHz have never been reliably measured with Earth-based observations. Furthermore, poor angular resolution has prevented detailed mapping of sources even at frequencies as high as 300 MHz. The mechanisms that modify the spectra at low frequencies through extrinsic (environmental) and intrinsic effects are described below.

The Razin-Tsytoich Effect

According to Tsytoich (1951), Eidman (1958), and Razin (1960), relativistic electrons embedded in a thermal plasma have their synchrotron radiation suppressed below the critical frequency given by:

$$\nu_R \approx 20 \frac{N_e}{B_\perp} \text{ Hz.} \quad (6)$$

The spectrum steepens in shape from

$$S_\nu \propto \nu^{-(\gamma-1)/2} \quad \nu > \nu_R$$

to (Lang, 1980)

$$S_\nu \propto \nu^{3/2-\gamma} e^{-3.7\nu_R/\nu} \quad \nu < \nu_R.$$

For typical interstellar gas densities of 0.1 cm^{-3} and $B \approx 10^{-6} \text{ G}$, $\nu_R \approx 10^5 \text{ Hz}$, well below 1 MHz. However, if the environments in which the particles are radiating have locally higher electron densities and/or lower B fields this effect could easily manifest itself in the VLF window defined above. The effect could be searched for in galactic objects such as SNRs and pulsars and in extragalactic objects such as active galactic nuclei (AGNs) and lobes of radio galaxies. Recognition of the unique spectral shape predicted by the Razin-Tsytoich effect is the primary means by which this mechanism would be identified in radio sources. The environment of such a source can be probed since the ν_R

depends only on N_e and B_\perp . An independent means of calculating one of the 2 parameters would immediately yield the second. For example, equipartition calculations of B_\perp and the observed value of ν_r yield the thermal gas density according to equation 6. Comparison of such calculations with Faraday rotation measurements made at higher frequencies would provide a consistency check and a direct test of the validity of equipartition calculations. Such a test would be of profound significance in understanding the physics of the interaction between magnetic fields and relativistic particles in radio sources.

Free-free (Thermal) Absorption

Plasma between the observer and the source can absorb radiation through the free-free transitions of ions. The optical depth of such a plasma to radio frequency radiation is given by

$$\tau_\theta \propto T^{-1.35} \nu^{-2.1} \int N_e^2 dl \quad (7)$$

which is unity at a frequency given by:

$$\nu_T \approx 0.3 T_e^{0.68} N_e l^{1/2} \text{ GHz} \quad (8)$$

where l is the path length in parsecs. Taking $T_e = 10^4 \text{ K}$ and $N_e = 0.1 \text{ cm}^{-3}$ the turnover frequency is a function only of l . Looking through the galactic plane, the turnover frequency is $\approx 1 \text{ MHz}$. Perpendicular to the plane, $\nu_T \approx 0.2 \text{ MHz}$. Extragalactic sources and distant galactic sources will therefore be strongly attenuated looking through the galactic plane and marginally attenuated otherwise. A statistical study of extragalactic sources could therefore be used to map out the distribution of thermal, ionized gas in the galaxy. Such a study can be combined with statistical studies of the Faraday rotation (e.g., Simard-Normandin, Kronberg and Button, 1980) to determine length averaged B fields through the galaxy. This would impact significantly on our very limited knowledge of the structure and strength of the global interstellar magnetic fields. Similar studies of discrete sources can be used to probe their local environments. A good example is the thermal environment thought to exist around extragalactic jets and lobes. If the thermal gas is mixed in with the radiating particles, the spectrum assumes a flatter shape given by:

$$S_\nu \propto \nu^{2.1-(\gamma-1)/2} \quad \nu < \nu_T.$$

If the absorbing gas is between the source and the observer then:

$$S_\nu \propto e^{(\nu/\nu_T)^{-2.1}}$$

In either case, the absorbed spectrum has a recognizable shape.

Synchrotron Self-Absorption

A source is opaque to its own synchrotron radiation when:

$$\nu_s \sim 34 \left(\frac{S_{\nu_s}}{\theta^2} \right) B^{1/5} \text{ MHz} \quad (9)$$

where B is in Gauss and θ is the angular size of the source in seconds of arc and S is in Janskys. Normally a radio source is self-absorbed under the most extreme conditions such as the cores of radio galaxies. However, for very low frequency these conditions can be less extreme. Consequently, the frequency turnovers of many more sources will be uncovered. A self-absorbed spectrum has a theoretical shape, below ν_s given by ($S_{\nu} \propto \theta^{2.5}$). In practice, the observed slope does not reach such high values because different parts of the source reach self-absorption at different frequencies. This dilution is minimized at very low frequencies because the absorption can occur over greater angular scales. Nevertheless, this important lesson from high frequency radio observations needs to be considered when interpreting the observations. The magnetic field of a self absorbed source can be derived very accurately because of its strong dependence on ν_s . In order to disentangle synchrotron self-absorption from other absorption effects, these searches should best be carried out at the higher frequency end of the VLF window (≈ 10 MHz). Once the self-absorbed sources are identified, their angular sizes can be determined from GHz observations, leaving the magnetic field as the only remaining variable. The determination of B for a large sample of radio sources is important in understanding their internal energetics and the lifetimes and replenishment of relativistic particles.

Coherent Plasma Processes

When the particles that make up a plasma are separated by scale lengths comparable to the wavelength of the EM radiation, collective effects can and do become important. If a population inversion of emitting particles exist ($\frac{\partial N}{\partial E} > 0$) this leads to stimulated emission which is a coherent process. This presents both an opportunity and a problem. The opportunity lies in the possibility of studying a new and interesting phenomenon as has been done in the solar system with solar radio bursts, and the magnetospheres of Jupiter, Saturn, Uranus and the Earth (Kaiser; Desch, this chapter). The parameters under which this process operates suggest that it may be observable in other stellar systems and in many radio sources where modestly high gas densities ($10^3 - 10^5 \text{ cm}^{-3}$) and B fields (0.01 - 1G) exist (Stone and Erickson, 1976). The problem lies not in the science but in the manner in which the data are analysed. Most interferometric techniques assume that source radiation is spatially uncorrelated.

Coherent radiation processes may, however, correlate over large spatial scales and the assumption is therefore invalid.

The VLF array is sensitive to:

$$V_{\nu}(\mathbf{r}_1, \mathbf{r}_2) = \langle E_{\nu}(\mathbf{r}_1) E_{\nu}^*(\mathbf{r}_2) \rangle$$

where V_{ν} is the measured correlation and E is the electric field at the two source locations, $\mathbf{r}_1, \mathbf{r}_2$. The normal simplifying assumption for incoherent radiation is that, at the source positions ($\mathbf{R}_1, \mathbf{R}_2$), $\langle E_{\nu}(\mathbf{R}_1) E_{\nu}^*(\mathbf{R}_2) \rangle = 0$ for $\mathbf{R}_1 \neq \mathbf{R}_2$. In the case of coherent radiation that assumption cannot be made. Spatially correlated radio emission can be mapped in the usual way but the interference pattern is a function of not only the relative antenna positions but also the *absolute* antenna positions. The data reduction techniques are therefore not as straightforward (Anantharamaiah, 1988).

In the case of interstellar scintillation the emission is coherent over short time scales (fractions of seconds). Extremely short *snapshots* can be used to record the instantaneous coherence pattern which can then be analysed using techniques analogous to speckle imaging (Dennison, this workshop).

Solar and planetary observations will make up a major fraction of the research effort of the array, particularly if frequencies below 1 MHz are used. Absorption effects are not important at the relatively short distances involved and observations in the kHz bands are possible. Such observations will allow better studies of the coherent processes that take place in the solar system. With the right combination of frequencies and angular resolution, it may be possible to spatially resolve the regions of coherent emission in the magnetospheres of the giant planets. The data reduction, in such cases, has the same complications discussed above.

Interstellar Scintillation

An EM wave travelling through an inhomogeneous plasma will have its phase altered in response to changes in the refraction index along its path. This leads to a bending of the propagating ray in a manner analogous to a random walk. The average angular deviation from a straight line-of-sight path determines the apparent angular size of the source. As discussed by Dennis on (this chapter) this leads to an effective lower limit on the angular size of any radio source, which at 1 MHz is ≈ 0.5 degrees. Since the effect is $\propto \nu^{-2}$ the limit approaches 1" at 30 MHz. Although this limits the resolution of the VLF array it also acts as a well defined constraint on its design. Under some conditions extra resolution may be achievable through deconvolution techniques and this may need to be taken into account when designing the array.

By inverting the problem, interstellar scintillation can be used to probe the nature of the scatters in the ISM. Comparing VLF and higher frequency measurements of the angular

sizes of a large number of extragalactic sources, statistical studies can be made to map out scintillation effects as a function of galactic longitude and latitude to gain insight into the global distribution of the scatters in the galaxy. The same technique can be used to study the properties of the IPM.

SUMMARY

The major research effort of the lunar based VLF array can be divided into 4 broad categories:

(a) Solar, planetary studies (≤ 1 MHz)

The low frequency end of the VLF window is ideally suited for solar and planetary work because of its sensitivity to coherent effects. Absorption effects are avoided since the sources are relatively nearby. The bulk of this research will be aimed at monitoring transient phenomena and resolution is therefore not an important issue. Nevertheless, the design of the array will allow for good directionality to avoid sidelobe interference, particularly from the Sun and Earth's magnetotail.

(b) Studies of the ISM (absorption effects, scintillation; ≈ 1 MHz)

Observations at frequencies near 1 MHz will be used to probe the ISM and the environments of radio sources. The Razin-Tsytoich effect, combined with high frequency Faraday rotation measurements can be used to estimate N_e and B in the local environments of radio sources. Thermal absorption of extragalactic sources can be used to measure the distribution of HII in the galaxy. These measurements can then be combined with pulsar dispersion measurements, and observations of foreground Faraday rotation to more accurately determine the column densities of HII, as a function of both latitude and longitude. Measurements of radio disks caused by scintillation can be used to probe the second moment of the density distribution ($\langle \Delta N_e^2 \rangle$).

(c) Discrete radio sources (galactic and extragalactic sources; 10 - 30 MHz)

Observations of synchrotron self-absorption allow the determination of intrinsic source magnetic fields. Consequently, energetics of radio sources can be better understood and the validity of equipartition assumptions can be directly tested.

The medium to high frequency portions of the VLF window provide observations of synchrotron spectra relatively free of absorption effects. Locating intrinsic low energy cutoffs will allow more accurate determinations of radio source luminosities which in turn improve calculations of source energetics. Studies of the long lived electrons that radiate at these frequencies will provide useful insights into source histories. The shape of the spectrum at low frequencies, and the locations of the low energy cutoffs are important

constraints of particle acceleration theories since these 2 parameters are model dependent.

(d) High resolution, all-sky survey (1 - 30 MHz)

History is the best judge of the importance of all-sky surveys. The precursor mission will provide initial low resolution maps of the sky. The lunar base array will produce high resolution, sensitive maps of the sky and generate a data base for detailed statistical studies and follow-up studies of individual sources. Most important, the survey will set the foundation for long term planning and optimal use of the array.

The VLF window is not just another portion of the radio spectrum. It is an unexplored spectral region which offers insights into phenomena impossible to study from the Earth or even in Earth orbit. It promises insights into the ISM and gaseous environments of radio sources. A window will literally be opened onto the uncharted fields of plasma effects and coherent processes. Serendipity is a factor whenever a new field is opened to exploration and we expect discoveries to shape much of the future research the VLF array will generate.

REFERENCES

- Anantharamaiah, K.R. 1988, in *NRAO Workshop on Aperture Synthesis*.
- Blandford, R.D. 1988, in *Supernova Remnants and the Interstellar Medium*, IAU Colloquium 101, p 309, Eds. R.S. Roger, T.L. Landecker (Cambridge University Press: New York).
- Cane, H.V. 1979, *M.N.R.A.S.*, **189**, 465
- Dennison, B. 1988, *This workshop*
- Desch, M.D. 1988, *This workshop*
- Douglas, J.N. 1988 *This workshop*
- Eidman, V.Y. 1958, *Sov. Phys. J.E.T.P.*, **7**, 91
- Erickson, W.C. 1988, *Preprint*
- Kaiser, M.L. 1988, *This workshop*
- Simard-Normandin, M., Kronberg, P.P. & Button, S. 1980, *Ap. J.*, **45**, 97
- Lang, K.R. 1980, in *Astrophysical Formulae*, p. 41, (Springer Verlag: New York)
- Razin, R.G. 1960, *Radiophysica*, **3**, 584
- Stone, R.G. and Erickson, W.C. 1976, *Experimental Proposal for the Lunar Polar Orbiter*, NASA proposal AO #8
- Tsytoich, V.N. 1951, *Vestn. Mosk. Univ.*, **11**, 27



VOYAGER RADIO ASTRONOMY AND THE LOW FREQUENCY NEAR-EARTH RADIO ENVIRONMENT

M.D. Desch
Laboratory for Extraterrestrial Physics
Goddard Space Flight Center
Greenbelt, MD 20771

ABSTRACT

I review the major features of the radio astronomy experiment onboard the two Voyager spacecraft. In addition, the major sources of noise in the near-Earth environment are identified. They are: (a) terrestrial atmospheric, (b) terrestrial kilometric radiation, and (c) solar Type III bursts. Interference from all but the last is eliminated by observing from the lunar far-side. Based on experience with numerous classes of spaced-based radio astronomy experiments, the use of relatively simple antennas with a sophisticated observing scheme seems not only expedient but most likely to operate effectively on the Moon. Finally, a science rationale for lunar-based planetary observations is presented.

1. Planetary Radio Astronomy on Voyager

The Planetary Radio Astronomy (PRA) receiver shares space on Voyager with 9 other instruments (Figure 1). The 198-channel swept-frequency receiver is driven by two 10-meter orthogonal monopoles. The input is alternately switched through a quarter-wave hybrid to sense right-hand and left-hand circular polarization. The PRA receiver covers the frequency range from 1 kHz to 40 MHz in 198 steps. Figure 2 shows how this band covers the well-known Earth-based transmitter frequencies and the natural planetary radio sources now recognized in the solar system.

Both Voyagers were launched in 1977. As illustrated in Figure 3, encounters with Jupiter occurred in 1979, with Saturn in 1980 and 1981, and with Uranus (Voyager 2) in 1986. Voyager 2 will encounter Neptune in August 1989. Thus far, every encounter has resulted in the discovery of new radio phenomena.

Figure 4 shows a 24-hour radio spectrogram. The frequency band ranges from 1 kHz at the top of each panel to 1320 kHz at the bottom of each panel in 70 equal steps. Both solar type III bursts and Saturn kilometric radiation (SKR) are clearly visible. Some Jovian emission (HOM) is visible near 1 MHz, especially from about 7 to 8 hours in panel 2. At the time this spectrogram was made, Voyager 1 was about 0.7 AU from Saturn and about 4 AU from Jupiter.

The spectrogram in Figure 5 illustrates a type of emission, namely SED, never before seen by Voyager. The SED, or Saturn Electrostatic Discharges, are visible as the short vertical streaks, extending from 40 MHz to 100 kHz.

Because of the way our receiver samples, we know that

the SED are actually very broadband (probably at least many hundreds of MHz) and of short duration (50 - 100 msec). They have been shown to originate in Saturn's atmosphere, near its equatorial region, and are very likely due to lightning-like emissions. By observing the low-frequency cutoff of these atmospheric emissions, we were able to generate a global model of Saturn's equatorial ionosphere density.

2. RF Environment Near 1 AU

Observations from Voyager and from other spacecraft carrying radio instruments have helped us assess the radio noise environment in the vicinity of 1 AU. Figure 6 shows a

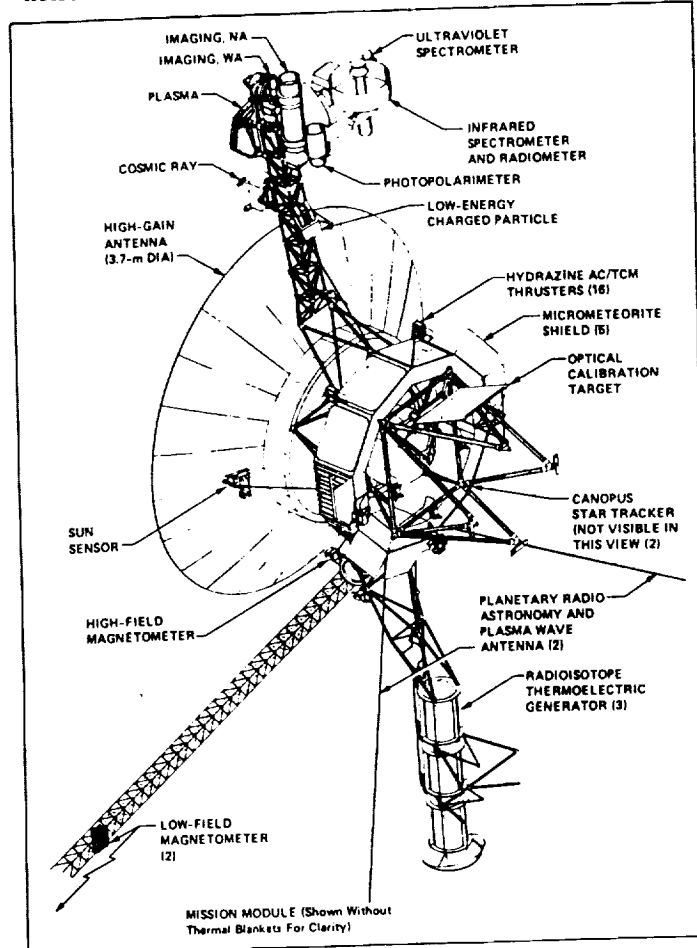
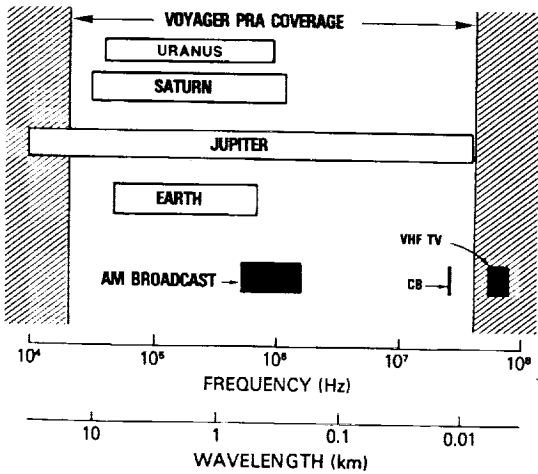


Figure 1. Line drawing of the Voyager spacecraft showing its complement of instruments.

34

VOYAGER PRA COVERAGE OF PLANETARY RADIO EMISSIONS



radio spectrogram of Voyager data when it was near Earth, shortly after launch. The spectrogram is dominated by the Earth's natural auroral radio noise (AKR). AKR is observed in the frequency band from about 50 kHz to 750 kHz. Also seen in this spectrogram is a type of noise generated at the antennas, due to coupling with the antennas to the solar wind. It is always observed when the solar wind plasma density is unusually large, say, greater than a few tens of particles per cubic centimeter. In the spectrogram, this antenna coupling noise (or thermal noise) occurs over the band from a few kHz to about 200 kHz. A solar type III burst can be seen in the first few hours of the spectrum. The top panel in this spectrogram illustrates the polarization signature of these emissions. Black represents LH circular polarization. The AKR appears LH polarized, while the Type III burst and the antenna coupling noise are unpolarized because they do not show a consistent polarization signature.

Figure 2. Frequency coverage of the radio astronomy instrument on Voyager. The radio emissions from Saturn, Uranus and the low frequency portion of the Jovian emission were unknown before Voyager.

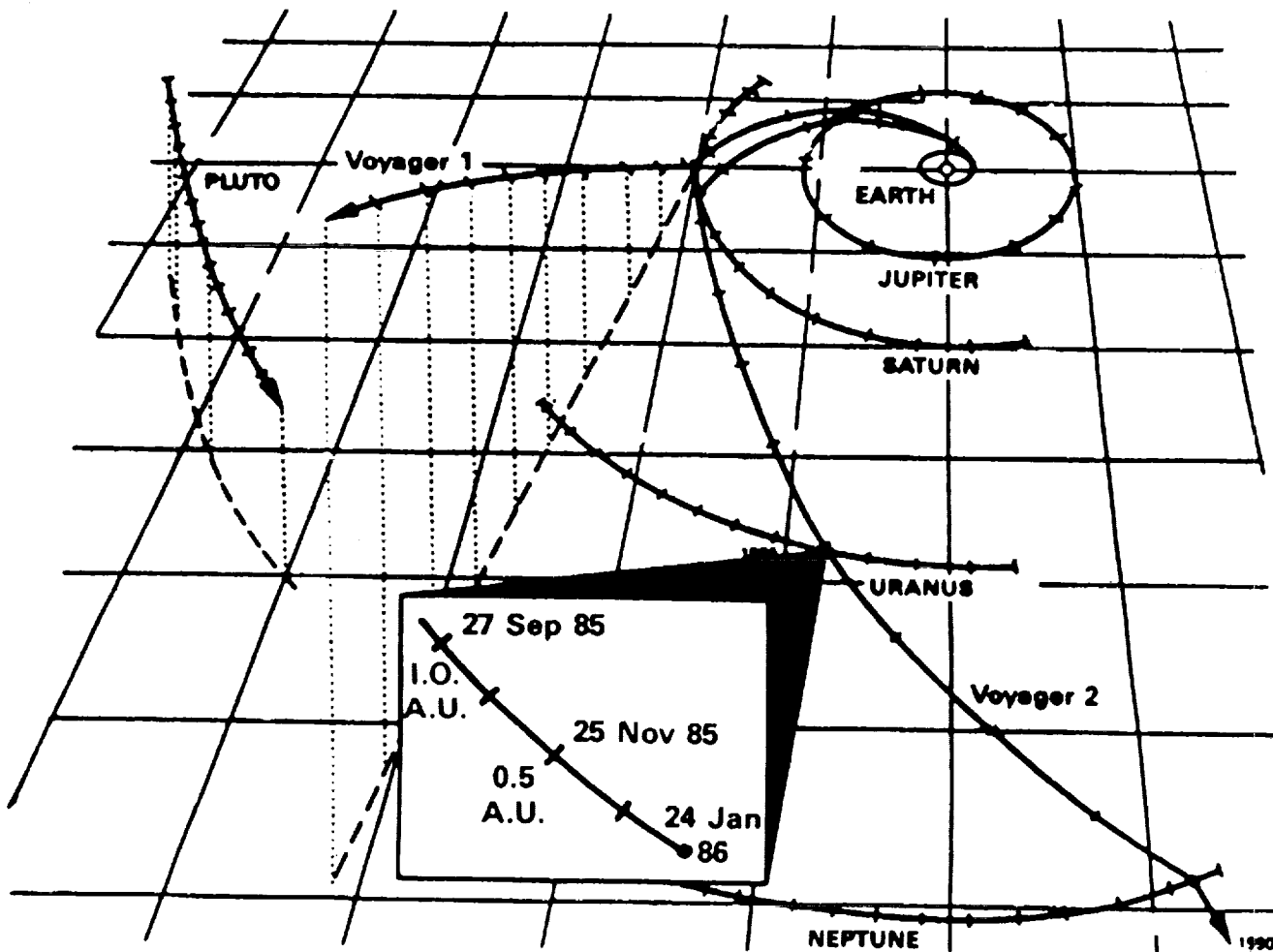


Figure 3. Trajectory of the two Voyagers. Voyager 2 encounters Neptune in August, 1989.

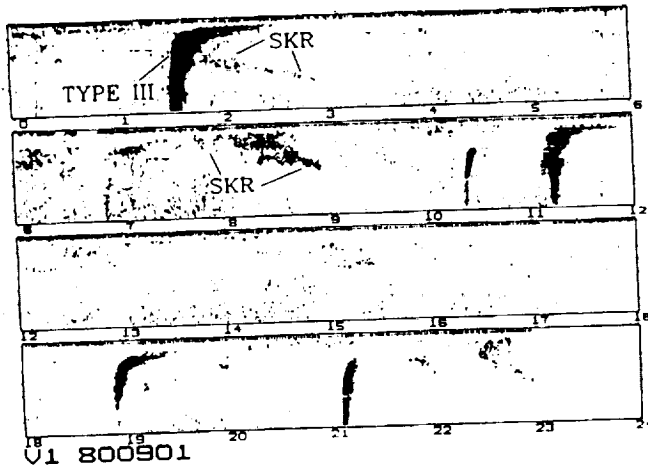


Figure 4. Radio spectrogram showing 24 hours of data from Voyager 1. In each frame, 1 kHz is at the top and 1320 kHz is at the bottom. Several solar Type III bursts and several episodes of Saturn kilometric radiation (SKR) are visible.

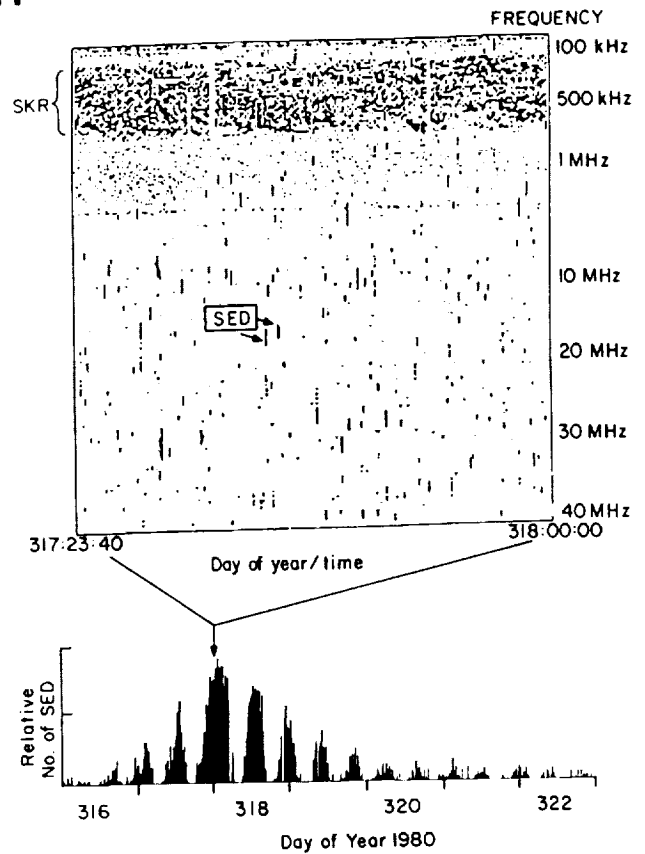


Figure 5. (top) Radio spectrogram taken near Saturn showing 20 minutes of activity during an intense period of SED (Saturn electrostatic discharge) activity. (bottom) Periodic nature of the SED 'storms' over a 7-day span from which it was deduced that the SED were coming from an equatorial storm system in the atmosphere of the planet.

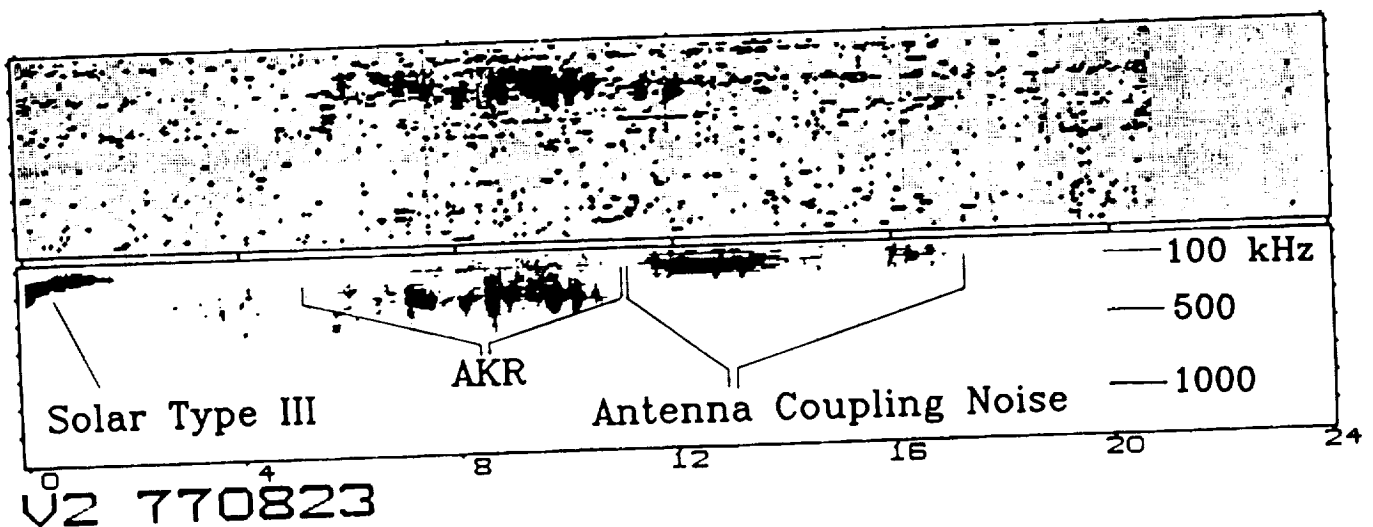


Figure 6. Typical radio spectrogram of radio frequency 'noise' environment near 1 AU.

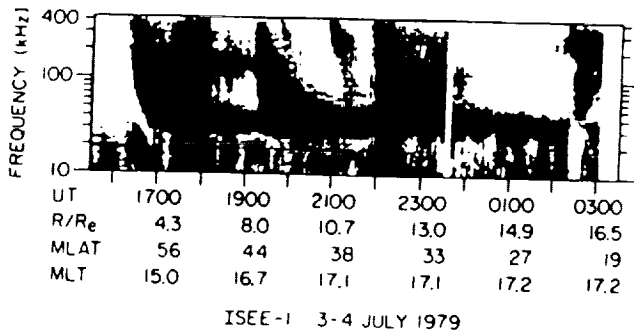
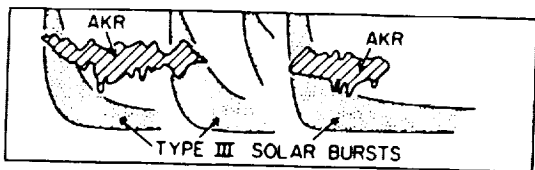


Figure 7. Radio spectrogram from ISEE-1 showing the intensity of solar Type III bursts [from Farrell and Gurnett].

Figure 6 does not give a good indication of the potential level of noise from solar Type III bursts. Figure 7, however, shows how the Type III bursts can completely dominate the noise background at times. The top panel cartoon is useful in helping to identify the Type III bursts and the AKR.

At somewhat higher frequencies, typically above 1 MHz, man-made noise and lightning rf contribute significantly to the general level of noise observable at 1 AU. Figure 8, from RAE (Radio Astronomy Explorer) satellite observations near 9 MHz, shows antenna temperature contour levels in dB above 300°K. The observations were made from an altitude of about 6000 km. Given the proper ionospheric conditions, almost any location on Earth can produce easily detectable noise in the terrestrial vicinity.

Figure 9 compares quantitatively some of the noise sources discussed above. The observations were made from the ISEE spacecraft from out near the Earth-Sun libration point, several hundred R_E from Earth. Lacking is the contribution due to man-made noise, which would dominate at

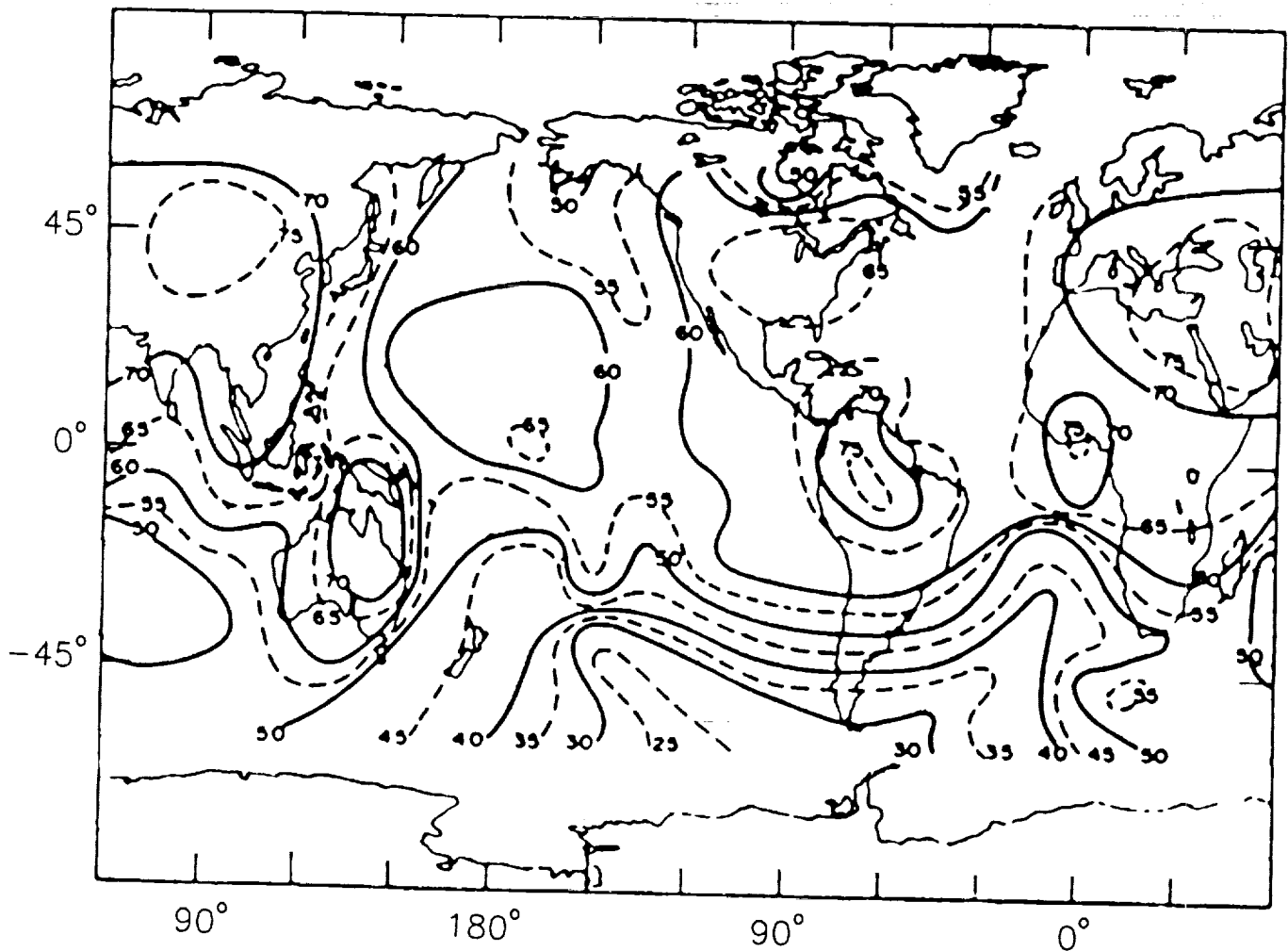


Figure 8. Isocontours of antenna temperature from RAE-1 observations at an altitude of 6000 km. Noise is due to the combination of lightning activity and man-made transmissions at 9 MHz.

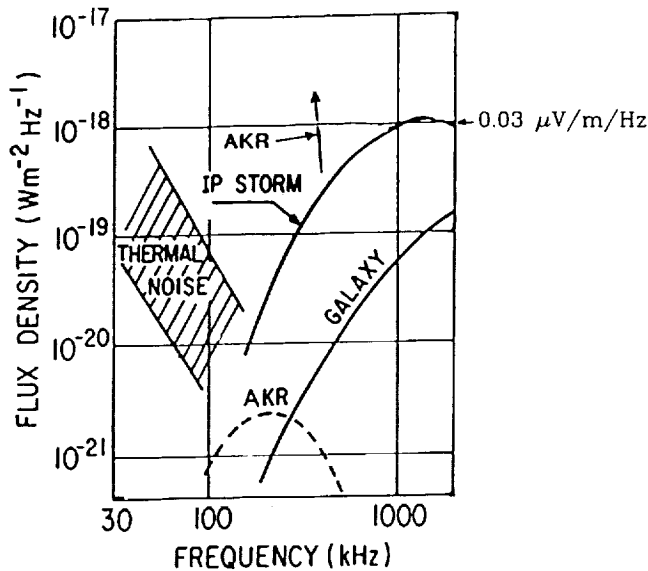


Figure 9. Flux spectrum showing typical noise levels of the most important noise sources at 1 AU. Included are AKR (lower limit), solar Type III emission (IP), and antenna thermal noise due to coupling with the solar wind.

frequencies above 1000 kHz. Man-made noise would certainly be comparable to the IP storm level above 1 MHz, however. Two spectra are shown for the AKR; the lower one (dashed) illustrates the intensity level of AKR when observed over the dayside of Earth, the higher one (solid) shows the level observed over the nightside. IP storm is the radio noise due to a succession of Type III solar bursts observed during an interplanetary (IP) "storm."

Table 1 provides a summary of the recognized low-frequency noise sources near 1 AU. They are tabulated in approximate order of importance. Items with an "X" in column 1 would be detectable on the lunar far-side. Others should be undetectable due either to the shielding provided by the Moon, or because, as with Uranus, the emission is too weak.

Table 2 provides a rough comparison of spacecraft antenna systems with which the author has had personal experience. A scorecard is included to evaluate the relative successes of each. It is clear, of course, that for planetary observations, 'going there' is the best bet. Hence Voyager, with only a 10-meter dipole, has detected the most planets. If confined to the near-Earth vicinity, then residing in an rf quiet neighborhood is the next-best thing. Hence ISEE, fixed at the Earth-Sun libration point on the Earth's dayside has done extremely well. If ISEE had to make observations above 9 MHz (the dayside critical frequency), however, it would not do very well owing to likely interference from terrestrial atmospherics. RAE, surprisingly, has not done that well

Table 1. Low-Frequency Noise Sources at 1AU

Source	Frequency	Pol	Level	Spacecraft
Terrestrial Atmospherics	1 MHz - Day	yes	v. strong	
x Type III Bursts	20 kHz - Day	no	strong	
AKR	20 - 750 kHz	yes	strong	
x AKR'	20 - 100 kHz	?	moderate	ISEE
x Antenna Coupling	dc - 200 kHz	no	strong	
x Jupiter	20 kHz - 40 MHz	yes	moderate	V1, V2, ISEE, RAE
x Saturn	20 kHz - 1 MHz	yes	moderate	ISEE
Uranus	20 kHz - 850 kHz	yes	v. weak	IMP-6 (?)
Neptune	?			

- Note that two of the major sources, namely, terrestrial atmospherics and AKR do not present a noise problem on the far side.
- Type III bursts would be detectable over approximately 1/2 of each lunation.
- AKR' (AKR prime) is a recently discovered low-frequency component of the AKR that is of moderate intensity, but very infrequently observed. It may originate on field lines far down the Earth's tail and would therefore be observable over half a lunation. This particular component may represent an important science objective of the array.
- Antenna coupling noise would be detectable during times when the array is immersed in the solar wind (approximately half a lunation) provided the solar wind density is extremely high (a few hours each month).
- Finally, the planetary sources Jupiter and Saturn should be relatively easy to detect and would represent important science objectives of the array.

considering the size of its antenna system. This is particularly true below 1 MHz. I believe this fact underscores the importance of the observing mode in helping to properly identify the myriad of signals incident on space-based receiver systems. ISEE, with a small antenna systems maintains a very good identification record due to the spinning platform from which the observations were made. Harmonic phase fits to the intensity modulations from various sources helped considerably in identifying sig.

Table 2. Spacecraft Antenna Systems: Comparison

Spacecraft	Antenna		Scorecard
	physical length	electrical type	
RAE	460 m	travelling wave V	J (not easily)
IMP-6	90 m	electrically short	J (easily), U(?)
ISEE	90 m	electrically short	J, S (both easily)
Voyager	10 m	electrically short	J, S, U

J=Jupiter
S=Saturn
U=Uranus

Summarizing, in low-frequency radio astronomy a quiet environment and a clever observing scheme are far more important than massive antenna structures. This general 'philosophy of low frequency radio astronomy' argues strongly for individual array elements that are very simple in design, such as simple short dipoles, rather than individual elements that are complex, such as log spirals or large Vee structures. This simplicity is more than made up for by the use of aperture synthesis, which is in a sense the modern-day equivalent of the spinning platform used on ISEE to identify the direction of arrival of incoming signals.

3. Science Rationale from a Planetary Perspective

As is apparent from Figure 10, most of the interesting work that can be done in planetary radio astronomy is below 1 MHz. The spectral peaks of the emissions discovered by the PRA experiment onboard Voyager are all in the neighborhood of 100 - 1000 kHz. These are radio components that cannot be observed from the ground, and can only be detected from space in quiet rf environments.

Planet by planet, the emission components of immediate interest and whose study would most likely have far-reaching implications for solar-system research are as follows:

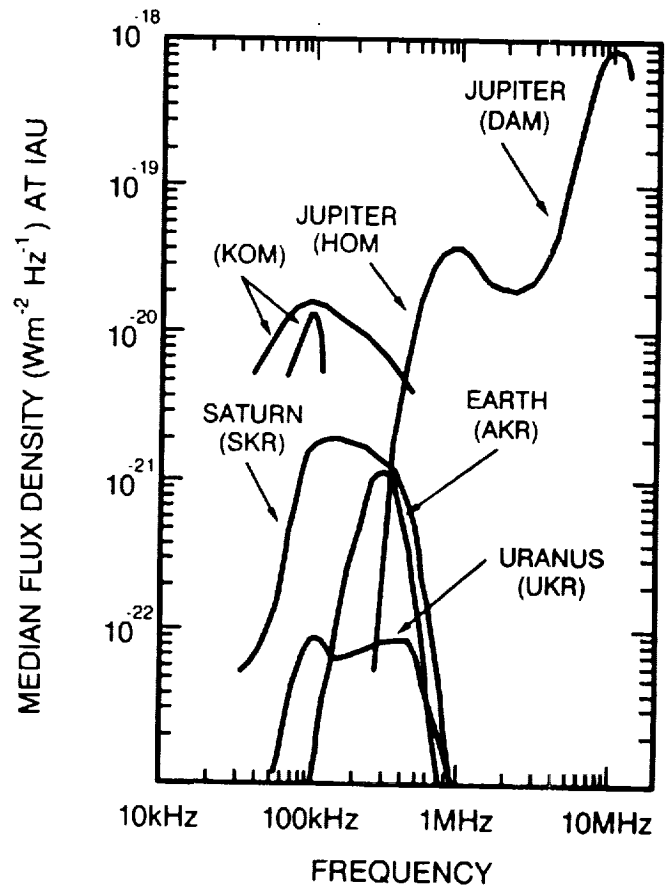


Figure 10. Median flux densities of the known planetary sources normalized to a standard distance of 1 AU. The dashed portion of the Jupiter curve is what was known before Voyager.

Earth Although the primary component of the terrestrial emission, AKR, is invisible from the lunar far side, of potentially great interest is the recently discovered (what I have called here) AKR' emission. It occurs only infrequently, but may be very important in mapping the plasma dynamics of the Earth's magnetic tail regions during disturbed, auroral-related, conditions. Very little is known about this emission at present, but if its importance to tail dynamics holds up, then a lunar monitoring platform would be ideal for its study.

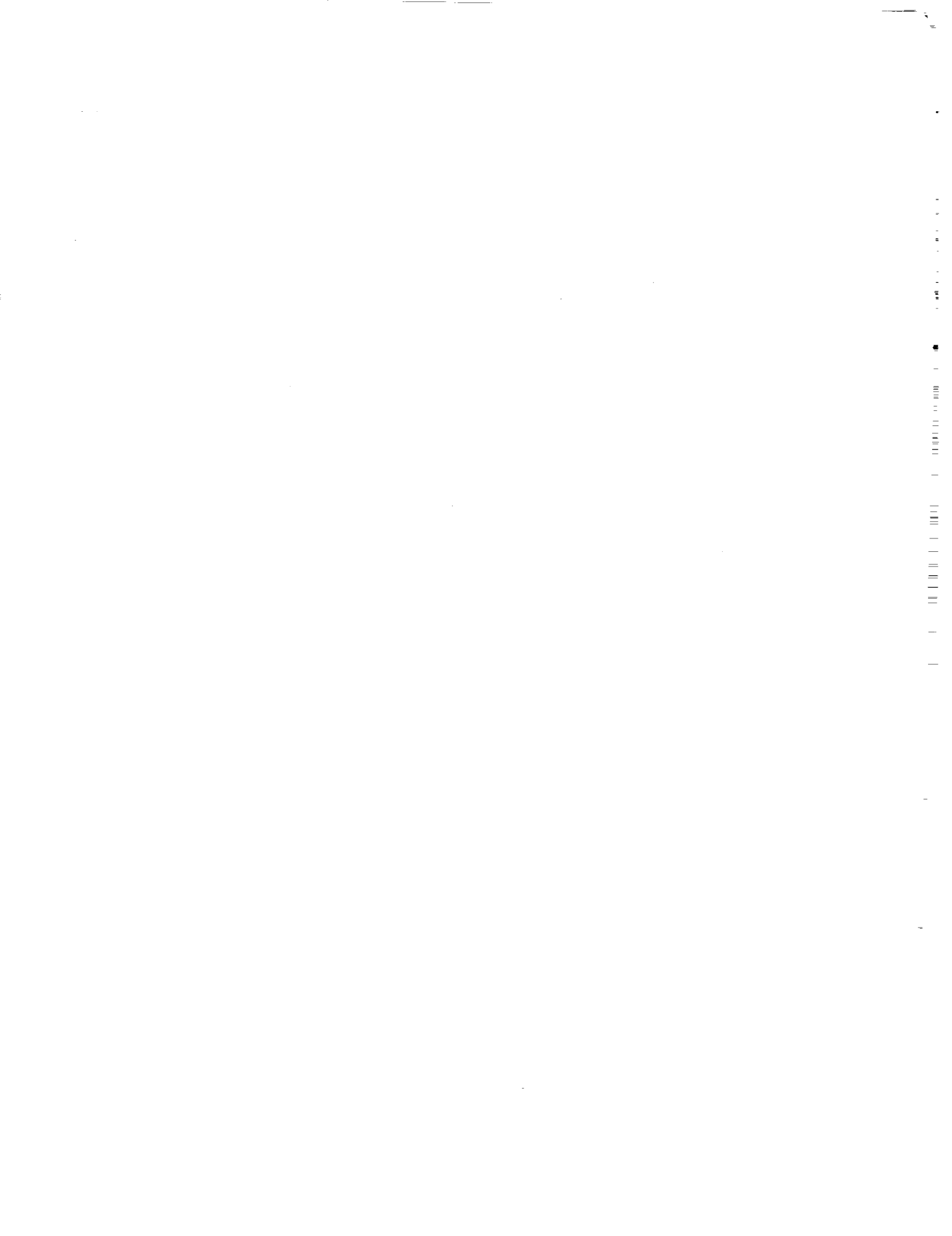
Jupiter The kilometer-wavelength components of Jupiter's emission (labelled KOM in Figure 10) are important in understanding the dynamics of the Io plasma torus. Presently, and for the foreseeable future, Io and its related plasma torus, play an extremely important role in understanding the physics of the Jovian system. Study of the KOM provides one of the

few ways, along with spectroscopy, in which the Io system can be monitored remotely.

Saturn The Saturn kilometric radiation (SKR) is fairly well understood, although further monitoring would almost surely turn up additional surprises. An important advantage in monitoring the SKR, however, is the fact that the SKR is strongly solar wind controlled. Therefore, a record of the intensity level of the SKR is also a highly reliable record of solar wind conditions, in particular the solar wind density, at a distance of 10 AU. This record may be of

importance in deconvolving the low-frequency synthesis maps from the effects of interplanetary scintillations.

In addition to the SKR, the Saturn Electrostatic Discharges, or SED, have provided extremely important information on Saturn's ionospheres, besides being an interesting phenomenon to study in their own right. Observations of SED near 5 MHz yield information on variations in the ionospheric density; there is no other remote sensing technique capable of doing this.



THE EFFECTS OF SCATTERING AND SCINTILLATION IN THE INTERSTELLAR AND INTERPLANETARY MEDIUMS

Brian Dennison
 Department of Physics
 Virginia Polytechnic Institute and State University
 Blacksburg, VA 24061

ABSTRACT

Radio waves are scattered in propagating through the interstellar and interplanetary mediums. This effect sets limits to the effective resolution that can be achieved with a low-frequency array. Here, we review the "standard model" for scattering, and we use it to estimate the limitations relevant to a lunar low-frequency array. At a frequency of 1 MHz, the maximum useful baseline several tens of kilometers. At higher frequencies the scattering is smaller, and therefore longer baselines can be used to achieve greater resolution. Within these limitations a wide range of forefront scientific investigations would be possible. Regarding propagation phenomena, lunar array has the distinct advantage of being outside the Earth's magnetopause in which significant refraction and birefringence occur at low frequencies.

INTRODUCTION

Density irregularities in the interstellar medium (ISM) and the interplanetary medium (IPM) are known to scatter radio waves; and in some cases cause fluctuations (scintillation) in the received amplitude, phase, and intensity. Because these effects occur in an ionized gas, they are stronger at lower frequencies. Not surprisingly, scattering phenomena result in fundamental limitations relevant to any low-frequency array.

In what follows, a simplified, heuristic presentation of the "standard model" for interstellar and interplanetary scattering is discussed, drawn mainly from Cohen and Cronyn (1974), and Dennison (1987, 1988). The reader should consult Rickett (1977) and Cordes et al. (1985) for greater detail. Using this model and extrapolating existing data, the limitations relevant to a lunar low-frequency array (LLFA) are then determined.

THE "STANDARD MODEL" FOR INTERSTELLAR AND INTERPLANETARY SCATTERING

It is well known that inhomogeneities on a range of spatial scales contribute to scattering. The power spectrum of electron density fluctuations can be adequately represented by

$$P_n = C_n^2 q^{-\alpha},$$

where q is the spatial wavenumber, and the coefficient, C_n^2 , quantifies the "strength of turbulence" at any particular location within the medium. The power law index, α , is in most cases thought to be in the range $3.5 < \alpha < 4.5$, with the Kolmogoroff value, i.e. $\alpha = 11/3$, frequently invoked. The power law dependence is generally valid over a range of spatial wavenumbers, given by $q_1 < q < q_2$, where q_1 and q_2 are referred to as the outer and inner scales, respectively.

A common situation is depicted in Figure 1. Because of the density irregularities (and the consequent irregularities in

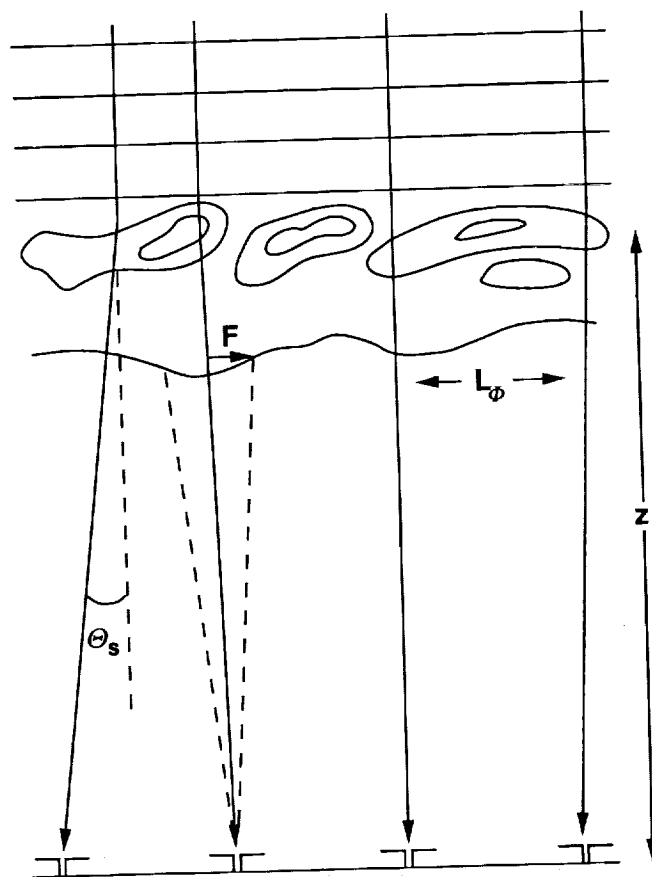


Figure 1. Weak scattering. Initially plane waves emerge from the screen corrugated, having phase coherence length L_ϕ . The rms deflection is θ_s . The dominant contribution to the diffraction integral for the complex voltage at an array element comes from a region of scale size $F = \sqrt{\lambda z}$, the Fresnel scale. For weak scattering $z\theta_s \ll F \ll L_\phi$.

refractive index), a wavefront emergent from the medium is corrugated, whereas it was previously plane, or more generally spherical. The phase fluctuation in the emergent wave decorrelates on transverse scale, L_ϕ . For $\alpha = 11/3$,

$$L_\phi \propto v^{6/5} \left[\int C_n^2(z) dz \right]^{-0.6}$$

where the integral is taken along a ray path through the medium. A direct consequence of the corrugated structure of the emergent wavefront is that ray trajectories are no longer parallel (for an initially plane wave). Hence, the rays are *scattered* through various angles. The width of this distribution is characterized by the scattering angle, θ_s , which is given approximately by

$$\theta_s \approx \lambda/L_\phi,$$

where λ is the wavelength of the radiation.

Weak Scattering

In Figure 1, the observer is located sufficiently close to the scattering screen that the ray displacements in the observer's plane due to scattering are much smaller than the phase fluctuation scale, L_ϕ . That is

$$z\theta_s \ll L_\phi,$$

where z is the distance to the scattering screen. (Many of the features of an extended medium may be approximately understood using this picture by setting z equal to the distance to the midpoint in the medium.) This condition is known as weak scattering. According to Fermat's principle, the complex voltage at each array element in the observer's plane is obtained by integrating the contributions from all parts of the wavefront, each of which is to be regarded as a radiation source. The dominant contribution comes from a region of scale size $\sqrt{\lambda z}$ at the screen, the Fresnel scale. Since this scale is just the geometric mean of $z\theta_s$ and L_ϕ , we have

$$z\theta_s \ll \sqrt{\lambda z} \ll L_\phi$$

for weak scattering.

Since the wavefront phase does not fluctuate significantly over the Fresnel scale, the phase at an array element is well determined from the optical path length of the ray reaching that element. Each array element then suffers some "propagation phase." The resultant shift in fringe phase on some baseline is just the difference in propagation phases for the two elements. Baselines much shorter than L_ϕ would have negligible corruption in the fringe phase ($\delta\phi_{\text{rms}} \ll 1$ radian). On baselines much longer than L_ϕ , the fringe phase would be essentially random, fluctuating on timescale

$\tau \approx L_\phi/v$, where v is the transverse velocity of the medium, relative to the line of sight. Note that no degradation of the instantaneous visibility amplitudes occurs. The amplitudes do, however, fluctuate slightly due to diffraction; for the limit discussed here, the corresponding intensity scintillation index is much less than 1.

These effects can also be readily understood as apparent images wander over angular scales $\approx \theta_s$, occurring on timescale, τ . Clearly, the fringe amplitude on baselines $> L_\phi$ is severely diminished if integration times $> \tau$ are used.

With a sufficiently short integration time ($\gg \tau$), the propagation-induced distortions of the fringe phase can be removed, if three or more array elements are used. This is possible because $(N^2 - N)/2$ independent fringe phase measurements are made per integration period. (N is the number of array elements.) Various well-known analysis techniques such as self-calibration and global fringe fitting have been developed to handle this problem. Therefore, recovery of much, if not most, of the source structure information is possible.

Scattering in the interplanetary medium is weak at frequencies $\gtrsim 300$ MHz, at solar elongations $\gtrsim 15^\circ$; and in the interstellar medium at frequencies $\gtrsim 7$ GHz, at galactic latitudes above 20° . An LLFA, however, can be expected to operate in domains in which these conditions do not obtain. Hence, it is necessary to consider strong scattering as well.

Strong Scattering

Figure 2 depicts a situation in which the observer is sufficiently far from the screen that

$$z\theta_s \gg \sqrt{\lambda z} \gg L_\phi.$$

This is the condition for strong scattering. Note that since $L_\phi \propto v^{1.2}$, and $\theta_s \propto v^{-2.2}$, this condition occurs in any case at a sufficiently low frequency. An observer receives an angular spectrum of rays of approximate width θ_s . If the instrumental bandwidth is sufficiently small ($\lesssim 2c/(z\theta_s^2)$), then interference among the received rays results in significant intensity fluctuations (strong scintillation, with index ≈ 1). Also, the phase in the observer's plane fluctuates randomly, decorrelating on spatial scales $\approx L_\phi$. Therefore, the fringe phase on baselines longer than L_ϕ is random, and it fluctuates on timescales $\approx L_\phi/v$.

For a *point source* of radiation, the fringes could, in principle at least, be recovered using techniques similar to those discussed in the context of weak scattering. Because both amplitude and phase scintillation are present, each element is corrupted by a complex factor, which varies on timescale, τ . With four or more elements, this corruption can be removed using phase and amplitude closure. The result, however, would be uninteresting unit visibility fringes! To be

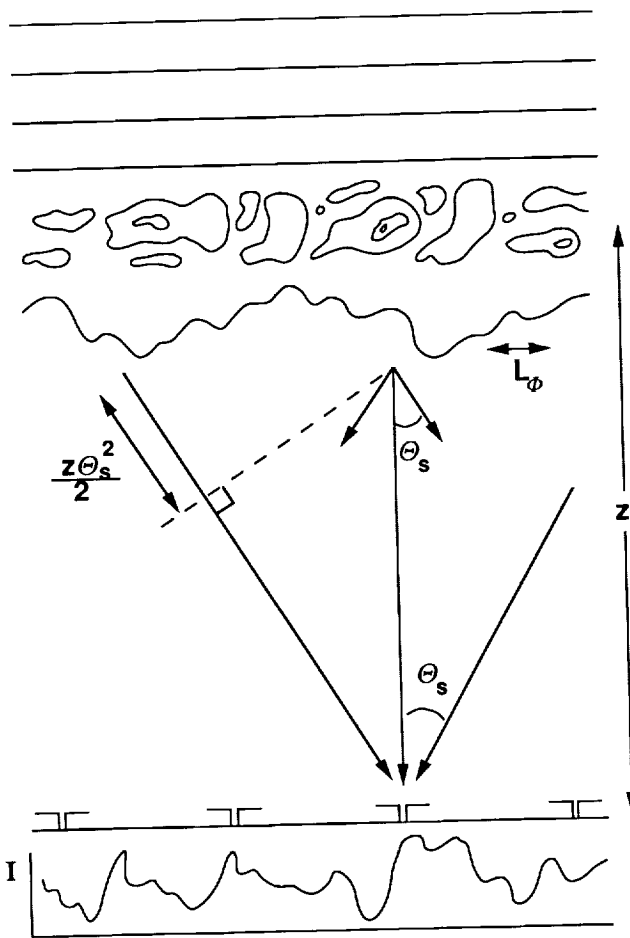


Figure 2. Strong scattering. In this case the ray displacements exceed the phase coherence scale, and an observer receives an angular distribution of rays of width, θ_s . Interference among the received rays results in intensity scintillations if a point source is observed with short time resolution, and if the bandwidth is sufficiently narrow that approximate coherence is maintained over the extra path length $(z\theta_s^2)/2$. The fluctuating intensity is shown schematically. In virtually all cases of interest, the scattering angle is a firm lower limit to the achievable angular resolution.

interesting, a source should have structure on angular scales resolvable by the array. If B_{MAX} is the longest baseline in the array, then to be at least partly resolved, the source should have structure on scales $> \theta \lambda / B_{\text{MAX}}$. It is important to compare this angular scale to the critical angle, θ_c , approximately defined as the angles subtended by the phase coherence length at the screen, i.e. $\theta_c \approx L_\phi / z$. If $\theta > \theta_c$, then the source can no longer be considered a point source, different parts of the source suffer uncorrelated phase corruptions, and the true source structure cannot be reconstructed. Conditions in the ISM result in a very small value for θ_c , much smaller than most sources of interest. For ultracompact

sources, such as pulsars, the baselines required to resolve angular scales comparable to θ_c , or smaller, are $\geq z\theta_s$. In most situations, this implies exceedingly long baselines of astronomical unit dimensions at GHz frequencies, given the constraints set by the ISM.

We find, therefore, that the structures examined with an LLFA would be considerably larger than θ_c . In this case, intrinsic structure is irretrievably smoothed by an angular distribution of width, θ_s , if the scattering is strong. This sets a firm limit to the achievable resolution. Baselines longer than $\lambda/\theta_s \approx L_\phi$ would show diminished visibility due to scattering. Hence, the longest useful baselines would be several times L_ϕ .

CONSTRAINTS ON THE LLFA

The Interstellar Medium

Interstellar scattering is typically strong for $\nu > 7$ GHz, along lines of sight to extragalactic sources at moderate to high latitudes (> 20 degrees) (Cordes et al. 1984). At lower galactic latitudes, the transition frequency (separating strong and weak scattering) is even higher. Clearly, we are well within the limit of strong scattering as far as the LLFA is concerned. Extrapolating from measurements made at GHz frequencies (Cordes et al. 1984), we have for the critical and scattering angles

$$\begin{aligned} \theta_c &\approx [10^{-10} \rightarrow 10^{-9} \text{ arcsec}] \nu_M^{1.2} \\ \theta_s &\approx [20 \rightarrow 120 \text{ arcmin}] \nu_M^{-2.2} \end{aligned}$$

for $|b| > 20$ degrees. ν_M is the frequency in MHz. The extrapolation is somewhat uncertain as the most appropriate value of the power law index is unknown. Also, there is considerable variation in the scattering magnitude from one line of sight to the next. Therefore, these magnitudes must be regarded as typical. Since the effective resolution cannot usefully be much better than θ_s , we find that we are limited to baselines

$$B \leq 50 \text{ km } \nu_M^{1.2}$$

It is also noted in passing that below about 1 MHz, the galaxy is at least partially opaque due to free-free absorption. Hence, this frequency is probably close to a lower limit for extragalactic, and many galactic, observations.

The Interplanetary Medium

Recently, Dennison et al. (1988) reported interferometric measurements of interplanetary phase scintillations at 327 MHz. Extrapolating their results to lower frequencies yields $L_\phi \approx 5$ to 15 km at 1 MHz and a solar elongation of 75 degrees. The corresponding scattering angles are 2 to 3.5

degrees. Since under these conditions the scattering is strong, these scattering angles represent resolution limits. Of course, the scattering angles will be somewhat smaller at larger elongation angles. At 1 MHz, then, the maximum useful baselines will be limited to several tens of kilometers. At somewhat higher frequencies, the limitations will be much less severe, since $\theta_s \propto \nu^{-2.2}$. These results are approximately consistent with Erickson's (1964) formula for θ_s , which predicts $\theta_s \approx 1.25$ degrees at an elongation angle of 75 degrees and $\nu = 1$ MHz. The minor difference between the two predictions may be attributable to the phases in the solar cycle when the respective data sets were taken.

In general, the limit set by interplanetary scattering is

$$B \lesssim 30 \text{ km } \nu_M^{1.2} \quad (\text{for strong scattering})$$

As indicated above, interplanetary scattering is strong in virtually all directions at 1 MHz. The transition to weak scattering occurs around 40 MHz at an elongation of 75 degrees, and varies with elongation angle. At the higher frequencies, at which the scattering is weak, the above limitation need not apply, provided sufficiently short integration times are used.

DISCUSSION AND CONCLUSIONS

The resolution limits set by interstellar and interplanetary scattering are comparable at very low frequencies. The maximum useful baseline is of order tens of kilometers at 1 MHz, and increases in rough proportion to frequency. Within these resolution limits, a wide range of forefront scientific investigations will be possible, including mapping of the galactic nonthermal emission, galactic thermal absorption studies, spectral observations of pulsars, supernova remnants, and extragalactic sources, and detailed studies of planetary emissions (Dennison et al. 1986). Indeed, an array of 10 km dimensions may well be quite appropriate for an initial deployment. Later stages could conceivably involve longer baselines which could be used profitably for detailed mapping of individual sources at frequencies ≈ 10 MHz.

Although scattering imposes limitations upon an LLFA, it is also an important object of investigation (Dennison et al. 1986). In this regard, as in other cases, an LLFA would be a unique instrument. By having baselines several times the phase coherence length, the apparent scattering disks of individual sources could be accurately mapped, and properties such as diameter and eccentricity determined. Interplanetary and interstellar scattering could be separated using the dependence of the former on solar elongation, as well as the fact that interplanetary scattering becomes weak at frequencies of tens of MHz. Since scattering size measurements would effectively be made for every source observed, it would be possible to map the galactic distribution of interstellar scattering. This has not been possible, since at higher frequencies intrinsic source sizes dominate over scattering. The combination of scattering size measurements and

low-frequency absorption measurements would facilitate a determination of the fractional modulation of the ionized gas density. Eccentricity in the scattering disks would indicate the presence of an anisotropy in the turbulence. By combining scattering measurements at very low frequencies with those at higher frequencies, it will be possible to accurately determine the power law index, and to search for the effects of an inner scale in the wavenumber spectrum. Finally, refractive scattering, if present, would produce noticeable distortions such as image doubling. It is widely suspected that refractive scattering occurs in the ISM, in addition to the diffractive scattering discussed above (Rickett et al. 1984; Simonetti et al. 1985).

Another medium which should be mentioned briefly is the Earth's magnetosphere. Close to the Earth significant refraction and birefringence are known to occur at low frequencies. In addition, intense auroral kilometric radiation (AKR) is generated at high magnetic latitudes. The lunar far side has the significant advantage of being well beyond the Earth's magnetopause, and therefore outside the region in which significant refraction and birefringence occur, even at 1 MHz. This site, of course, has the tremendous advantage of being shielded from the interfering effects of the AKR (as well as man-made terrestrial interference).

REFERENCES

- Cohen, M. H., and Cronyn, W. M. 1974, *Astrophys. J.*, **192**, 193.
- Cordes, J. M., Ananthakrishnan, S., and Dennison, B. 1984, *Nature*, **309**, 689.
- Cordes, J. M., Weisberg, J. M., and Boriakoff, V. 1985, *Astrophys. J.*, **288**, 221.
- Dennison, B. 1987, in *Radio Astronomy from Space*, ed. K. W. Weiler (National Radio Astronomy Obs.: Green Bank, WV), p. 137.
- Dennison, B. 1988, in *Future Astronomical Observatories on the Moon*, NASA Conference Publication 2489, eds. J. O. Burns and W. W. Mendell, p. 105.
- Dennison, B., Weiler, K. W., Johnston, K. J., Simon, R. S., Spencer, J. H., Hammarstrom, L., Wilhelm, P. G., Erickson, W. C., Kaiser, M. L., Desch, M. D., Fainberg, J., Brown, L. W., and Stone, R. G. 1986, Naval Research Laboratory Memorandum Report Number 5905.
- Dennison, B., Simmon, R. S., Ananthakrishnan, S., and Fiedler, R. L. 1988, in *Interstellar Scattering and Scintillation*, eds. J. M. Cordes and D. C. Backer, in press.
- Erickson, W. C. 1964, *Astrophys. J.*, **139**, 1290.
- Rickett, B. J. 1977, *Ann. Rev. Astron. Astrophys.*, **15**, 479.
- Rickett, B. J., Coles, W. A., and Bourgois, G. 1984, *Astron. and Astrophys.*, **134**, 390.
- Simonetti, J. H., Cordes, J. M., and Heeschen, D. S. 1985, *Astrophys. J.*, **296**, 46.

PART IV — DESIGN CONSIDERATIONS FOR A LUNAR VLFA

ENGINEERING FOR A LUNAR FAR-SIDE VERY LOW FREQUENCY ARRAY

Stewart W. Johnson
The BDM Corporation
June 1988

PRELIMINARY CONSIDERATIONS

The design drivers for a lunar far-side very low frequency array (VLFA) for astronomical observations from the lunar surface are listed in Table 1. The VLFA must be designed to gather data at frequencies of interest. It must achieve the desired sensitivity to small changes in brightness and also capability to respond to wide ranges of brightness. It must achieve spatial and temporal resolution to meet the needs of the community. A reasonable field of view of an appropriate part of the sky must be achieved. The operational mode must be selected whether it be scanning or aperture synthesis.

Options discussed at the workshop included having a large area sparsely populated with dipoles, a small area densely populated, a small area densely populated with outriggers, and finally a large area densely populated with dipoles.

The individual units of the array were discussed with the outcome being a conclusion that the individual units should be kept simple. Two options were dipoles and three-axis dipoles. Cross-links between the individual units and groupings of units are required and can take several forms including wires between units, radio links, fiber optic links, and some hybrid mix of linkages.

A computer capability is required for the VLFA. The questions discussed related the computer being in situ at the VLFA on the lunar far-side or in lunar orbit or elsewhere. Other questions discussed related to the time-phasing of the establishment of the VLFA and the prospects for enhancing its capability over time (Table 2). A phased development is desirable commencing with precursor missions to the Moon and evolving to an initial capability which can subsequently be enhanced.

Table 1. VLFA Design Drivers and Issues

Drivers for Design	Design Results	
<ul style="list-style-type: none"> • Frequency • Bandwidth on Frequency • Numbers of Frequencies • Range of Brightness very dim to very bright • Brightness Sensitivity distinguish narrow ranges of brightness • Polarization • Spatial Resolution (angular) • Temporal Resolution (time) • Field of View • Operational Mode 	<p>LARGE AREA sparse</p> <p>SMALL AREA dense</p> <p>DENSE with outriggers</p> <p>LARGE AREA densely populated</p> <p>Individual Units monopoles dipoles three axis dipoles Long vs. Short</p> <p>Crosslinks wires, fiber optics, radio, mix</p>	<p>Computational Algorithm</p> <p>Computer Capability</p> <ul style="list-style-type: none"> • in situ • orbit • other locations <p>Time to Build</p> <p>Enhancing Capability Over Time</p>

Table 2. Phased Development

Precursor

- Rudimentary Capability
- What Frequencies and Mode of Operation...and Why?
- Area/Volume/Mass/Power/Data
- Data Processing
- What do we need to learn early?

Initial

- Areal Extent, Numbers and Locations and Sizing of Dipoles
- Frequencies and Modes of Operations
- Features for Growth
- Constraints

Initial plus Enhancements

- Fill in and extend area?
- More frequencies of interest and why?
- Mass and volume of components
- Constraints

Initial Design

During workshop discussion it was decided that a strawman preliminary layout would involve 300 dipoles sited in a 17 km circle on the lunar far side. The suggested location is in the crater Tsiolkovsky which has some relatively flat mare-like surfaces and is at reasonable latitude for viewing and longitude to escape Earth-originating interference. The operating frequencies range from 1 to 30 MHz and the mode of operation is as an interferometer rather than a phased array. The resolution achievable at 1 MHz is to be 1°. A power law distribution of dipoles within the 17 km diameter circle is desirable. The properties of the lunar array suggested are as in Basart and Burns Table 2 in this volume with incremental dipoles each one meter long, observing frequencies of 1, 3, 10, and 30 MHz; bandwidths such as 20 kHz at 1 MHz; and beamwidths ranging from 1° at 1 MHz to 2' at 30 MHz. The engineering challenge is to design and deploy this array at the preferred site on the far side of the Moon.

Engineering for the VLFA

The need for the VLFA is to engineer the installation with the technologies that make it possible for the VLFA to perform well for long periods of time with minimal intervention by humans or robots. Contamination and interference can best be limited by reducing the need for nearby operations which produce rocket plumes, space suit effluents, other gases, particulates, ground shock, and extraneous radio frequency signals. Technology needs for the VLFA are listed in Table 3 and the engineering challenges are enumerated in Table 4.

Table 3. Technology Needs for the VLFA

- Deployment Capability (Vehicle with Robot)
 - Delivery to Site
 - Surface Transport
 - Variable Terrain Accommodation
 - Positioning Capability
- Dipoles
 - Solar cell
 - Battery
 - Radiation-hardened chip receiver
 - transmitter
- Communication links between dipoles and central station
 - Broad bandwidth with high radio band (GHz)
 - Receiver Chips with Very-Large-Scale Integrated Circuitry (VLSIC)
- Central Station
 - Computer
 - Shielding (from cosmic rays, UV, infrared, meteoroids, etc.)
 - Power
 - Transmitter/Receiver
 - Thermal Control
 - Solar Flare Shelter for Human Visitors
 - Vehicular servicing/control station
- Computer Algorithms
- Avoidance of Radio Interference
 - Internal versus other VLFA components
 - External operations not associated with VLFA

Table 4. Engineering Challenges for the Array

- Deployment in a Dusty Environment on Cratered, Unprepared surface; crater depth to diameter ratio 1 to 5; many blocks/boulders even on mare surfaces.
- Performance in Vacuum/Vacuum Outgassing
- Maintaining Calibration in Thermal Environment
 - temperature range 384 K to 102 K.
 - temperature change 5 K degrees per hour at sunset
- Designing Parts/Components for Temperature Extremes and Thermal Gradients
- Note: Number of cycles about one per month compared to LEO with about 480 per month.
- Radiation Hardening/Radiation Shielding for Cosmic and Solar Radiation Particularly for Electronics and Software
- Environmental Degradation (e.g., from Ultraviolet Radiation Induced Degradation of Thermal Control Coatings)
- Micrometeoroid Impact/Damage and Debris

A transportation system is needed to deliver the observatory components (the 300 dipoles and the central station) to the site in the crater Tsiolkovsky on the far-side of the Moon. Surface transportation is needed to deploy the 300 dipoles in the desired power law distribution within a 17 kilometer diameter circle. Navigation options for the vehicle are noted in Table 5. Construction capability is needed to set up and shield the central

station with is computer, transmitter/receiver, power supply, batteries, and thermal control capability.

Table 5. Deployment Vehicle

OPTIONS:

- Inertial Navigation Units
- External Beacon satellite
- Dead Reckoning steering angle and wheel rotation and slippage estimator
- Human operator (direct or telepresence)
- Hybrid-combination of capability

The surface mobility units first used for deployment should subsequently be useful in maintenance and repair of the array.

VLFA COMPONENTS AND DESIGN

Table 6 presents some design considerations for the components of the VLFA. Dipoles offer opportunities for innovative design. Each of 300 dipoles involves wires one meter in length, solar cells and batteries for power, a receiver and transmitter requiring radiation-hardened chips, and thermal control which may be either passive or active to assure that high and low temperature bounds are not violated.

Table 6. Design Considerations for VLFA Components

- Electronics Packages — Sizes, Power, Reliability, Redundancy, Repair, Aspects of Radiation Hardened Electronics—How Hard? Shielding required vs. hardness aspects; temperature range for operation vs. thermal control; heterodyne receiver?
- Recording of Data — how much, what type
- Data Processing — computational capability on the Moon
- Data Transmission

Frequencies	Uplinks	separation
Bandwidths	Downlinks	
- Compatibility with Science
- Compatibility with Satellites for Communication
- Power sources
 - solar RTG (Radioisotope Thermal Generator)
 - batteries DIPS (Dynamic Isotope Power System)
- Lifetime of system and how to plan for life (degradation, upgrade capability, etc.)

The communications links between dipoles and the central station offer opportunities for technological innovation and creative engineering. Each of the 300 or more dipoles must have its own radio frequency probably in the GHz range. Very-large-scale integrated circuitry is rapidly advancing (according to Basart) and may lead to a compact lightweight solution to the communications links problem.

Table 7. Options for VLFA Observatory Operation (The Human Interface)

- Never visited by humans—completely automated (completely remote operation)
- Human presence on site at time of need
 - Initial setup
 - Maintenance and troubleshooting
 - Upgrading of capabilities
- Human presence via telepresence and telerobotics

The design of the VLFA must involve a human interface aspect that is presented in Table 7. If the site is to never be visited by humans, there is called for a high level of sophistication in automation and robotics which may not be attained in a reasonable time frame. The options for involving humans in VLFA on-site development and upgrades need further trade-off studies before decisions are made as to which option or combinations of options are feasible. Human presence via telepresence and robotics is hampered by the long delay times if the communications are to a far-side site from a near-side lunar base or an Earth-based monitor. Human presence at the VLFA, even periodically, will require furnishing adequate shelter to protect people in the event of a solar flare. From 2 meters up to 3-1/2 meters of compacted lunar soil may be required according to Silberberg and coworkers (1985).

INFRASTRUCTURE FOR VLFA

A transportation system, communications, data processing/data reduction/interpretation, and Earth-based VLFA science center are essential. The maintenance/resupply network and the upgrading planning/implementation activity are also essential if the long-term mission of the far-side VLFA is to be completed over a 10-year lifetime. Life-cycle costing of the VLFA cannot avoid any of these five major categories of support listed in Table 8.

Table 8. Infrastructure for Far-Side VLFA

- Transportation System
 - VLFA delivery capability (to far side)
 - Surface transportation within an on-site 17 km diameter circle
 - Access from lunar orbiting station — periodic
- Communications System
 - Data relay satellite in lunar orbit
 - Data relay satellite in earth orbit
 - Earth orbiting space station monitor
- Maintenance/Resupply Network
 - Robotics
 - Telepresence
 - Human EVA intervention capability
- Upgrading Planning/Implementation Activity
 - Relates to Earth-based VLFA science center
 - Monitor health/status of system
 - Programs/executes modifications and upgrades

Table 8 highlights the support the VLFA on the far side of the Moon will probably require at various locations to function successfully.

Table 9. Mass To Be Delivered to Far-Side Site*
(Offered to Stimulate Discussion)

- Central station (could be reduced)
Note: The ALSEP mass was about 136 kilograms including power/communication, and science packages according to the ALSEP Review by Bendix Corporation of August 1972 (NASA CR 128597). 800 kilograms
 - Dipoles
One dipole with solar power, battery, receiver, transmitter, thermal control, shielding — 2 to 5 kilograms (could be much less) For 300 dipoles
600 to 1500 kilograms
 - Vehicle with associated robotics, sensors, power, guidance, communications, construction options 2000 kilograms
Note: (fully loaded with two astronauts, suits, and supplies, the Apollo LRV was 708 kilograms)
 - Backup equipment/redundancy kit (optional) 500 kilograms
- 3900 to 4800 kilograms

*(Rough Estimates)

MASS TO BE DELIVERED TO VLFA SITE

Table 9 presents rough estimates of the mass of the VLFA to be delivered to the far-side site. The VLFA may require

more than 4000 to 5000 kilograms delivered to the far side. Shielding of the central station will be with compacted lunar regolith to a depth of two meters to protect the computer and software from upsets caused by cosmic rays and solar flare radiation. The compacted lunar regolith is a poor conductor so waste heat rejection from the central station may require use of heat pipes. Heat pipe technology is available for such applications.

POWER NEEDS

The most significant uncertainties in masses associated with the dipoles and central station are in the power supplies, batteries, and thermal control systems. The day-night cycle on the Moon requires long-life batteries which are probably unavailable at this time if solar power is to be used. Batteries are likely to drive up the masses associated with power and thermal control systems. Fortunately, the power needs (Table 10) of the system are relatively modest and battery development is being pursued for other applications.

Table 10. Power Needs for VLFA*
Rough estimates for discussion purposes

Central Station	500 to 1000 watts (upper bounds)
Each Dipole	1 watt* (upper bound)

*Basart suggests power needs at each dipole may be in the milliwatt range

The central station is a candidate for an RTG and DIPS power system. The Apollo Lunar Surface Experimental Package or ALSEP was powered with a SNAP27 radioisotope thermoelectric generator (RTG) which furnished about 70 watts. The Dynamic Isotope Power System (DIPS) requires future development but is being considered for some systems.

THE DEPLOYMENT VEHICLE

Energy requirements for the vehicle to deploy the dipoles will probably be greater than noted for the Apollo LRV. On Apollo 17 LRV energy consumption (Carrier, 1988) was 1440 watt-hours for a distance traversed of nearly 36 kilometers in three EVAs. Vehicle energy consumption in deploying the dipoles will be a function of vehicle parameters and the length of the traverses, the amount of soil compaction as the wheels interact with the soil, the surface roughness, and the elevation change. Soil compaction is a factor here because more compaction leads to greater rolling resistance which leads to greater energy consumption. The cratered, unprepared surface and the low lunar gravity restricted Apollo LRV maximum cruise speed to 6 to 7 km/hr. This LRV could not climb slopes greater than 19°–23°. The nature of the site

determines the vehicle energy consumption. Is the floor of the crater Tsiolkovsky comparable in trafficability to the sites encountered by Apollo 15, 16, and 17 LRV? It may be. That hypothesis of comparable trafficability should be verified before a vehicle and its power supply are decided upon to serve the VLFA. Carrier (1988) points that a wheeled vehicle will perform satisfactorily if ground contact pressure is no greater than 7 to 10 kPa. We lack experience with more massive vehicles on the Moon. The fact that the Apollo LRV was successful cannot lead to the conclusion that a vehicle twice as massive would respond satisfactorily in the same mission. Ground contact pressure and other factors must be taken into account. It is possible to become stuck with wheels spinning on the lunar surface as did happen with the Apollo LRV. The resolution of this problem was for the astronaut operators to lift the vehicle and move it to better ground. Such an option will not exist for an unmanned or much more massive vehicle.

ENVIRONMENTAL EFFECTS ON VLFA COMPONENTS

Surveyor III components including a television camera, a soil mechanics scoop, and sections of tubing, some polished and some painted, were returned to Earth by Apollo 12 astronauts after 31 months on the Moon. Tests after recovery verified the integrity of most parts even after the extended exposure to the lunar environment. There were some failures which related to thermal cycling (e.g., a tantalum capacitor and some glass envelopes).

Thermal control coatings were noted to have degraded because of exposure to the environment on the Moon. Inorganic coatings originally white became tan in appearance because of solar radiation, adhering lunar dust, and effects of outgassing from spacecraft parts. As the appearance of the coatings was altered, the solar absorptance, which was originally 0.2, more than doubled. Lunar soil particles adhered to all surfaces and were noted to significantly alter the properties of thermal coatings. A small amount of adhering lunar soil could increase absorbed solar thermal energy by a factor of 2 or 3. The Lunar Module (LM) engine was a significant source of dust found on Surveyor III components. Apparently the descent engine accelerated dust to velocities in excess of 100 meters per second so that the effect was to literally sandblast Surveyor III's painted surfaces, even though the LM landing was 155 meters from Surveyor III. Landings near a VLFA will have to be planned to avoid comparable sandblasting and dust contamination by accelerated dust particles. Keep-out distances required may be as great as 300 to 400 meters. Counts of hypervelocity impact pits on Surveyor III parts place bounds on this meteoroid threat to VLFA parts. Solar wind sputtering was noted to have had little effect on the returned tubing after 31 months of exposure.

Several points which apply to the VLFA are apparent from a review of Surveyor III and other data:

- Protection of thermal control surfaces is essential (degradation with time must be a design factor).
- Shielding of sensitive components from micrometeoroid impact may be necessary.
- Laboratory investigations of degradation of operational integrity are necessary during development.

Components of the VLFA should be designed to survive in the lunar environment and then be subjected to extensive tests to assure that degradation will be not excessive over the lifetime of the system. For example, thermal-vacuum tests will be essential in development and preflight preparations of components. These tests are necessary to show that components can operate under cold and hot conditions and survive large thermal gradients. Connections involving dissimilar metals which result in thermal stress should be of particular concern in the design and testing phases of VLFA development.

PRECURSOR MISSIONS

Enhanced understanding of degradation processes and their rates is a reasonable goal for precursor missions to the Moon. We have a limited knowledge of lunar surface degradation of proposed VLFA components. Our knowledge can be enhanced by revisiting selected Apollo sites and recovering components for study. Also, an effort is needed to quantify the amount of disturbance and dust contamination occurring when an EVA astronaut does maintenance on the VLFA Central Station. Table II lists questions to be addressed on early missions to the Moon.

Table II. Engineering Questions for Precursor Missions

- Position locations on far side need improvement (≈ 10 km now in some areas) and better knowledge will help deployment operations.
- Sites—details of topography needed for deployment robot and/or final site selection. Contour maps needed.
- Verify trafficability parameters for specific competing sites for vehicle power/energy needs. Reduce ranges of uncertainty.
- Obtain information for terrestrial engineering tests of deployment vehicle system and risk analyses/trade studies of alternative deployment systems.
- Instrumental long-term degradation on Moon (needed to quantify design margins and reduce risk).
- Lunar ionosphere uncertainties
 - Diurnal variation?
- Simplified VLFA with dipoles deployed by inexpensive means on Moon
 - Impactors
- Terrestrial precursor of lunar VLFA
 - Dipole arrangement
 - Computational algorithms
 - Answer what-if questions

THE INITIAL ENGINEERING EFFORT

The VLFA that is finally deployed on the lunar surface should be the result of a phased development that involves careful design and test of each component and includes not only hardware but also software. A terrestrial prototype should be built and tested. It could be operated at somewhat higher frequencies to show the visibility of the system and the readiness of components. The terrestrial prototype and associated hardware and software could be applied to the task of reaching a near optimal layout and helping improve algorithms and data interpretation capabilities. The initial terrestrial prototype could be a very simplified version of the proposed lunar VLFA.

REFERENCES

- Basart, John P. and Jack O. Burns. (1988), "Lunar Far-Side Very Low Frequency Array," in these *Proceedings of the Workshop on A Lunar Far-Side Very Low Frequency Array*, NASA, in press.
- Bendix Corporation, ALSEP Review, NASA CR 128597, Aug. 72, 88 pages.
- Carrier, W. David III. (1988), Chapter 7, "Physical Properties," in *The Lunar Source Book*, Cambridge University Press.
- Johnson, Stewart W. and John P. Wetzel. (1988), "Advanced Technology for a Lunar Observatory," in *Engineering, Construction, and Operations in Space*, American Society of Civil Engineers, N.Y., N.Y., pages 1102-1113.
- Johnson, Stewart W., G. Jeffrey Taylor, and John P. Wetzel. (1988), "Environmental Effects on Lunar Astronomical Observatories," submitted for publication in the *Proceedings of the Second Symposium on Lunar Bases and Space Activities in the 21st Century*, NASA-JSC, Houston, TX.
- Johnson, Stewart W. (1988), "Engineering for a 21st Century Lunar Observatory," *Journal of Aerospace Engineering*, Volume 1, Number 1, pp. 35-51.
- Johnson, Stewart W. (1988), "Design of Lunar Base Observatories," in *Future Astronomical Observatories on the Moon*, NASA Conference Publication 2489, NASA, pages 127-134.
- Silberberg et al. (1985), "Radiation Transport of Cosmic Ray Nuclei in Lunar Material and Radiation Doses," in *Lunar Bases and Space Activities of the 21st Century*, W.W. Mendell, editor, Lunar and Planetary Institute, Houston, TX, pages 663-669.

LUNAR FAR-SIDE VERY LOW FREQUENCY ARRAY

John P. Basart
Department of Electrical and Computer Engineering
Iowa State University
Ames, Iowa 50011

and

Jack O. Burns
Institute for Astrophysics
University of New Mexico
Albuquerque, New Mexico 87131

ABSTRACT

We suggest an initial general design for a low-frequency array for the lunar surface. Deployment would occur over several phases. In the first phase, incremental dipoles would be placed in a semiregular pattern over a region 17 km in diameter. This would provide a resolution of 1° at the lowest operating frequency of 1 MHz. Operating frequencies for the array would range from 1 to 30 MHz. The array would operate in an interferometric mode rather than as a phased array. During subsequent deployment phases, additional antennas would extend the array to a larger size.

INTRODUCTION

It is appropriate to initiate the design of a low-frequency radio telescope array at this time, even though a possible launch date for such an instrument is many years away, because the large expense of deployment demands that many stages of planning and rethinking of the entire design be executed before any Earth-based hardware construction is initiated. In this paper we discuss the principal attributes of a lunar array, and suggest a base plan from which future plans can evolve.

The justification for installing a radio telescope on the Moon is to avoid the effects of the Earth's environment. It follows that the telescope would be placed on the lunar far side in order to shield the telescope from radio radiation from the Earth. The spectral region for which it is impossible to do radio astronomy from the Earth is the low-frequency region below the plasma frequency of the Earth's ionosphere. In this region the ionosphere totally blocks all celestial signals. In the range from the plasma frequency to several times the plasma frequency, the ionosphere corrupts the signals so badly that it is nearly impossible to collect reliable high-resolution data. To maximize the amount of information collected versus the cost of implementation, it is appropriate to consider collecting data over as much of the low-frequency range as possible. A suitable frequency range for initiating discussion is from 1 to 30 MHz.

ARRAY SIZE

With the frequency range roughly specified as above, the next consideration is the physical size of the array. This depends upon the frequency of operation and the resolution desired. In the very low frequency part of the spectrum, the resolution limit will be determined by wave scattering in the interstellar medium. A suitable formula for the calculating this is

$$\theta_s = 1.1^\circ \nu_{\text{MHz}}^{-11/5} (\sin |b|)^{-3/5}$$

where ν_{MHz} is the observing frequency in MHz and b is the galactic latitude. If we choose a latitude of 90° , which is the best case, the scattered size of a point source is 1° . While a telescope of 1° resolution seems rather crude, it would be vastly superior to anything available at 1 MHz at this time. The length of an array operating at 1 MHz and 1° resolution is 17 km. This length could be assumed as a lower limit on the array diameter.

The upper limit on array size is determined by the desired resolution at the upper end of the frequency band which produces smaller scattered size. At 30 MHz the scattering size is roughly 2 arc seconds. The array size for this resolution is approximately 1000 km. This is an appreciable fraction of the lunar circumference and may be totally inappropriate to consider. In practice, the upper limit would be set by cost and deployment problems. We suggest a multi-stage deployment program with 17 km being the diameter of the antenna array at the first stage. Subsequent stages would gradually increase the array size, considering both resolution and beam shape, until the maximum resolution at 30 MHz would be obtained.

Array expansion can be divided into two broad categories. The first method is to simply expand the array in all dimensions with the same mathematical law for the antenna element separation as the initial array. The second method of expansion is to place the new elements at a significant distance beyond the initial array. This would increase the

resolution more quickly. The trade-off is that large sidelobes are created.

SCANNING VS. APERTURE SYNTHESIS

The two principal modes of operation for an array of antennas are scanning a beam in real time using a phased array, and recording data and later synthesizing a beam via signal processing. The trade-offs between these two procedures are outline in Table 1. One of the most serious problems for a lunar array is the transportation of a lot of mass to the Moon. This problem essentially eliminates the use of copper wire to interconnect the elements. The table shows an alternate method of relaying signals by radio. We will discuss the trade-offs in the suggestions made in the table.

Antenna Element. In a harsh environment, such as the moon, we do not want any array element that requires mechanical movement. Beam movement must be done electronically. The simplest type of antenna is a dipole whose length could be either an appreciable fraction of a wavelength, such as $\lambda/2$, or it could be much less than a wavelength. In the latter case, the antenna is called an incremental dipole.

The advantage of a long dipole is that it has a directivity that can partially screen out unwanted signals coming in off the side of the main beam. A dipole's pattern goes to zero off the end of a dipole. Patterns for nine dipoles whose overall lengths range from $1/2$ to 2.7λ are shown in Figure 1. In our application, we can think of the physical size of the antenna being fixed, and the pattern varying as the operating frequency varies. A disadvantage of the pattern is that we would have to place a second set of dipoles orthogonal to the first in order to have complete sky coverage. A second disadvantage is that the pattern changes with wavelength. If the antenna were $\lambda/2$ long at 1 MHz, the same antenna would be 15 wavelengths long at 30 MHz. As can be seen in Figure 1, longer dipoles have complicated patterns. The beams split into multiple lobes pointing in unwanted directions.

The messy pattern situation can be eliminated by using a dipole whose length stays well below a wavelength at all operating frequencies. At the upper operating frequency of 30 MHz, the dipole length could be, say, one tenth of a wavelength. A $\lambda/10$ dipole has a three-dimension pattern like a very fat doughnut with a tiny hole in the center. As the frequency is lowered, the dipole pattern grows in fatness

Table 1. Scanning Array Vs. Synthesis Array

Attribute	Scanning Array	Synthesis Array
Antenna element	Incremental dipole	Incremental dipole
Antenna config.	Roughly $n \times m$ uniform array	Nonuniform spacing
Relative number of elements	Most	Least
Element connection	2×2 elements in group	2×2 elements in group
Group connection	Rows with possible amplitude taper Connection by wire or optical fiber	None
Phase shifters	Within rows and groups	Within groups
Large-scale connection	Radio relay at each row	Radio relay at each group
Phasing control path	Transmit to rows, run wires to groups	Transit to groups
Sidelobe level	Highest	Lowest
Observing time	Relatively short, depends on integration time	Few Earth days
Transmission-line mass	Most	Least
Computer controlled?	Yes	Yes
Backend processing	Simple	Complex

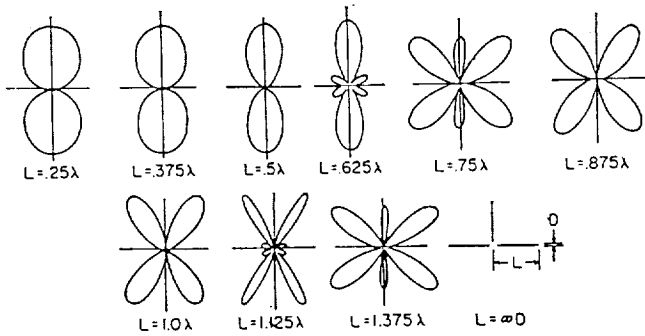


Fig. 1. Patterns for dipoles of varying lengths in terms of wavelength. L is one-half the dipole length. The dipole axis is the horizontal line through the center of the pattern. (after Jasik 1961.)

somewhat. Generally, the shape of the pattern would not change very much throughout the entire operating range of the array. While the incremental dipole would allow us to easily track a source without physical movement, it could not reject an unwanted signal coming in from some other direction. Source discrimination is obtained when the dipole elements are used either in a phased array or in a correlator (interferometer) array.

Antenna Configuration. Aperture synthesis imposes the least constraints in the placement of array elements. In an extreme case, elements can be placed randomly. The only requirement is a phase-stable communication link between each element and the control area. On the other hand, to create a real-time beam and scan it with minimal complications requires a dense uniformly-spaced array of antennas. Dense arrays have elements spaced on the order of one wavelength apart. A high density is required to keep side-lobe levels low. But with a synthetic aperture array, sidelobes are reduced by tracking a source over a wide range in the uv plane (spatial frequency domain) and combining the data later. Consequently, fewer elements are required in synthesis and the spacing is non-critical. Unfortunately, real-time use of a synthesis array is impossible unless the celestial signal source is so strong that sidelobe effects can be ignored.

One way to reduce the number of communication paths between the elements and the control area could be to group the elements in some fashion. One of the simplest groups is a mini-array of two elements by two elements. The elements within a group could be phased to produce a small amount of beam shaping. Phasing information would be sent to the group center where the phasing occurs. For synthesis, no more interconnecting is necessary. The group output would be transmitted via radio, or possible infrared, to the control area.

For a phased array, much more interconnection is needed beyond the group level. One possibility is to connect the

groups in rows and then interconnect the rows in a column arrangement. If appropriate, tapering could be applied at the group level or the row level to further shape the beam. Signal strength would be lowered, but the loss generally would not be significant since celestial sources in the very low frequency region are strong. The interconnection between groups could be made with optical fibers to keep the transportable mass low.

One strong disadvantage of a phased array in our application is that the pattern of the entire array changes with wavelength. Figure 2 shows a set of antenna patterns for 16 uniformly spaced antenna elements placed in a single line (linear array). The spacing between elements is fixed physically, but changes electrically as the wavelength changes. Horizontally, across the top, the numbers give the spacing between elements in terms of wavelengths. Hence as we change the operating frequency of the array, we are changing columns. Vertically, along the left side, are numbers giving the phase relationship between the elements. T represents the period of the observing frequency. Notice the large variation in shapes of the antenna pattern. We could design an array so as to minimize the pattern variation from one frequency to another, but the remaining variation would still cause difficulties in operation and data analysis.

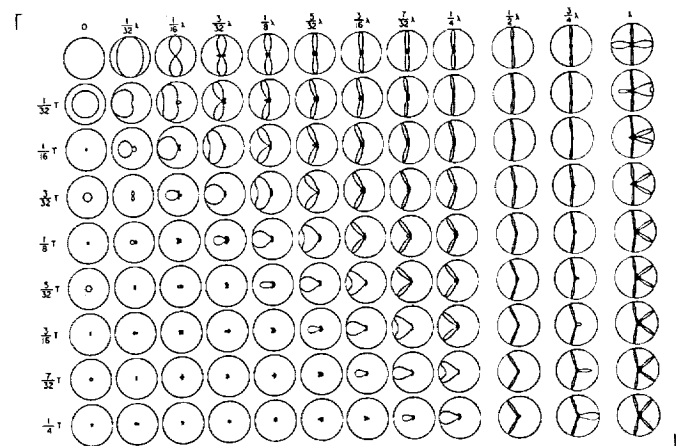


Fig. 2. Element patterns for linear array of 16 elements. The individual elements have no directivity. The patterns show variations caused by changing frequency, and by changing the phasing between the elements. (after Jasik 1961).

In both types of array configurations, a problem can arise if there is no beam shaping before the signals are sent from an array element, or elements, to the electronic equipment. Hardware always has a limited linear dynamic range. A strong unwanted signal could drive the electronics beyond the linear dynamic range. The small desired signal would either be lost completely or badly distorted. It may be necessary to shape the beam somewhat before sending the signals to the electronics.

Sidelobe level and observing time. A phased array would have a sidelobe level determined at the time of design. Element location in wavelengths and element type completely specify the sidelobes. This is also true for a synthesis array, but since element spacing is equivalently determined by the tracking time, we can lower the sidelobes by longer tracking. The longest tracking time would be for about 1/2 of a lunar day which would be about 14 Earth days. Thus, for low sidelobes, the trade-off is the complexity of a phased array vs. long tracking time for a synthesis array.

Other considerations. Regardless of array type, there would be a computer in a control area. For a phased array, the computer would be busy sending signals to the elements throughout the observation, but there is only one output signal from the array. It would easily be put into an image format by forming a raster. For a synthesis array, any element phasing would be minimal. However, the imaging is complex. The number of antenna elements chosen may have to be limited by the availability of computer power.

ARRAY EXAMPLE

To provide a focus for the characteristics of a very low frequency lunar array, we discuss a specific array element, the incremental dipole, and a square array of nonuniformly spaced array elements.

Properties of an incremental dipole are shown in Table 2 for four frequencies within the operating range of the lunar array. Attributes of the dipole and their units are listed in the left column. The physical length of the dipole is one meter in all cases. This was chosen so as to make the dipole's electrical length (length in wavelengths) 0.1λ at the shortest wavelength of 10 meters. Over this wide frequency range from 30 to 1 MHz, the directivity and the beam solid angle are essentially constant. This constancy is the principal reason for choosing the incremental dipole. No corrections to the mapping operation as a function of frequency will be necessary due to the dipole pattern. A directivity of 1.5 means that the dipole collects very little power more than an isotropic antenna which by definition has a directivity of one.

The fifth row lists the effective aperture area of the dipole. This effective area does not relate to any physical area as in the case of a paraboloidal antenna. The effective aperture area for a lossless antenna is defined as 4π times the wavelength squared divided by the directivity. As a wavelength increases with the directivity remaining constant, we get huge numbers for the effective aperture area. While the effective area of an aperture antenna, such as a dish, is smaller than the physical area, the effective aperture area of a wire antenna is much larger than the projected area of the wire because the physical wire intercepts a very small amount of power. Electrically, the wire looks much bigger than its physical size.

The last two rows of the chart illustrate the wide variation in impedance of the dipole over the frequency band. The radiation resistance is a measure of how much power a transmitting dipole radiates into space. The power radiated by the dipole is dissipated by this fictitious resistor. As resistance decreases, the radiated power decreases. The reciprocity theorem of antennas assures us that this property applies to receiving dipoles. Thus, as the radiation resistance decreases, the amount of received power appearing at the antenna terminals decreases. This characteristic is acceptable for the lunar array because the celestial signals are strong. The relevant property is resolution, not the total amount of power appearing at the antenna terminals.

The last item in Table 2 is the input resistance. Input reactance, which is not shown, becomes increasingly negative (capacitive reactance) as frequency decreases. The input resistance and reactance determine the dipole's impedance characteristics as seen by a transmission line connected to the center terminals of the dipole. This impedance varies considerably over the frequency band causing a variable power loss due to an impedance mismatch between the dipole and the transmission line. Again, the loss would be sustained rather than minimized by installing impedance matching devices since the absolute power level is not of primary importance. The total amount of power received when observing would be calibrated against a standard celestial reference source.

Table 2. Characteristics of a One-Meter Dipole

Attribute	Frequency, MHz			
	30	10	3	1
Wavelength, meters	10	30	100	300
Electrical length, λ	0.1	0.03	0.01	0.003
Directivity	1.5	1.5	1.5	1.5
Beam Solid Angle, Ster.	8.4	8.4	8.4	8.4
Effective aperture area, m^2	8×10^2	7×10^3	8×10^4	7×10^5
Radiation resistance, ohms	2×10^{-1}	2×10^{-3}	2×10^{-5}	2×10^{-7}
Input resistance, ohms	2	2×10^{-1}	2×10^{-2}	2×10^{-3}

ORIGINAL PAGE
BLACK AND WHITE PHOTOGRAPH

Figure 3 shows an example of a dipole with the receiver box attached which contains the receiver and solar power supply. The antenna rising vertically from the box receives and transmits information to the central control area.

Properties of a synthesis array are shown in Table 3. The table has two sections. The left half is for Phase One, initial deployment, in which the array size is confined to 17 km. In Phase Two, the array would be considerably expanded to increase the resolution at the high frequencies. The large dimension of 1000 km may be unrealistically large, but it sets an important goal of nearly one arcsecond of resolution at 30 MHz.

For convenience of this initial design study, array properties were calculated for a square array configuration with elements spaced at locations 2^n wavelengths at 30 MHz in both rows and columns. The smallest spacing is one wavelength ($n=0$). This configuration would give uv plane coverage similar to that of a uniformly spaced array after several days of tracking a source. This drops the synthesized sidelobes to a maximum of 13 dB below the main beam without any deconvolution procedure.

The number of elements in the two cases, 169 and 361, is minimal considering the large size of the two arrays. However, the number of correlations between all possible pairs of elements is substantial. The number of correlators shown is for two correlations between each pair. In synthesis we must correlate both real and imaginary parts of the signal.

The directivity entries in the table were obtained from the

theory of uniformly spaced arrays. Hence, they apply to the synthesized beam after several days of tracking, and not to an "instantaneous" beam obtained with a "snapshot" of data. Because of the similarity to a filled uniformly spaced array, the effective aperture area of the synthesized array is essentially the same as the physical area.

The resolutions listed represent the narrowest fringewidths at the various frequencies. Sources not passing over the zenith of the telescope would have lower resolutions decreasing as cosine of the smallest zenith angle during the observation run. Actual synthesized beam widths would be comparable to the figures shown.

The synthesized sidelobe level is stated as 1 dB below the main beam for all cases. It does not decrease for the larger array since the sidelobe level for a uniformly spaced array is always 13 dB down regardless of the array length. One significant effect has been neglected in the array calculations. This is mutual impedance between the elements. At the lowest frequency, many array elements will be less than a wavelength apart. Accounting for the mutual impedance between these elements will alter the array characteristics. Nevertheless, the numbers tabulated will be similar to those obtained from more detailed calculations.

An example of a circular array in the Crater Tsiolkovsky is shown in Figure 4. The element spacing is dense near the center and decreases radially outward. This is an indication of how the Phase I deployment would appear.

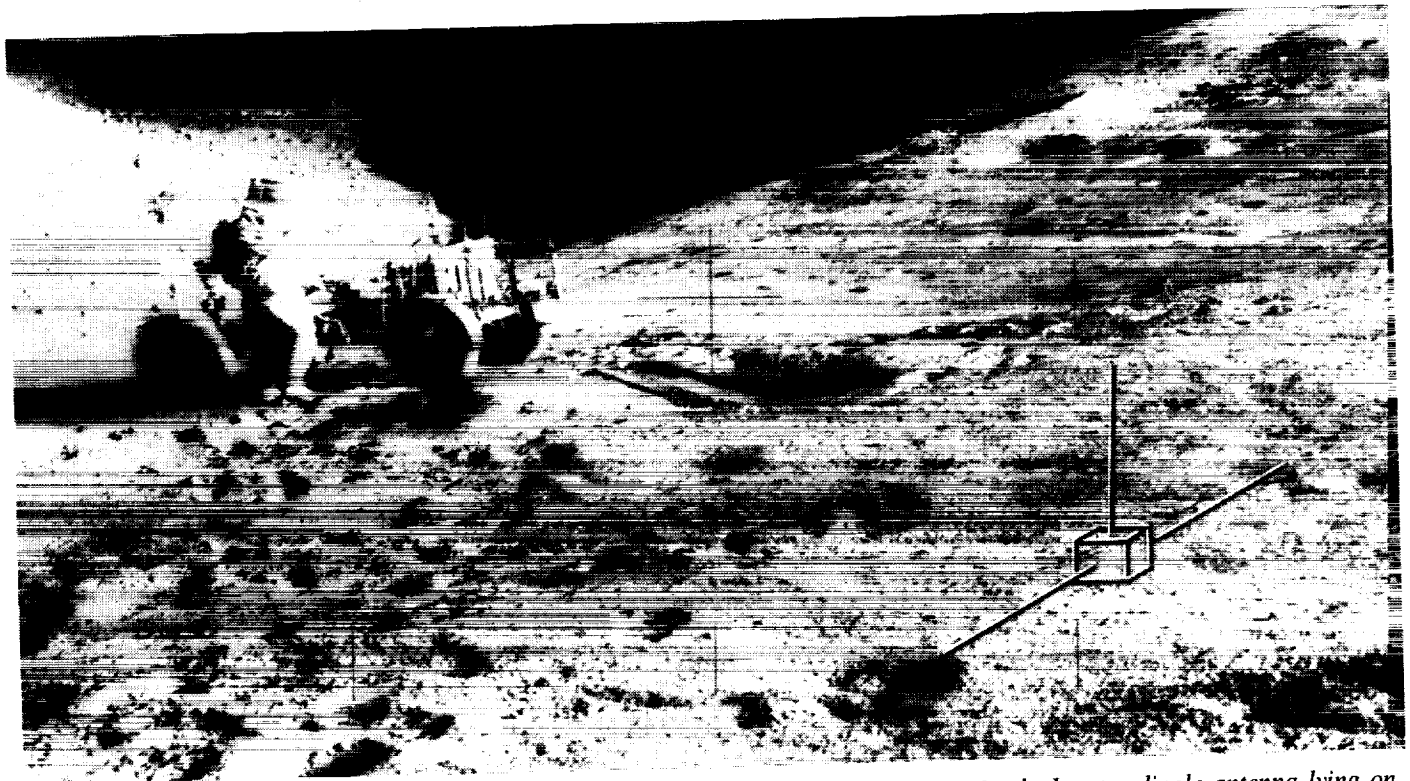


Fig. 3. Schematic illustration of a lunar low-frequency radio telescope illustrating a simple 1-meter dipole antenna lying on the lunar surface, an antenna to relay data back to a central processor, and a box to house the electronics. For scale, the dipole antenna is shown superposed on an Apollo 15 photograph.

Table 3. Synthesis Array Characteristics

Attribute	Frequency, MHz							
	1	Phase One			1	Phase Two		
		3	10	30		3	10	
Length & Width, km	17	17	17	17	1000	1000	1000	1000
Physical Area, km ²	289	289	289	289	10 ⁶	10 ⁶	10 ⁶	10 ⁶
Number of Elements	169	169	169	169	361	361	361	361
Number of Correlators		28392				129960		
Directivity Effective	8×10 ⁴	7×10 ⁵	8×10 ⁶	7×10 ⁷	3×10 ⁸	2×10 ⁹	3×10 ¹⁰	2×10 ¹¹
Area, km ²	289	289	289	289	10 ⁶	10 ⁶	10 ⁶	10 ⁶
Resolution	60'	20'	6'	2'	44"	15"	4"	1.5"
Sidelobe Level, dB	-13	-13	-13	-13	-13	-13	-13	-13

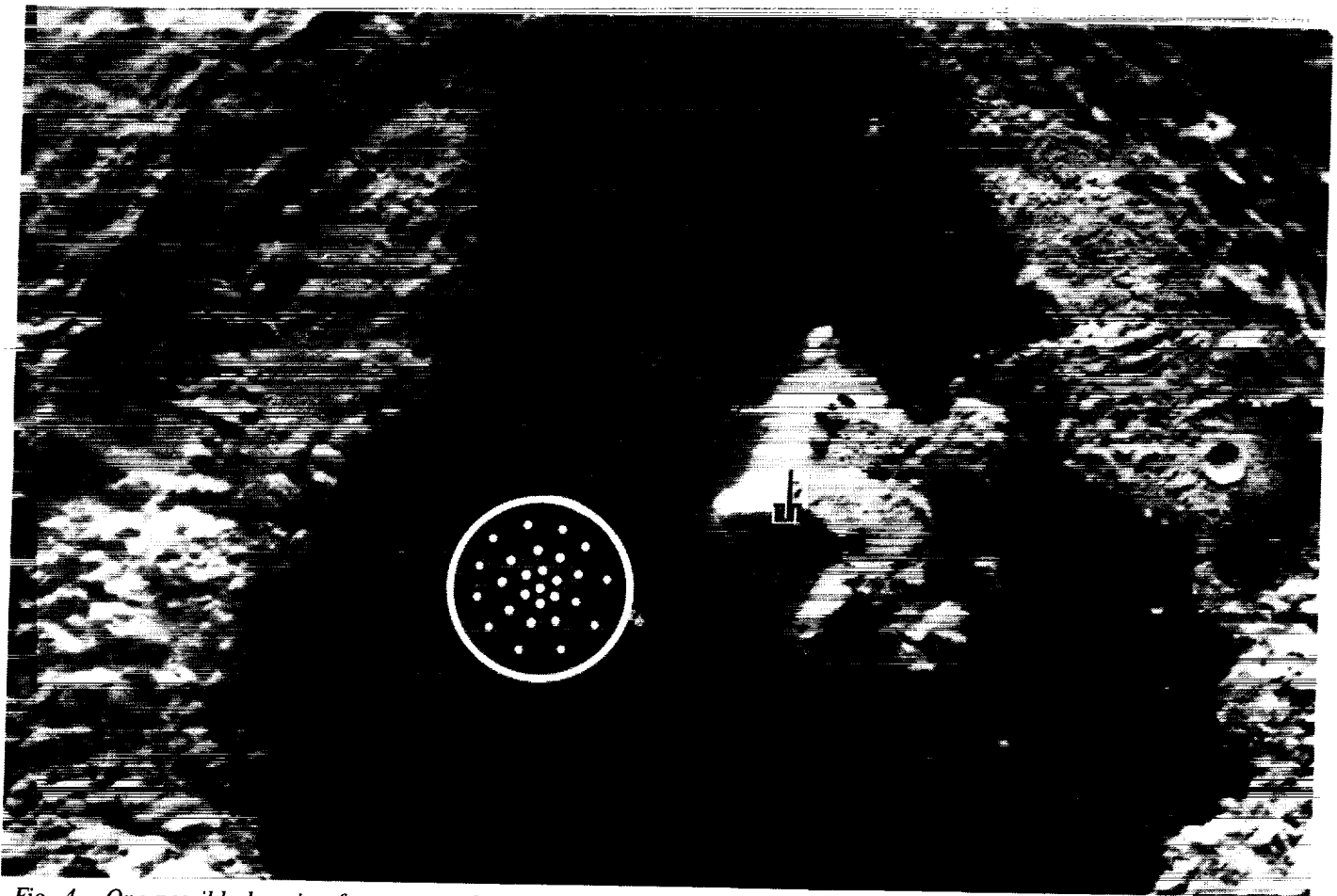


Fig. 4. One possible location for array on lunar far side within the crater Tsiolkovsky. The circle is about 20 km diameter. Dots represent a subset of 300 dipoles that will be deployed in a circular, power-law pattern.

COMMUNICATION LINK

With either a phased array or a synthesis array, considerable attention must be given to the communication link. For a phased array, many control signals with phasing information must be sent from the central area to the elements. For a synthesis arrays many signals from the antenna elements must be sent to the control area. The simplest communication method which avoids the transportation of mass to the Moon is to use either infrared or radio links. Transmitters and receivers for line-of-sight paths would be small electronic chips. One advantage of a radio link, rather than IR, is that the chip at each antenna element could be phase-stable a radio relay. The celestial signal would be upconverted and transmitted on to the control area. The local oscillator at the array element would be kept phase stable by a reference signal sent to it from the control area. A small box containing a solar cell, a battery, and a radiation hardened chip could easily be deployed by each dipole at the same time the dipoles are deployed.

The large number of communication links between the elements and the control area would require a significant amount of bandwidth in the electromagnetic spectrum. To obtain this bandwidth, the transmittal signals would need to be at a high radio band in the GHz portion of the spectrum. However, with the advancing technology in very-large-scale

integrated circuits, receiver chips may be available in the appropriate frequency range by the time the lunar radio telescope project is financed.

An example of a receiver-relay is shown in Figure 5. It receives signals at the four principal frequencies, one at a time. Control signals must be sent from the central control area to each receiver-relay to change observing frequencies. This is done at the frequency at which the receiver is currently operating. The digitally encoded signals are trapped by the decoder and sent to a controller which selects the appropriate bandpass filter, the receiver gain, and the down converter local-oscillator frequency. Upon the completion of this operation, the incoming radio waves from the celestial radio source, containing no digitally coded control signals, are passed through the encoder to the upconverter and then transmitted to the control center.

In addition to frequency switching information, the receiver-relay must receive a master local oscillator signal from the central control area for synchronizing its own local oscillators. This information is sent by radio to each receiver-relay. With a closed-loop path between the central control area and the antenna element, samples from the local oscillators can be sent to the master oscillator for synchronization purposes. The near vacuum of the lunar atmosphere will keep phase fluctuations due to propagation at a minimum.

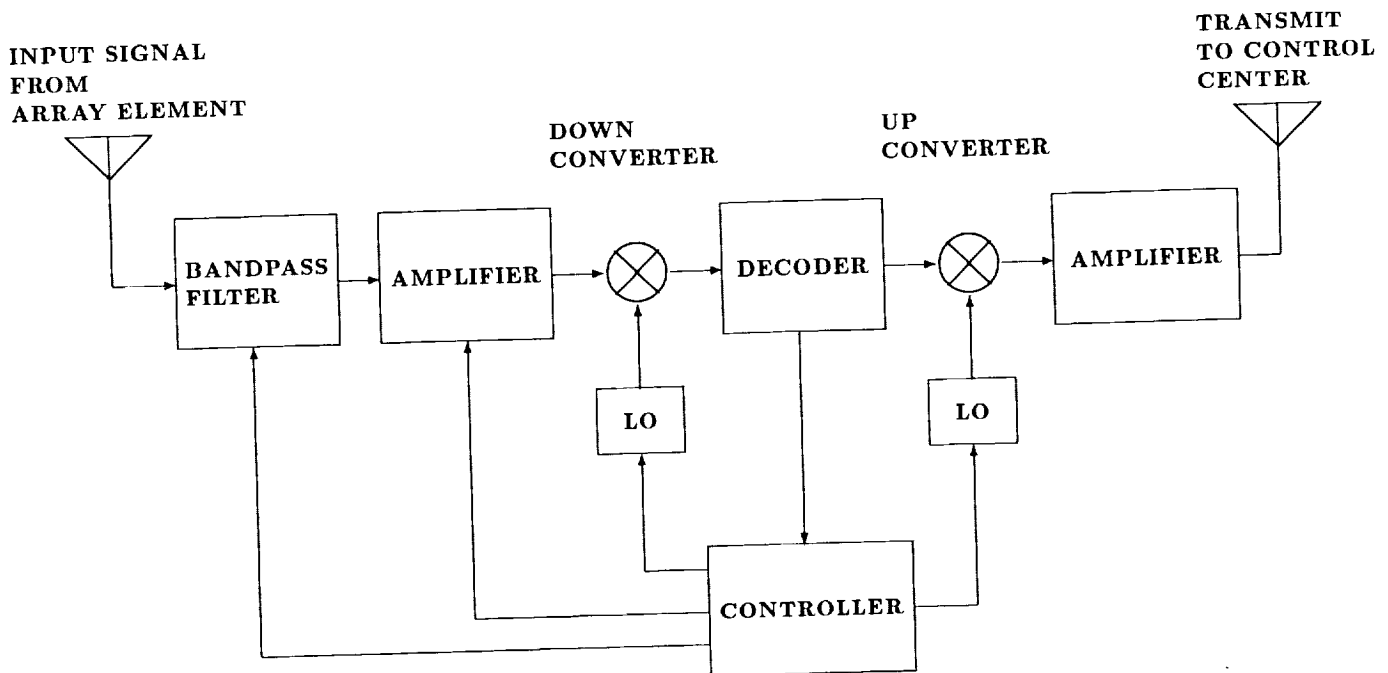


Fig. 5. Simplified block diagram of a receiver-relay. The device receives commands from the central control area through its receiving antenna in addition to the celestial signals. The celestial signal is upconverted and transmitted to the central control area.

COMPUTER CONTROL AND PROCESSING

The real-time computer systems' functions are to control the entire array operation, correlate all the signals received from the receiver-relays, and store the output. Several computers can be used for the various functions. One computer controls the transmission and reception of signals to the receiver-relays. A second computer controls the correlator system which itself is a special purpose computer. The data storage computer serves as a link between the on-line system and the off-line system.

The amount of operations to be performed per second depends upon the sampling frequency of the relayed signals. Assume for illustrative purposes that the bandwidth of each receiver is a maximum of 5 MHz. This must be sampled at 10 million samples per second. For 361 receiver-relays, we acquire roughly four billion samples per second. These signals are fed to the 130,000 correlators. The fringe rate is very slow on the Moon so a considerable amount of signal averaging can be performed on the correlator outputs, perhaps for minutes. Assuming one-minute averages, the system would output about 2000 numbers per second for a single polarization.

At the present rate of performance increase in computer systems, several future minicomputers will be able to handle the computer requirements for the very low frequency array.

PROPOSED ARRAY

Table 4 contains a brief summary of our suggestions for the general properties of a lunar array. We have chosen synthesis over a phased array because of the complications of the phasing in a phased array, and because of the flexibility offered by synthesis. The detailed suggestions are offered as a starting point for further evolution of a design. This array has a minimum resolution of 1° at the lowest observing frequency of 1 MHz and a maximum of $1''$ resolution at 30 MHz for the Phase II array. One frequency would be observed at a time, but future evolution of the instrument could include simultaneous observations at four frequencies since the incremental dipoles have frequency independent patterns. Also, a second polarization could be added. The technological advancements in electronic chips will keep the hardware at each element to a physically small size. We conclude that a lunar synthesis array that operates at frequencies and spatial resolutions significant for the advancement of astronomical research is technically feasible.

REFERENCES

Jasik, Henry, ed., (1961), Antenna Engineering Handbook, McGraw-Hill, New York.

Table 4. Lunar Radio Telescope Properties

Mode of operation:	Synthesis
Antenna elements:	Incremental dipoles about one meter long
Characteristic size:	17 km for Phase I 1000 km for Phase II
Impedance matching:	Ignore impedance matching. Large signal levels allow a loss
Observing frequencies:	1, 3, 10, 30 MHz
Bandwidth:	5 MHz maximum with several smaller bandwidths
Beamwidth:	1° @ 1 MHz, $20'$ @ 2 MHz $6'$ @ 10 MHz, $2'$ @ 30 MHz for Phase I $1''$ minimum @ 30 MHz for Phase II
Dynamic range of electronics:	At least 1000
Polarization:	Linear

PART V — POTENTIAL LUNAR VLFA SITE

SITE SELECTION CRITERIA

G. Jeffrey Taylor
Institute of Meteoritics
University of New Mexico

We have identified several criteria that must be considered when determining where to locate an astronomical observatory on the Moon. These are the following: longitude and latitude, topography, distance from a lunar base, value of the site to lunar geoscience, and value as a materials resource.

LONGITUDE AND LATITUDE

The high background of very-low frequency (< 10 MHz) radio waves emanating from Earth requires that a VLF array be located on the lunar far side. Because of librations of the Moon, only sites with longitudes $>98^\circ$ (East and West) are permanently shielded from Earth. However, because of growing radio-frequency interference on Earth, it is in general desirable to place all radio telescopes on the far side. An exception is the Moon-Earth Radio Interferometer (MERI), which employs one or more radio antennas on Earth, hence must tolerate radio interference. On the other hand, even this would benefit by location on the far side because it might afford a way to distinguish interference from the signals of interest.

To view the entire sky, telescopes must be deployed over a wide range of latitudes. However, a complex VLF (or optical) array is almost certain to be a unique facility, so an optimum latitude must be chosen. Because objects of interest occur in both Northern and Southern skies, it seems sensible to locate a VLF array within 20° of the lunar equator. Also, polar sites are weak for viewing the planets in our solar system as all the objects of interest would be at the horizon.

TOPOGRAPHY

The Moon's surface is divided into two distinct terrains, the highlands and maria. The highlands compose the oldest lunar crust and are densely cratered. Relief differences are large over relatively short distances. For example, central peaks and walls of large craters can rise 3–4 km above their floors. Some large basins (craters >100 km across) have floors that are relatively smooth and light-colored; the floor materials represent either volcanic flows different in composition from darker mare flows or are impact-generated, fluidized materials (which is the case of the smooth plain on which Apollo 16 landed). Because of the highlands' great age, they are covered with a thick regolith of impact-generated debris, hence tend to contain fewer large blocks of rocks. The maria are younger than the highlands and formed when lavas

erupted onto the lunar surface and filled low-lying regions. Mare surfaces tend to be much smoother than highland surfaces and are much less cratered. However, they also have thinner regoliths, so crater ejecta blankets tend to contain numerous blocks of rocks.

Topography enters into the selection of a site for an observatory more for ease of deployment and operation of the facility than for scientific reasons. The rugged terrain in the highlands makes it difficult for elements of an array to communicate by line of sight with a single central processing station. Also, deployment vehicles would need to maneuver around many hills and valleys created by old, degraded craters. On the other hand, blocks of rocks would be less of a hazard than in the maria. Overall, the optimum site would be a relatively old (>3.5 billion years) mare surface. The old age would permit a relatively thick, unblocky regolith and the presence of mare basalt flows would create relatively low relief across a large region.

DISTANCE FROM A LUNAR BASE

An observatory needs to be isolated from an active lunar base, especially if the base is the site of extensive mining operations. Several factors must be taken into account when estimating how far an observatory needs to be located from a lunar base. These are the distance from a lunar base located on a limb (90° longitude), seismic noise, atmospheric contamination, and dust.

Distance from a limb site. It might be desirable to locate a lunar base close to a nearside limb. For example, the Mare Smythii region holds great promise for lunar geoscience investigations and for lunar resource extraction (P. Spudis, oral presentation at AIAA meeting, Reno, 1988). To keep Earth in view (for both psychological and operational reasons), the base could be no farther than about 90° E. However, lunar librations cause sites up to 98° to be sometimes in view of Earth. Consequently, a radio array would need to be at least 240 km east of a lunar base located at 90° E longitude (1° equals 30 km at the lunar equator). Furthermore, radio waves from Earth would be diffracted. Assuming a perfectly spherical Moon, the diffraction region for very low frequency radio waves (300 m wavelength) is 75 km (see, e.g., Jackson, 1975, p. 447). Thus, this distance must be added to that caused by librations: a radio telescope must be located at least 315 km from 90° longitude.

Seismic noise. Lunar base activities will increase the general seismic background on the Moon. This might affect radio telescope antennas, especially dishes, and would almost certainly affect an array of optical telescopes. Using data from the signal strengths generated by charges placed on the lunar surface by astronauts and from impacts of the Apollo 17 lunar module, Cooper and Kovach (1975) developed an empirical relation between ground motion and seismic energy, $A = KE^{0.5}/r$, where A is the amplitude (nm), E is the energy (ergs), and r is the distance (km). K is an empirical constant, 2×10^{-5} . To estimate the effect of lunar base activity, let us assume that surface mining takes place continuously and calculate the ground motion (amplitude) generated by dropping 1 m^3 of soil from a height of 2 meters. This generates about 6×10^{10} ergs, assuming soil density of $2 \times 10^3 \text{ kg/m}^3$. This produces the following ground motions:

distance (km)	ground motion (nm)
1	5
10	0.5
100	0.05

The lunar seismic background produces ground motions on the order of 1 nm, so it is clear from the above that even an optical-telescope array will not be affected if it is located more than 10 km from a mining operation. This analysis does include the additive effects of each mining scoop. This would seem to be important because seismic waves are not attenuated rapidly on the Moon; for example, a signal damped out in minutes on Earth lasts hours on the Moon (Lammlein et al., 1974). However, it is unlikely for the signals from successive scoops to be in phase, so they will not simply add to one another. The above analysis also does not consider more potent sources of energy such as blasting operations. We are looking into the effects of these sources. Nevertheless, we can conclude confidently that artificial seismic disturbances will not affect radio observations on the Moon.

Artificial atmosphere. The Moon's tenuous atmosphere makes it ideal for astronomical observation. However, lunar base operations could lead to a significant increase in atmospheric density, as was first pointed out by Vondrak (1974). This problem has been addressed recently by Burns et al. (1988). Even considering the worst case, mining for ^3He (which might contribute as much as 1 kg/sec into lunar atmosphere), Burns et al. (1988) concluded that no significant growth of the atmosphere occurs beyond 10-100 km from a lunar base, roughly the range at which seismic pollution becomes negligible. However, if lunar base activities contributed $> 10 \text{ kg/sec}$, significant damage to the environment could occur.

Dust contamination. In principle, this could be a serious problem located within 1-10 km of a lunar base because of dust accelerated by rocket landings and lift-offs. However, this could be mitigated by construction of landing pads, so we do

not consider it to be a serious problem, but a quantitative analysis needs to be made. It is almost certainly of little concern for radio telescopes.

VALUE TO LUNAR GEOSCIENCE

The site for any astronomical observatory on the Moon ought to be chosen for its suitability for that purpose. Nevertheless, other factors, including operational considerations such as communications, being equal, it seems reasonable to propose choosing the site that has the greatest interest to lunar geoscientists. If this done, any visit by a crew to repair or expand the facility could include geologic sampling as well. Even during deployment by automated vehicles, geophysical instruments could be deployed as well, although this might add to the cost and complexity of the deployment.

VALUE AS A MATERIALS RESOURCE

Mining and astronomy are probably incompatible, so sites that hold obvious resource potential ought to be avoided. An alternative would be to designate areas for astronomy (and other sciences) within regions processing resources, keeping in mind the criteria for distance from a lunar base.

CANDIDATE SITE FOR A VLF ARRAY: TSIOLKOVSKY

The large crater Tsiolkovsky (Figure 1) is an excellent candidate for the site of a VLF radio array. The crater is 180 km across, rim to rim, and its floor is 113 km across, providing ample space for even an advanced array. It is located on the lunar far side at 20°S latitude and 130°E longitude. Thus, Tsiolkovsky is in the equatorial zone and far from any base established on the nearside: even a base on the eastern limb at 90°E would be 1200 km away.

The crater's floor is covered by high-Ti mare basalt (Wilbur, 1978) with an age similar to those of the Apollo 11 landing site, ≈ 3.6 billion years. The floor is smooth, except where punctuated by craters. Based on its age, a thick regolith ought to be present, thereby lessening hazards from boulder field near small craters. The central peak rises 3 km above the smooth plains. The central station located on the highest point could receive signals from anywhere on the floor: on a sphere with the Moon's radius, the horizon would be 102 km away when viewed from a mountain top 3 km high.

Tsiolkovsky is also interesting geologically (Guest and Murry, 1969; Guest, 1971; Wilbur, 1978). It represents an opportunity to study a relatively well-preserved large crater. The central peak probably represents uplifted, deep-seated materials, an ideal place to study the field relations of highland crustal rocks. It also provides an opportunity to study eruption mechanisms and post-volcanic tectonic processes.

There are two drawbacks to Tsiolkovsky as the site for

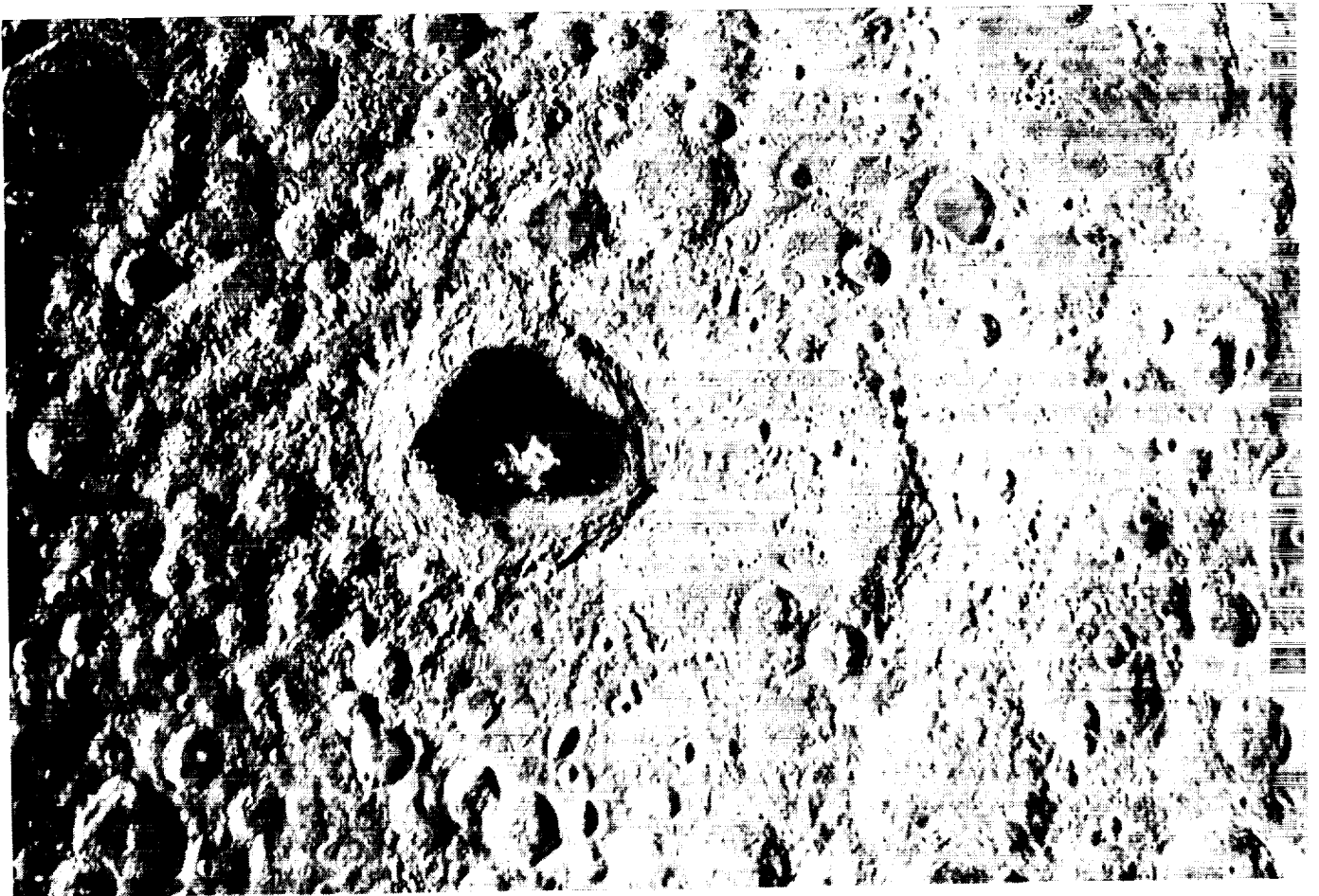
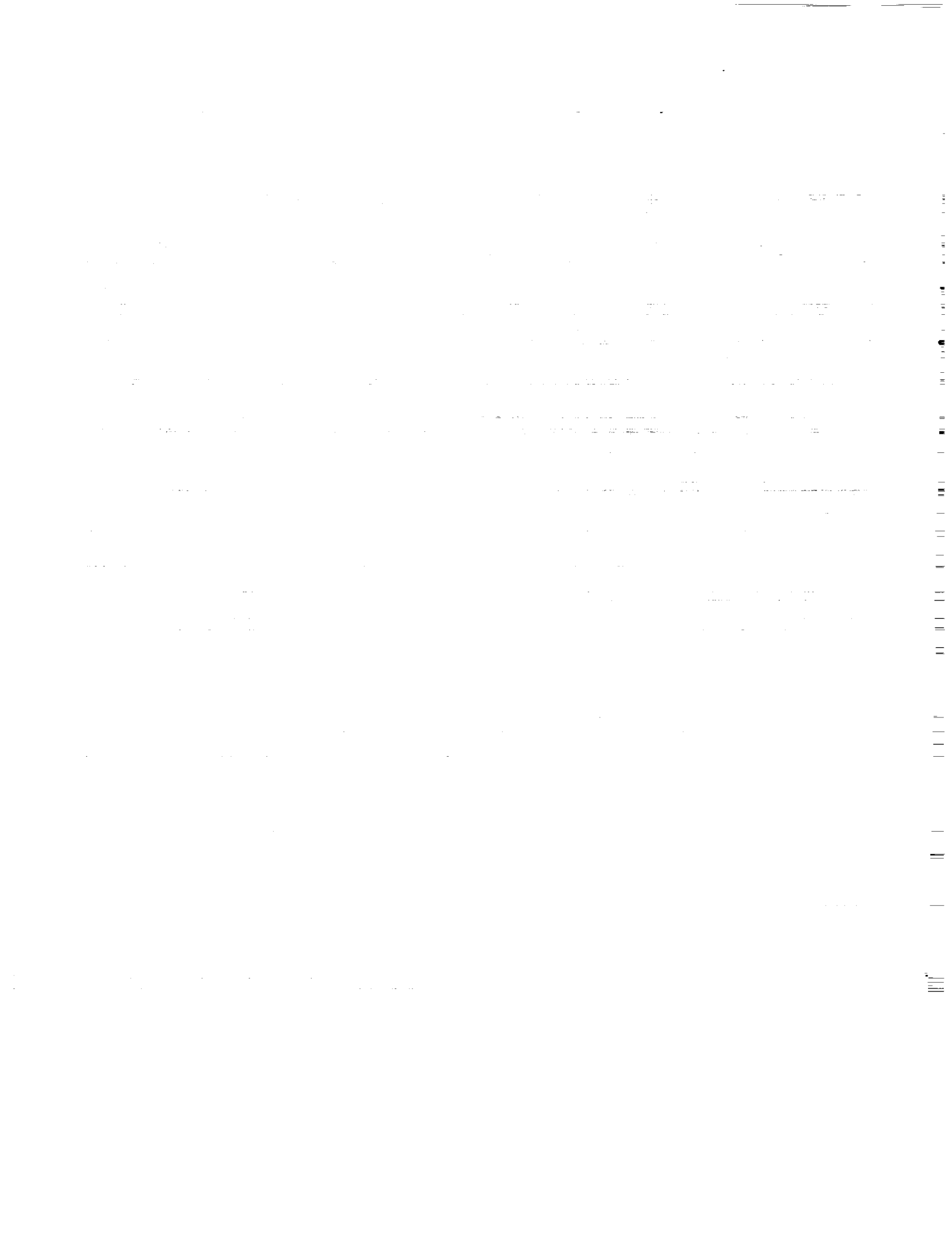


Figure 1.

the VLF array, although neither is a fatal flaw. One is that the walls rise 4 km above the floor, thus limiting the view of the horizon to $>6^\circ$ above the horizontal (if the array is centered 40 km from the crater wall). The second problem is that the mare basalts that help make the floor smooth are of the high-Ti variety. This makes the regolith in the crater a potential source of ^3He , which is found in greater abundance in high-Ti materials. However, development of ^3He -based fusion reactors for commercial power production is far in the future and Tsiolkovsky represents only a few percent of the total amount of high-Ti basalt on the Moon, so it would not need to be exploited. Furthermore, although high-Ti basalts are the richest source of He, all lunar soils, mare and highland, contain He in extractable quantities. If Tsiolkovsky turns out to be the best site for the VLF array, it ought to be declared a scientific preserve, closed to resource exploitation.

REFERENCES

- Burns, J.O., Fernini, I., Sulkanen, M., Duric, N., and Taylor, J. (1988) Artificially-generated atmosphere near a lunar base. *Lunar Bases & Space Activities in the 21st Century*, submitted.
- Cooper, M.R. and Kovach, R.L. (1975) Energy, frequency and distance of moonquakes at the Apollo 17 site. *Proc. Lunar Sci. Conf. 6th*, 2863-2879.
- Guest, J.E. (1971) Geology of the farside crater Tsiolkovsky. *Geol. Phys. Moon* (G. Fields, ed.), 93-103. Elsevier, Amsterdam.
- Guest, J.E. and Murry, J.B. (1969) Nature and origin of Tsiolkovsky Crater, lunar farside. *Planet. Space Sci.* 17, 121-141.
- Jackson, J.D. (1975) *Classical Electrodynamics*. John Wiley & Sons.
- Lammlein, D.R., Latham, G.V., Dorman, J., Nakamura, Y., and Ewing, M. (1974) Lunar seismicity, structure, and tectonics. *Rev. Geophys. Space Phys.* 12, 1-21.
- Vondrak, R. (1974) Creation of an artificial lunar atmosphere. *Nature* 248, 657.
- Wilbur, C.L. (1978) Volcano-tectonic history of Tsiolkovsky. *Lunar Planet. Sci. IX*, 1253-1255. Lunar and Planetary Institute, Houston.



PART VI — PROPOSAL FOR PRELIMINARY STUDIES

PRECURSOR MISSIONS

G. Jeffrey Taylor and Jack O. Burns
The University of New Mexico

VLF radio observations from the Moon could be made prior to installation of an array. These could be made by including appropriate antennas on missions planned primarily for other scientific purposes, such as deployment of a geophysical package, for engineering measurements, or as dedicated astronomy missions.

I. PRECURSOR MISSION

The only lunar mission currently planned by NASA is the Lunar Observer. This mission has been detailed by the Lunar Geoscience Observer Science Workshop Members (1986). It might be launched as early as 1994. Although its primary goals are to gather geochemical, mineralogical, and geophysical data about the Moon, it could carry an antenna to detect very low frequency radio waves. The mission is scheduled to last a year, so the spacecraft could have about six months of observing time shielded from the Earth during the portion of its orbit on the far side. Such an experiment was proposed for the Lunar Observer's original incarnation, the Lunar Polar Orbiter.

Automated landers have been proposed by various groups, most recently by the Lunar and Planetary Sample Team (1988, report in preparation). They fall into two categories. One class of missions is designed to establish a global network of stations (seismometers, heat flow probes, magnetometers, atmospheric monitors). There ought to be at least eight of these, approximately half of which would be located on the far side. These might be deployed by penetrators dropped from orbit, or perhaps by soft landers. The other category of missions is a series of Luna-type sample-return missions. Their purpose would be to perform geological reconnaissance of areas of interest. Geophysical and sample-return missions could be combined. Most important, any of them could carry VLF radio antennas, which might be used to establish a long baseline, but low density, array. Such additions to geoscience missions could, besides making astronomical observations, provide valuable engineering data to help design the best possible antennas for the VLF array and would provide a crucial test of the concept.

The above discussion envisions that VLF experiments are additions to missions whose main goals are to better understand the nature and origin of the Moon. However, one can also envision missions dedicated to astronomy, carrying payloads such as a dipole antenna, a radio dish, and an optical telescope for photometric measurements (Zeilik, 1988). Such missions need to be planned in detail.

II. SCIENTIFIC OBJECTIVES OF PRECURSOR MISSIONS

There are a number of important scientific objectives for very low frequency radio astronomy that might be met using relatively simple instrumentation on precursor missions. These include:

1. Detailed measurements of the lunar ionosphere. Our knowledge of the density and scale height of the ionosphere on the Moon is very poor at present. Yet this information is of critical importance in developing a design for a far-side VLFA. Is there a 100-m thick layer of ionized gas that hugs the lunar surface on the day side as suggested by Vondrak (1988)? If so, lunar dipole antennas would have to be placed on 100-m poles to rise above this layer of attenuating atmosphere. Short, tunable dipole antennas that transmit and receive low frequency radio waves can be used to probe the lunar ionosphere either from orbit or on the surface. From orbit, this radio frequency system could be used in conjunction with a laser ranging device to accurately determine the scale height of the lunar plasma.
2. All-sky survey at low frequencies. We have very limited knowledge of what the sky looks like below 30 MHz. We desperately need accurate, reliable maps of the sky down to 0.5 MHz for the purpose of detailed planning for the VLFA. Source counts could provide information on the numbers of sources we might expect to observe with the VLFA and the required sensitivity, and could contribute to observational cosmology. This survey would be the natural follow-up mission to the RAE. V-shaped antennas on an orbiting vehicle or on a far-side lander could perform this survey. Either spacecraft could be shielded from the Earth's interfering signals thus allowing sensitive observations free from the strong sidelobes produced by the Earth.
3. Study of signal propagation effects through the ISM. One of the more interesting (and complicating) effects at very low frequencies the effect of scattering by turbulent cells in the interstellar medium (ISM). Images are smeared and attenuated by this plasma process. We have only cursory observational data at present with which one can compare with models. To understand the effects that the ISM will have on lunar VLFA observations and how the VLFA might constrain models of turbulence in the ISM, we need observations at a variety of low frequencies, at a variety of galactic latitudes, and over reasonable time baselines. Such observations could be performed with simple dipole antennas on precursor missions.

4. Monitor variable sources. Flickering of extragalactic sources (i.e., rapid time variability) is believed to be due to scintillations of the ISM especially at low frequencies. High time resolution observations could, once again, constrain the nature of the ISM turbulence using a third dimension of information. Intrinsic variations of active galaxies and quasars are believed to be caused by accretion processes near the central black hole. Variations at low frequencies will sample a somewhat different environment in the outer corona of the black hole accretion disk. Dipole antennas on board long-lived precursor missions could begin sampling the extent and measuring the positions of very low frequency variable sources.

III. POSSIBLE CONFIGURATIONS FOR LOW FREQUENCY OBSERVATIONS ON PRECURSOR MISSIONS

A. Lunar Orbiter

A V-shaped, short (about 10 meter), low gain antenna would be most useful on an orbiting spacecraft. It would operate over at least a few frequencies possibly centered on a few MHz. The receiver should have a short time constant to allow monitoring of flickering of radio sources. Occultations of radio sources would be an important experimental capability. Therefore, the orbit of the spacecraft should be fairly elliptical with a major axis of about 36,000 km from Earth. The antenna plus receiver would probably have a mass of a few kilograms and occupy a volume of about 0.01 m³.

B. Lander: Impacter or Soft-Lander

If impacters are used to survey the far side, then simple short dipoles deployed from the impacters could perform

some important observations for both astronomy and geoscience. Such dipoles could be deployed in a manner similar to the telemetry antenna. If several impacters are used, then a long-baseline (hundreds to thousands of km) interferometric array can be established. Such an interferometer could be used to accurately determine the positions of new low frequency sources. Similarly, the array could use known sources to accurately determine the relative positions of the landers (thus providing an important position reference frame for lunar geographic surveys). Such an array might be particularly useful for long-term monitoring of magnetospheric activity of the planets and solar flares.

C. Landers: Rovers

Semi-autonomous rovers could carry a few dipole antennas plus receiver packages and "plant" them during their traverse. Once again, the dipoles could then be linked together as a simple interferometer with baselines over a few tens of kilometers.

REFERENCES

- LGO Science Workshop Members (1986), Contributions of a Lunar Geoscience Observer (LGO) Mission to Fundamental Questions in Lunar Science, Southern Methodist University, 86 pp.
- Zeilik, M. (1988), Lunar Automatic Photoelectric Telescopes (LAPTs), *Space 88*, in press.

PART VII — SUMMARIES, CONCLUSIONS, AND PROPOSALS FOR FUTURE WORK

SUMMARY REMARKS

James N. Douglas
The University of Texas at Austin

The best summary of this meeting and of this subject was offered by a visitor, who remarked that we "had a solution looking for a problem." It is clear that with a modest projection of extant technology a lunar-far side low-frequency telescope could be deployed. It is equally clear that none of the participants in the meeting could offer an astronomical problem of sufficiently transcendent interest and urgency to justify the investment, although a large number of routine tasks are obvious and, it could be argued, produce a cumulative justification. But such arguments are difficult to make, as is the argument for serendipity. So the first job for those interested in a lunar far-side array is to focus the case for low-frequency astronomy, and let such arguments drive the design and deployment strategy.

I. THE CASE FOR LOW FREQUENCY ASTRONOMY

1. The move to high frequencies

Radio astronomy began with observations at long wavelengths. Nature provided abundant and interesting steep-spectrum radio sources which were readily detected by the relatively low-frequency systems which were dictated by the receiver technology of the time and by antenna economics. Observations at these wavelengths were fundamentally limited by the optically active terrestrial ionosphere, which restricted the field coherence length and thus the resolution obtainable, and to add insult to injury, the same ionosphere at longer wavelengths propagated abundant and frustrating terrestrial interference into the systems at strengths fully capable of driving them into non-linear behavior.

Radio astronomers accepted these limitations and got on with a first-order inspection of the sky, uncovering phenomena of great importance. But many a radio astronomer of the day, in contemplating the design for a new generation telescope, wished for an observatory on the far side of the Moon, or alternatively, for lower noise high-frequency receivers and the funding to put up big dishes instead of wires.

The move to higher frequency is of course what has happened. The benefits of higher resolution (first anticipated and emphasized by Grote Reber in the 1930s) have been obtained, although in practice this was just as much a result of reduced ionospheric phase fluctuations permitting synthesis over very long baselines and of reduced radio frequency interference permitting continuous reliable observations as of the shorter wavelength itself. Steep-spectrum sources are of course weaker at these higher frequencies, but the sensitivity of

modern systems more than makes up for the weaker flux. Furthermore, new populations of flat or inverted-spectrum sources were uncovered, in numbers hitherto unsuspected. Increased understanding of the emission processes responsible for discrete radio sources pointed to the highest frequencies as being produced most directly by the underlying energy source, with the low frequencies being produced by old electrons. Not only was the observing better (and easier) at high frequencies, but the science seemed more promising as well.

Thus, the centroid frequency of observational radio astronomy has moved from 50 MHz (1930s and 1940s) to 100 MHz (1950s) to 400 MHz (1960s) to 5000 MHz (1970s and 1980s). A data point at 1400 MHz is now considered to be low-frequency, and one at 400 MHz is very low-frequency and probably suspect (and often with good reason!). And the frequency range below 100 MHz has been ignored by most astronomers since the 1950s.

2. The terrestrial low-frequency funding cutoff

The only general purpose synthesis telescope capable of operation below 100 MHz — Bill Erickson's TPT at Clark Lake — was recently cut off from NSF funding and shut down. A similar fate has also befallen the Culgoora array. Although steps to instrument the VLA at 75 MHz are now being undertaken, this recent history has discouraged designers of ground-based low-frequency arrays, and should be studied by those who propose low-frequency astronomy in space or on the Moon. What causes the lack of interest by the general astronomical community in frequencies below 100 MHz, and particularly in frequencies below 30 MHz?

i. Resolution

The primary reason, as suggested by Bill Erickson during this workshop, has to do with the low resolution of even the most modern low-frequency telescopes. To an astronomical community accustomed to seeing maps of sources with arc-second resolution, data obtained at lower frequencies with resolution of a few arcminutes — *ten thousand times worse* — is hardly worth considering, unless driven to it by scientific necessity. But comparing the maps of sources sufficiently nearby to be adequately resolved at low frequencies with their high-frequency maps shows only second order differences; thus far nature has not provided a compelling argument for low-frequency source mapping. To be sure, spatially averaged spectral information is obtained

for comparison with models, but such information is of ever poorer quality as the wavelength becomes longer, as the resolution becomes worse, and as the precision obtainable becomes limited by confusion and by ionospheric and calibration problems.

ii. Low-frequency phenomena play a support role

There are a number of phenomena which can *best* be studied at low frequency, such as galactic synchrotron emission, absorption by HII regions, and some domains of interstellar and interplanetary scattering. While all of these areas have their interested investigators, none have generated widespread interest and excitement; and the data obtained are more of a supplementary nature than a sole or even primary avenue of direct investigation.

iii. Unique phenomena are of specialized interest

Some phenomena can *only* be studied at low frequency, such as planetary and solar non-thermal emission. These phenomena are of enormous complexity, and are of considerable importance as their understanding involves an understanding of plasma instabilities in configurations which are impossible to produce in the laboratory. The theoretical insights potentially obtainable are of direct relevance both to laboratory plasmas and to the larger cosmic plasmas which are of great interest to astronomers. However, astronomers have generally abandoned the study of these phenomena to solar physicists and to space physicists, and support is diffused across several disciplines. This could be a position of strength, but historically it has been one of weakness — at least from the perspective of the astronomers.

3. Making the case for low frequencies

An outstanding but ultimately unsuccessful effort was made by Bill Erickson and his colleagues to make the case for ground-based low-frequency astronomy as practiced at the Clark Lake Radio Observatory. What additional weight can be added to the arguments in the context of a lunar farside VLFA?

i. What can we do with high resolution?

The resolution obtainable with ground-based low-frequency telescopes is limited by the ionosphere at all frequencies below a few hundred MHz, and less fundamentally but equally importantly by the omnipresence of RFI, making continuous operation — so necessary to many synthesis schemes — virtually impossible. Even when mapping is attempted by techniques such as hybrid mapping and other restoration schemes, dynamic range is limited by the ionosphere, as is knowledge of position and flux density.

On the lunar far side, absolutely calibrated arc-second resolution maps with good dynamic ranges could be accomplished at frequencies as low as 100 MHz and possibly as low as 30 MHz. The absolute position calibration of such far-side maps solves otherwise difficult position registration problems and the flux scale of the maps would be known. Extending the spectral base of precision mapping in this way down a decade or even two in frequency from 1.4 GHz dramatically expands the catalogue of interesting investigations that could be undertaken. For example, HII regions and SNRs would be resolvable in many more distant galaxies; extremely small knots of absorption could be noticed in our own galaxy. The quantitative results obtainable from the spectrum of such objects could open new possibilities of understanding the nature of the interstellar medium in a large sample of other galaxies than our own. These investigations will also produce information on the integrated emission along hundreds of thousands of lines of sight through our own galaxy, yielding new knowledge of the distribution and homogeneity of the Milky Way plasma.

A concerted effort should be made by interested astronomers (and particularly by theoreticians) both to consider these possibilities and to suggest and work out others. The question is: what can we do with VLA-resolution maps obtained at 10 meters wavelength?

ii. Extending the low-frequency window

The lunar far side will have an ionosphere—at least one and possibly two orders of magnitude less dense than that of the Earth. This implies far side observations could be made down to 1 MHz or possibly to 100 kHz; but even at 1 MHz other phenomena are beginning to limit performance. Interstellar and interplanetary scintillation limit resolution to about one degree at 1 MHz, and absorption by interstellar ionized hydrogen produces optical depth unity within a hundred parsecs or so. Still, the appearance of the radio sky at one degree resolution below 10 MHz is still unknown, and benefits (other than the obvious but still useful one of extending the spectra of sources known from higher frequency work) can be expected. Quite strong but very steep spectrum sources could exist at 1 MHz whose presence would be quite unsuspected from any work done to date. We have no reason to expect such sources—but suppose brown dwarfs were highly non-thermal emitters and also comically abundant (a suggestion due to John Wheeler)? Other obvious lines of inquiry include the distribution of local HII and synchrotron plasma and the behavior of interstellar and interplanetary scintillation mechanisms.

A coherent program of first-order exploration of this currently unknown territory should be organized, for implementation during an intermediate phase in the deployment of a VLFA on the lunar far side.

iii. Solar system non-thermal emission

Ground-based observations of meter and decameter non-thermal emission from the Sun have been made since the 1940s, and of the decameter radiation from Jupiter since 1955. The observational problems in these cases have always been different from galactic and extra-galactic work: the phenomena are quite reasonably strong, so that modest antenna systems suffice for adequate signal (although not of course for mapping!), but the radiation is also quite incredibly complex, leading to dynamic spectral observations on very short time scales in multiple polarizations in attempts to unravel things.

It has also been plain from the beginning that much of interest is just beginning to be visible at the longest wavelengths accessible from the ground and the early radio astronomy from space, such as the RAE missions and the more recent Voyager missions, have uncovered an amazing amount of detailed phenomenology—and not only from the Sun and Jupiter, but from Saturn, Uranus, and from the Earth as well.

From the point of view of planning low-frequency radio observations in space, perhaps the most dramatic result of the early missions was the impressive demonstration by the lunar-orbiting RAE II that Earth was an impossibly noisy object at all frequencies, producing antenna powers one to two orders of magnitude higher than background noise at all frequencies, but that when the RAE II was on the far side, the Earth disappeared (as expected).

Thus, developing a compelling case for further study—and particularly for synoptic study—of solar system non-thermal radiation automatically provides a strong argument for the lunar far side VLFA. As indicated earlier, this is a cross-field subject, without an influential general constituency among astronomers. It is up to planners of the VLFA to organize this as a strength rather than as a weakness, and to involve interested observers and particularly theorists from other disciplines.

Solar system non-thermal radiation is an important and unique observing opportunity for the lunar array, as was cogently argued by Mike Kaiser and Mike Desch at this workshop, and is suitable both for early stages of a lunar observatory, when copies of RAE or Voyager hardware could be deployed with only slight modification, and for succeeding stages, when increased sensitivity and mapping capability could support an ever more complete characterization of the phenomena.

II. THE LUNAR FAR-SIDE VLFA

The lunar far side has appealed to daydreaming radio astronomers for decades, as it has been presumed to supply the cure for two very real limitations to telescope performance: man-made and natural RFI (particularly important at decameter wavelengths), and irregular refraction and absorp-

tion in the atmosphere and ionosphere (important at any wavelength). The extension of the observable radio spectrum one or two decades lower in frequency is a bonus of potential if not demonstrable great importance.

What are the limitations on performance on a lunar far-side VLFA? What are some practical forms such as an array might take? And what are the areas where further investigation is merited before some preliminary version is needlessly frozen into too many people's plans?

1. Performance limitations

i. Geometry

The equatorial diameter of the Moon is 3476 km; the diameter of any array must be less than this if the vital benefit of shielding is to be enjoyed. Inasmuch as the various elements of an array must be capable of seeing the same bit of sky at the same time, the north-south dimension must be significantly less than this to make a reasonable range of lunar declination accessible to the array: if a range of $\pm\delta$ is desired, the extreme range of lunar latitude useable is $\pm(90-\delta)$. Librations and diffraction of RFI around the lunar limb must also be considered. A symmetric aperture of diameter of 2000 km would lead to a range in lunar declination of about $\pm 55^\circ$. Of course in principle the entire farside could be sprinkled with elements, and appropriate and best subarrays used for various directions in the sky. For purposes of further discussion, though, let us consider a 2000 km aperture, which would correspond to a one arcsecond beam at 30 MHz and a one-half arcminute beam at 1 MHz.

ii. Scattering

Scattering by the interplanetary medium (IPS) will affect all observations, and interstellar scattering will affect observations of galactic and extragalactic sources. Both processes probably vary at the 2.2 power of wavelength, with ISS being about 0.7 arcsec and IPS being about 42. arcsec at a frequency of 30 MHz (these numbers are from Douglas and Smith, and are in rough agreement with numbers presented by Denison at this workshop). At 1 MHz, the scattering angles become about 0.4 degrees and 1.2 degrees. If these numbers are taken to be correct for the sake of argument, the lowest frequency at which one arcsec mapping would be useful would be about 45 MHz, requiring an aperture of about 1340 km, while the largest worthwhile aperture at 1 MHz would be about 15 km.

iii. Absorption

For galactic and extragalactic observations one must take into account the increasing optical depth due to interstellar HII. The optical depth is proportional to wavelength squared, and is a few tenths at high galactic latitude at 1 MHz for lines

of sight that don't intersect HII regions. At low galactic latitudes, optical depth becomes large before one gets out of the local few hundred parsecs. At 1 MHz discrete HII regions will be opaque, even if of very low emission measure. Of course, this state of affairs is one of the things that makes observations below 30 MHz and particularly below 10 MHz astronomically interesting—but it will certainly produce a patchy view of the external universe.

iv. Lunar ionosphere

The Moon certainly has an ionosphere—the question is: how dense is it? Participants in the workshop were all mildly surprised that no one seemed to have better numbers than those quoted by Douglas and Smith, which came from lunar occultation observations in the 1960s. Those observations suggested an upper limit of $100/\text{cm}^3$, corresponding to an electron plasma frequency of 90 kHz. Apollo observations showed the presence of a neutral atmosphere of 10^{-12} torr; if fully ionized, this would correspond to around $4(10)^4/\text{cm}^3$, or a plasma frequency of 1.8 MHz. It is clearly vital for planning purposes to clear this matter up. Not only is the lower frequency limit of utility of the VLFA affected, but even at higher frequencies, resolution may be limited by the lunar ionosphere rather than by IPS.

2. Practical forms of the VLFA

i. Some basic assumptions

The entire spectral range below 50 MHz constitutes a bandwidth equal to one VLA channel—well within the routine data handling capability of modern digital circuits. Noise figures of front ends are low, and furthermore, the sky brightness temperature goes up (as $\lambda^{2.5}$ or so) with wavelength so that antennas whose efficiency decreases with wavelength can be tolerated without reduction in system signal-to-noise. These considerations led to a consensus of participants that it was probably possible to contemplate individual self-contained short tri-pole elements which are individually in communication, via satellite or optical link, with a central processor (located possibly on Earth, with daughter processors on the lunar surface or in appropriate orbit). It was also assumed that calibration could be achieved by lunar orbiting calibration transmitters, thereby removing the usual requirement of individual interferometer baseline elements which could see enough sources to calibrate themselves. Of course, all these assumptions about technology need to be checked out.

ii. The individual array elements

Elementary considerations of the theory of short antennas and matching circuits suggest that the efficiency of

impedance-matched short dipoles is inversely proportional to wavelength cubed, and inversely proportional to the fractional bandwidth of the matching circuitry. It may be, when matters are carefully investigated, that elements more nearly 10 meters in length than one meter would be required at the lowest frequencies—even after taking the sky brightness into consideration—if one wishes to avoid degradation of the speed of the array. But it may be that the well-known preference of low noise amplifiers to operate in a mismatched condition removes this problem. It may also prove advantageous to accept the degradation (if any) for the benefit of the shorter dipoles. This sort of investigation could be begun at any time.

The practical advantages of a synthesis array of individual and self-contained short dipole units were pointed out: the elements can be deployed by impactor, by robot vehicles which have been soft-landed, as well as by astronauts; their location need be known only approximately, and even that knowledge can come after the deployment; the elements can probably be designed so weight and power requirements are minimal, and tens or hundreds may be deployed per trip. The elements themselves are all identical, and considerable investment in their construction is possible, with custom VLSI chips housing the electronics, together with carefully designed solar power systems and deployment devices to cause the system to spring upright after having been literally tossed on the surface.

The specifications of the electronics package interact with what is deemed to be possible technically. Ideally, the system should be broadband—say 50 MHz to 100 kHz instantaneously—but in all likelihood this will be impossible. Alternatively, it should be multi-channel in that range, or perhaps dual-mode—broadband and inefficient (for solar system studies) and multi-channel and efficient (for galactic and extra-galactic studies). Clearly, the data rate from each element is also a consideration, and probably will be the limiting factor in the context of handling hundreds or thousands of elements. Although it would be premature to attempt a final specification now, a first trial balancing of all these factors would be highly desirable, and has not yet been done.

iii. The array configuration

Given the concept of N individual self-contained elements, it is a straightforward matter to run computer simulations of the performance to be expected (subject to assumptions about a possible lunar ionosphere). Enough such simulations have been run in other contexts to establish that the resolution of the system will be that of the aperture over which the elements are spread. The effective area of the system will be the number of elements times the effective area per element and the dynamic range will depend on the number of elements and on the accuracy of calibration. Thus,

$$(\Delta S)_{\text{array}} = \frac{2kT_{\text{sys}}}{NA_{\text{el}}\sqrt{\beta}\tau} = 1.341(10)^{-26} \frac{T_{\text{sys}}}{N\lambda^{1.5}\sqrt{\alpha}\tau}$$

for short dipoles, where $\alpha = \beta/f$ is the fractional bandwidth. The system temperature T_{sys} will be set by the sky brightness temperature T_{B} , which increases rapidly with λ down to about 4 MHz, and then more slowly. Taking the average sky brightness from Alexander (1970), which was based on ground-based and RAE data

$$T_{\text{B}} = 10750\lambda^{1.324} \quad (f < 4 \text{ MHz}) \quad T_{\text{B}} = 52.0\lambda^{2.53} \quad (f > 4 \text{ MHz})$$

we have

$$(\Delta S)_{\text{array}} = \frac{5284f^{0.176}}{N\sqrt{\alpha}\tau} \text{ Janskys, for } f \text{ (in MHz)} < 4 \text{ MHz}$$

and

$$(\Delta S)_{\text{array}} = \frac{24820f^{-1.05}}{N\sqrt{\alpha}\tau} \text{ Janskys, for } f \text{ (in MHz)} > 4 \text{ MHz}$$

The brightness temperature sensitivity of a synthesis array depends on the filling factor and on the bandwidth and integration time:

$$\frac{(\Delta T_{\text{B}})_{\text{array}}}{T_{\text{sys}}} = \frac{A_{\text{array}}}{NA_{\text{el}}\sqrt{\beta}\tau} = \frac{D^2}{2632N\lambda^{1.5}\sqrt{\alpha}\tau}$$

where D is the diameter of the equivalent synthesized aperture. The fractional error in brightness temperature reaches unity for $D = D_1$, where

$$D_1 = 51.31N^{0.5}(\alpha\tau)^{0.25}\lambda^{0.75}$$

The fractional error in brightness temperature at aperture diameter D is then $(D/D_1)^2$.

iv. Performance of a benchmark array

For purposes of a benchmark, let us consider a lunar array of $N=100$ elements, with 10% fractional bandwidth ($\alpha=0.1$), and a $\tau=10^5$ second integration. The column labelled S_{408} is the flux density at 408 MHz of a steep spectrum (spectral index = -0.8) point source which would have a flux of ten times the rms map noise at the observing frequency.

The rms map flux density is independent of the diameter D of the equivalent synthesized aperture and is adequate for studies of steep-spectrum point sources to a 408 MHz flux density of about 0.1 Jy, or about two hundred thousand objects.

Table 1. Properties of an Array with $N\sqrt{\alpha}\tau=10^4$

f (MHz)	$(\Delta S)_{\text{array}}$	S_{408}	D_1 (km)	Δ/T_{sys} (for $D=20$ km)
1.0	0.53 Jy	0.043 Jy	369.86	.0029
3.0	0.64	0.126 Jy	162.26	.0152
10.0	0.22	0.114 Jy	65.77	.0925
30.0	0.07	0.087 Jy	28.85	.4806

To attain near arcsecond maps one uses a large D (say, 2000 km) at 30 MHz. Such a system could produce 100-pixel maps for sources with 408 MHz flux brighter than about 9 Jy. This performance is useful, but by no means matches the VLA. One order of magnitude improvement would be realized by ten times the number of elements, or by stacking 100 maps (each of which represents a day's observation). It could also be attained with $N=100$ elements, each of which has a gain of 10 relative to a short dipole, but with attendant increased deployment and control problems.

The 100-element system when deployed to produce a synthesized aperture $D=20$ km would be useful for brightness temperature maps at 10 MHz and below, with resolution of about 5 arcminutes at 10 MHz and 50 arcminutes at 1 MHz. This 10 MHz performance is similar to the Clark Lake TPT at 100 MHz and the 1 MHz performance (neglecting probable scattering limitations) is similar to that of the original 80 MHz Mills' Cross.

In summary, the 100-element VLFA would be very useful for source spectra and for extending brightness temperature maps to low frequencies, but could produce arcsecond class maps of only the brighter sources in the sky. Our ultimate goal should be centered on arrays of a thousand or more elements.

3. Further investigations

A number of areas require further investigation before serious design work can be undertaken, while many other (perhaps most) problems are probably best uncovered and addressed by undertaking a serious (if preliminary) design study.

i. Interplanetary and interstellar scattering

Performance of the array at low frequencies will definitely be limited by interplanetary and interstellar scattering. Although a substantial amount of work has been carried out in both fields, which has formed the basis of extrapolations used above, much more can and should be done. In the final analysis, however, we must be prepared to find our predictions imperfect, and should arrange the deployment of early stages of the array to permit verification of predictions.

ii. Effects of the lunar ionosphere

Investigation of this problem is the most urgent of all issues: half of the case for a lunar location is based on the presumption that the ionosphere will be at least an order of magnitude less distorting than that of the Earth (the other half is RFI shielding afforded by the lunar far side). What is the density and scale height and variability of the lunar ionosphere? What are the correlation scales? We need to direct the attention of ionospheric physicists to this problem immediately, and plan on experiments to verify predictions in early stages of array deployment.

iii. Check basic assumptions

As noted above, we have been assuming many things are possible: active calibration of the elements and determination of their exact location through this process; individual communication possible without totally saturating link bandwidths; total mass per element small enough to contemplate many elements, and so on. Particularly noteworthy and worthy of careful examination is the short-dipole efficiency, and its bandwidth and stability if it needs to be matched. Although the possibility of higher gain elements was mentioned, it needs to be more carefully examined since such a direct impact on system performance would be produced by (for example) using local clusters of short dipoles as elements, rather than single units.

iv. Do a serious design study

Accept whatever uncertainties exist, and carry out a serious and complete design study, with the input assumptions carefully listed. This process will be more effective than any other method in uncovering problems and areas where tradeoffs are beneficial, and discovering just what the ultimate practical limitations on the array may be. The danger is that such an early design might become embedded in administrative concrete; this danger could be minimized by funding more than one group to carry out the study.

III. DEPLOYMENT OF THE LUNAR FAR-SIDE VLFA

This ambitious project will grow over a period of time, and the problem of setting forth a sensible sequence of stages must be addressed. Questions of scientific justification and administrative timing are of great importance and must be considered together with the purely technical ones of design checks and array performance. The following is a skeleton outline, intended to stimulate further thought on the matter.

1. Stage I—the return to the Moon

i. Lunar orbiter

A lunar orbiter with 0.1–30 MHz receivers is deployed, which is also capable of transmitting on a variety of frequencies in this range on command. The receivers would be used for passive occultation studies of solar system sources, including deliberately generated terrestrial signals; the transmitters would be used as probes for low-frequency occultation studies of the lunar ionosphere, as well as later for calibration signals for VLFA elements on the lunar surface.

ii. Early landers

A one-element system for solar system studies is deployed, capable of swept frequency and high time resolution. Several elements are deployed at a spacing of, for example, 20,200 and 2000 km, to be used interferometrically to check on limitations posed by the lunar ionosphere and by interplanetary and interstellar scattering and to verify the effectiveness of our calibration procedures. Although not very sensitive, even this system has the capability of detecting astronomical surprises.

iii. Tests of robot deployment

As a test of robot deployment, the beginnings of a cluster of antennas — perhaps 10 elements—are deployed over a region of 5–10 km. The elements should be linked to the central processing site by the system ultimately to be used; a data relay satellite should be in place and continuous processing begun. This is actually a useful if small system.

2. Stage II—the hundred-element array

i. Robot deployment of the hundred-element VLFA

This array would be deployed over a region of about 20 km, and should yield the performance discussed as a benchmark above. Many astronomical problems can be addressed at the two to fifty arcminute resolution of this system.

ii. High-resolution interferometry

The 20-km cluster of 100 elements will be used against one or more outlying elements hundreds and thousands of km away, producing a synthesized high-sensitivity interferometer. In addition to providing information necessary to the ultimate expansion of the system, preliminary information on the decimeter sky at this resolution is obtained.

3. Stage III—the arcsecond mapping instrument

i. Modified element design

Earlier stages will have suggested modifications in element design, which can be incorporated at this stage. In particular, to reach the 1000-element performance level needed, the competing possibilities of 100 ten-element clusters soft-landed and robot deployed or thousands of individual elements which are hard-landed must be decided.

ii. Deployment and incorporation of elements

Deployment would presumably occur over a period of years, with new elements brought on line as they are available; the system performance would gradually grow—

and could be biased in directions of new targets of opportunity discovered at earlier stages of the array.

IV. SUMMARY

The lunar far-side VLFA appeals to the observational radio astronomer as an achievable instrument of great potential. It will never be deployed unless a focused and convincing argument for its utility can be made. These remarks do not constitute such an argument but hopefully we will in due course find or assemble a compelling case. It is important to include as primary partners in this endeavor those solar and space physicists whose interest in the solar system non-thermal radiation processes can form part of the bedrock on which the structure is erected.



SUMMARY AND CONCLUSIONS

Jack O. Burns
The University of New Mexico

The workshop concluded with a general consensus on the scientific goals and preliminary design for a lunar far-side very low frequency array. Our major conclusions and recommendations are as follows:

(1) The lunar far side is the only viable location within the inner solar system from which to conduct sensitive, very low frequency (0.5 to 30 MHz) astronomical observations. Ground-based observations are severely limited by a generally opaque ionosphere, electrical discharges in thunderstorm activity, and man-made interference. Earth-orbit observations are similarly constrained by terrestrial atmospheric, leakage of radio and television transmissions through the ionosphere, and auroral kilometric radiation produced by plasma processes in the Earth's magnetotail. A far-side VLFA will be shielded from these interfering signals by the Moon.

(2) A lunar VLFA is technically feasible. The dipole and receiver components are simple, off-the-shelf technology. The data at the anticipated rates can be processed with current specialized correlators, such as those present at the Very Large Array radio telescope, and computers. Data transmission back to Earth can be accomplished with a communication satellite in lunar orbit. Although the thermal and cosmic ray environments are harsh on the Moon, they do not present any substantial engineering or maintenance problems for the array. The major new technology that must be developed for this observatory is an automated robot for remote deployment of the dipoles.

(3) Unlike radio telescopes operating at higher frequencies, the system temperature (i.e., noise characteristics) will not be limited by receiver or internal electronics noise, but by the brightness of the sky. The astronomical signals that we anticipate will be strong. Therefore, impedance matching of the dipoles to the system electronics is not a crucial issue. So, short dipoles of about 1 meter length (much smaller than a wavelength) will be adequate. This will greatly simplify deployment and reduce the mass of the array.

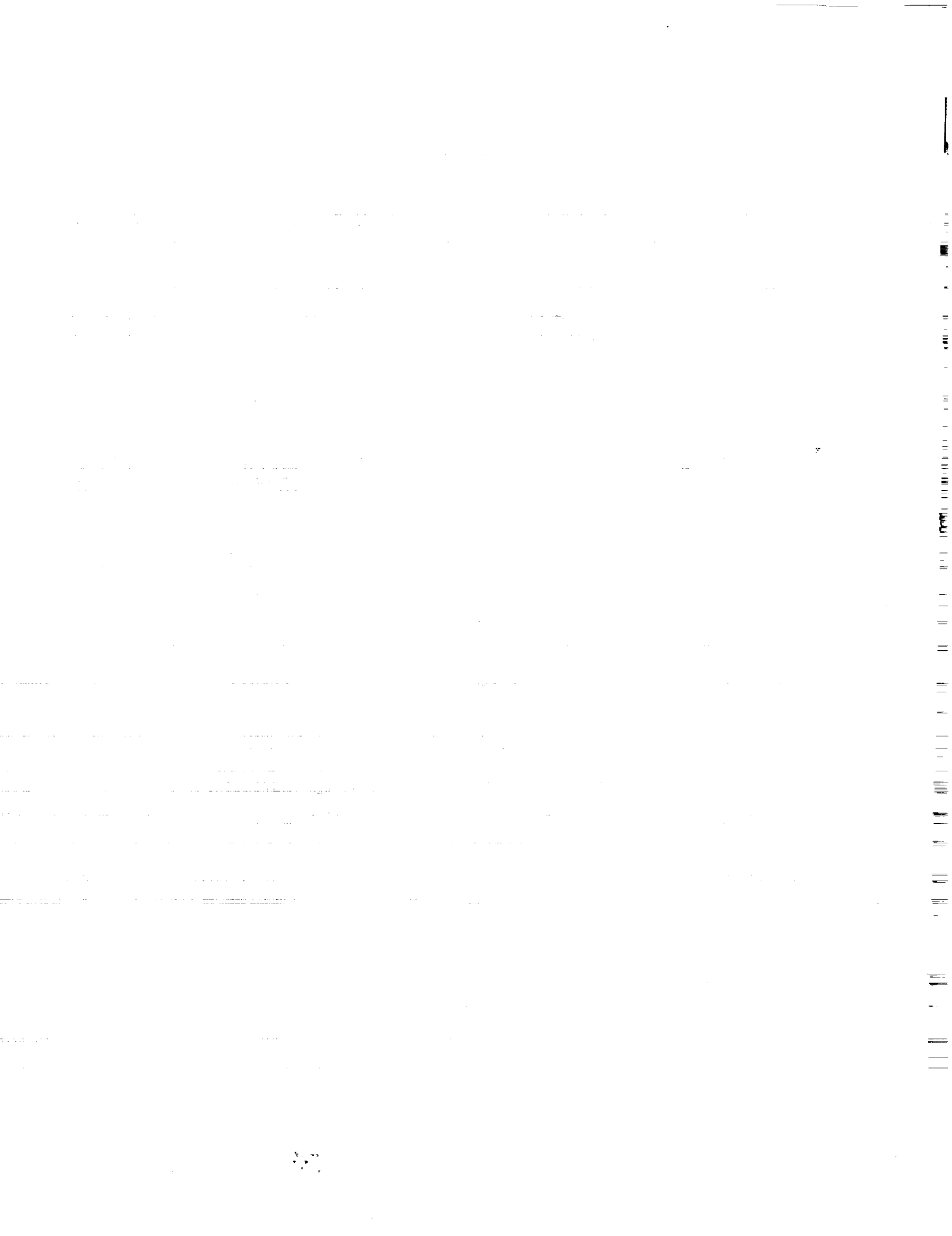
(4) The beam size and shape, and the directivity for a short dipole are all relatively poor. To improve upon these characteristics, we propose to group the dipole antennas into mini-arrays consisting of two by two elements. The elements within a group could be phased to produce a small amount of beam shaping and improve the pointing.

(5) The initial, phase I array would consist of roughly several hundred dipoles spread over a circle with a diameter 17 km. Since interstellar scintillation limits the resolution at 1 MHz to about 1° , there is no reason to build an array with longer baselines at this frequency. This would also produce several arcminute resolution at 30 MHz. For the higher frequencies, one would like to extend the baselines to diameters of at least 1000 km in phase II. The phase I array could be deployed in a spiral-like pattern with a high density of antennas near the center and lower density near the periphery. We suggest antenna spacings that increase with radius roughly as a power-law (i.e., r^n) where the index of the power-law (n) would be determined by computer simulations. In analogy to the VLA, we expect this pattern to produce good instantaneous u-v coverage (i.e., a good synthetic aperture). The emplacement of individual dipoles is not at all crucial with variations of tens of meters around the nominal pre-selected positions possible due to terrain considerations.

(6) The preferred mode of operation for the array is aperture synthesis. This will produce the best beams with lowest sidelobes and the least complications in communication between elements. The post-processing of data in this mode is more complicated than in a scanning mode but no more so than the current VLA. Operationally, aperture synthesis is simpler and more reliable.

(7) The scientific motivation for a lunar VLFA is potentially very strong. One could map the propagation of electron streams through the corona of the Sun produced by solar flare activity. Magnetospheric plasma processes near Mercury, Jupiter, and Saturn tend to produce low frequency radiation that can be monitored and analyzed with the VLFA. The galactic thermal and nonthermal background can be mapped to study the properties of the interstellar medium, and the origin and propagation of cosmic rays. Measuring the low frequency spectrum of extragalactic sources would be useful in understanding the process by which radio emission is generated, and how relativistic particles are accelerated and evolve with time. One might also find evidence of coherent radiation processes in extragalactic sources that are common in solar system magnetoactive plasmas. These exciting scientific goals require further study to tailor their applications to the VLFA.

PRECEDING PAGE BLANK NOT FILMED



SUGGESTIONS FOR FUTURE WORK

Jack O. Burns
The University of New Mexico

Not unexpectedly, the workshop generated many new questions about the lunar VLFA that must be addressed before any serious design studies can be undertaken. We divide these questions into two categories: Science and Engineering.

I. FURTHER SCIENCE INVESTIGATIONS

(1) The general consensus of the workshop participants was that the scientific justification for low frequency radio astronomy in general is not well focused or detailed. There is a great deal of potentially exciting and important astronomy that might be conducted with the VLFA, but at present the scientific goals are too vague and general. In particular, more study must be undertaken of the potential observations of the planets and the Sun. Within the general topics, such as the interstellar medium and extragalactic radio sources, we must develop stronger quantitative, theoretical arguments for observations with the VLFA. Predictions with specific observational signatures would be useful. We suggest that theoreticians be asked to join the working group on the VLFA. The scientific goals must be well established before detailed design work can begin.

(2) Some effort must be made to "sell" the VLFA to the astronomical community once the scientific justification is better focused. We will likely be in competition with other branches of astronomy for funding. Thus, our arguments for the VLFA must be at least as intriguing as those for x-ray and infrared astronomy. Unlike these other fields, however, low frequency radio astronomy has yet to fly its first survey instrument. We are effectively in the same position as x-ray astronomy in the early 1970s when the UHURU satellite was launched. These other fields have had an opportunity to discover many new exciting sources of radiation and, thus, to mature. Low frequency radio astronomy is still in its infancy. Serendipity will play a large role in a lunar VLFA since we are not really sure what the sky looks like in this uncharted window. This puts us at a distinct disadvantage with respect to other, more developed areas of astronomy.

(3) Some very useful survey work at low frequencies could be performed on precursor missions that might be launched in anticipation of the establishment of a permanent lunar base. A simple dipole or V-shaped antenna could be placed on board a lunar geoscience orbiter. This would be the successor of the RAE satellite. This instrument could survey the sky at low resolution and low background levels when the spacecraft orbit takes it above the lunar far side. Similarly, if robotic spacecraft were landed on the far-side for geological survey work, dipole antennas could operate from these

vehicles. If several were landed, simple interferometry at low frequencies could be performed to survey and locate radio sources at higher resolution. Such precursor missions would help to address the scientific questions described in (1) and (2) above.

(4) More theoretical study is needed on the limitations that will be placed on the lunar VLFA by scattering and refraction from the interplanetary and interstellar media. These plasma effects ultimately limit the resolutions and frequencies of the VLFA. Therefore, the effects must be well understood so that they can be incorporated into the design of the VLFA.

(5) A better investigation of the ionosphere near the surface of the Moon is critically needed. At present, good global and near-surface values of the electron density do not exist. These are crucial to the design of the array. We must know, for example, if a 10^4 electron/cm³ layer hugs the day side of the Moon as recently suggested by Vondrak (1988). These investigations could be carried out by a combination of remote, ground-based observations, reanalysis of RAE and Apollo data, and new measurements made from the lunar surface by precursor and/or early lunar base missions.

(6) In an effort to better understand the scientific limits of the VLFA, we suggest that some initial computer modeling be undertaken to investigate the type of radio source structure that one might be able to map with VLFA. For example, one could "observe" an extragalactic radio source (particularly, the expected low-frequency, extended components) via the computer as it would be seen by the VLFA. Beginning with a model, we can convolve the hypothetical source with the response of the array (i.e., uv coverage) and add noise at the appropriate level to examine what structures one might expect to observe. This will constrain both the science and the design.

(7) We propose that consideration should be given to precursor missions before the establishment of a lunar VLFA. These missions would be used to accurately determine the density and extent of the lunar ionosphere, to perform a preliminary low-resolution all-sky survey at very low frequencies, to study the signal propagation effects through the interstellar medium, and to begin monitoring low frequency variable sources. These missions could be conducted from lunar orbit and from the surface as part of a survey of the lunar far-side.

II. ENGINEERING STUDIES

(1) There should be continued trade studies of various options for the array elements: long versus short dipoles, dipoles versus tripoles, dipoles versus Beverage antennas (J. Kierein, private communication).

(2) The frequency range must be further investigated. One is limited to frequencies above about 1 MHz for galactic and extragalactic observations. However, some of the more interesting planetary emissions occur between 100 kHz and 1 MHz. What should be the lower bound on the frequency of the array?

(3) Computer studies should be undertaken to design the optimum number and configuration of dipoles. Studies of the instantaneous and longer term uv coverage (i.e., synthetic aperture) can be performed with currently available software and computers.

(4) More thought must be given to problems involving noisy data that are anticipated from the VLFA. Questions of self-calibration, phase retrieval, refractive errors, and three-dimensional Fourier transforms must be considered.

(5) Consideration of observing strategy would be useful at this early phase. How does one maximize the range of objects to be studied in detail and minimize the observing time with the proposed VLFA configuration?

(6) One should study the design of a VLSI chip that could perform most of the receiver functions needed at each dipole. This would simplify the electronics, reduce the weight requirements, and potentially make the antennas more reliable.

(7) The power requirements and power storage are still uncertain. We expect that each element will need less than a watt of continuous power during operation. However, how

will this power be supplied, especially during the 14-day nights? Will solar cells with battery storage be adequate? How will this impact on the expected limitations on the mass of the array and the deployment?

(8) An intelligent, robotic vehicle must be designed to remotely deploy the antennas. Given the delay time between the far side and Earth and between the far and near sides, the robot will most likely have to operate in a semi-autonomous mode. Thus, questions of telepresence and artificial intelligence enter into the design. We see this as the most difficult engineering hurdle for the VLFA.

(9) We suggest that a ground-based model of a mini-VLFA be built to test observing and deployment strategies, and to debug the electronics and communications for remote operation. This model would operate at 30 MHz, a window that is accessible (but often polluted by interference) from the ground. The array would be relatively inexpensive since it can be built from currently available components. We would plan to simply deploy these antennas, as on the Moon, with each dipole having an electronics and communication package. The data would be transmitted to a central location via a radio link and recorded on magnetic tape. We may be able to use currently available correlators (e.g., the VLBA correlator) to produce source fringes and visibilities that can be made into sky maps. This model would test the feasibility of the design and operational mode for a future lunar far-side observatory.



Report Documentation Page

1. Report No. NASA CP-3039		2. Government Accession No.		3. Recipient's Catalog No.	
4. Title and Subtitle A Lunar Far-Side Very Low Frequency Array				5. Report Date November 1989	
				6. Performing Organization Code	
7. Author(s) Jack O. Burns, Nebojsa Duric, Stewart Johnson, and G. Jeffrey Taylor, Editors				8. Performing Organization Report No.	
				10. Work Unit No.	
9. Performing Organization Name and Address The University of New Mexico Institute For Astrophysics Department of Physics and Astronomy Albuquerque, New Mexico 87131				11. Contract or Grant No.	
				13. Type of Report and Period Covered Conference Publication	
12. Sponsoring Agency Name and Address National Aeronautics and Space Administration Washington, DC 20546				14. Sponsoring Agency Code	
15. Supplementary Notes Jack O. Burns and Nebojsa Duric, Institute for Astrophysics, The University of New Mexico, Albuquerque, New Mexico 87131; Stewart Johnson, The BDM Corporation, 1801 Randolph Dr. SE, Albuquerque, New Mexico 87106; G. Jeffrey Taylor, Institute of Meteoritics, The University of New Mexico, Albuquerque, New Mexico 87131					
16. Abstract <p>This document contains papers presented at a workshop held to consider very low frequency (VLF) radio astronomical observations from the moon. In part I, the environment in which a lunar VLF radio array would function is described. Part II is a review of previous and proposed low-frequency observatories. The science that could be conducted with a lunar VLF array is described in part III. The design of a lunar VLF array and site selection criteria are considered, respectively, in parts IV and V. Part VI is a proposal for precursor lunar VLF observations. Finally, part VII is a summary and statement of conclusions, with suggestions for future science and engineering studies. The workshop concluded with a general consensus on the scientific goals and preliminary design for a lunar VLF array.</p>					
17. Key Words (Suggested by Author(s)) Astronomy, Astrophysics, Telescopes, Celestial bodies, Lunar bases, Lunar environment, Radio telescopes, Interferometry, Low-frequency observatories, Far-side observatories			18. Distribution Statement Unclassified--Unlimited Subject Category 91		
19. Security Classif. (of this report) Unclassified		20. Security Classif. (of this page) Unclassified		21. No. of pages 88	22. Price A05

